

**Elementary Photocatalytic Chemistry on TiO₂ Surfaces**

Journal:	<i>Chemical Society Reviews</i>
Manuscript ID:	CS-REV-06-2015-000448.R1
Article Type:	Review Article
Date Submitted by the Author:	05-Aug-2015
Complete List of Authors:	Guo, Qing; Dalian Institute of Chemical Physics, State Key Lab Zhou, Chuanyao; Dalian Institute of Chemical Physics, State Key Laboratory of Molecular Reaction Dynamics Ma, Zhibo; Dalian Institute of Chemical Physics, Ren, Zefeng; Peking University, 2. International Center for Quantum Materials and School of Physics Fan, Hongjun; Dalian Institute of Chemical Physics, State Key Laboratory of Molecular Reaction Dynamics; Dalian Institute of Chemical Physics, State Key Lab of Molecular Reaction Dynamics Yang, Xueming; Dalian Institute of Chemical Physics ,

For submission to Chem. Soc. Rev. 2015-08-05

Elementary Photocatalytic Chemistry on TiO₂ Surfaces

Qing Guo^{1,#}, Chuanyao Zhou^{1,#}, Zhibo Ma¹, Zefeng Ren^{2,3,*}, Hongjun Fan^{1,*},
Xueming Yang^{1,*}

1. State Key Laboratory of Molecular Reaction Dynamics, Dalian Institute of Chemical Physics, 457 Zhongshan Road, Dalian 116023, Liaoning, P. R. China
2. International Center for Quantum Materials and School of Physics, Peking University, Beijing, 100871, P. R. China
3. Collaborative Innovation Center of Quantum Matter, Beijing 100871, P.R. China

#) Who made equal contributions to the writing of this manuscript.

*) To whom all corresponding should be addressed: zfren@pku.edu.cn,

fanhj@dicp.ac.cn, xmyang@dicp.ac.cn

Abstract

Photocatalytic hydrogen production and pollutant degradation provided both great opportunities and challenges in the field of sustainable energy and environmental science. Over the past few decades, we have witnessed a fast growing interests and efforts in developing new photocatalysts, improving catalytic efficiency and exploring reaction mechanism at the atomic and molecular level. Owing to the relative high efficiency, nontoxicity, low cost and high stability, TiO_2 becomes one of the most extensively investigated metal oxides in semiconductor photocatalysis. Fundamental studies on well characterized single crystals using ultrahigh vacuum based surface science techniques could provide key microscopic insight into the underlying mechanism of photocatalysis. In this review, we have summarized recent progresses in the photocatalytic chemistry of hydrogen, water, oxygen, carbon monoxide, alcohols, aldehydes, ketones and carboxylic acids on TiO_2 surfaces. We focused this review mainly on the rutile $\text{TiO}_2(110)$ surface, but some results on the rutile $\text{TiO}_2(011)$, anatase $\text{TiO}_2(101)$ and (001) surfaces are also discussed. These studies provided fundamental insights into surface photocatalysis as well as stimulated new investigations in this exciting field. At the end of this review, we have discussed how these studies can help us to develop new photocatalysis models.

1. Introduction

The seminal work of photocatalytic water splitting on TiO_2 electrode by Honda and Fujishima¹ attracted great interests in the field of renewable energy, given the limited fossil resources and their pollution to environment during utilization. Great progresses have been made in solar energy conversion and environmental remediation by making use of TiO_2 heterogeneous photocatalysis.²⁻¹⁰ In addition, fundamental studies targeting at understanding photocatalysis mechanism at the molecular level have also attracted growing attentions.¹¹⁻²² Investigation using the combination of ultrahigh vacuum (UHV) based surface science techniques such as ensemble-averaging desorption/photonic/electronic spectroscopy and especially atomic-resolved scanning probe microscopy, and well characterized single crystal model catalysts provides key insight into the underlying mechanism of heterogeneous photocatalysis.

Rutile TiO_2 (r- TiO_2) (110) surface (Fig. 1A), one of the most extensively studied metal oxide surfaces, has become a prototype for surface chemistry and photochemistry research. The structure of r- TiO_2 (110) has been very well understood. On the surface, fivefold coordinated Ti^{4+} ions (Ti_{5c}) and twofold coordinated bridge O^{2-} ions (O_b) run alternatively along the [001] azimuth. Reduction leads to the creation of surface bridging oxygen vacancies (O_v) and subsurface Ti^{3+} interstitials (Ti_{int}) which contribute to the band gap states. In addition to r- TiO_2 (110), the structures of r- TiO_2 (011) and anatase TiO_2 (a- TiO_2) (101) surfaces have also been investigated, though less extensively. The most stable phase of r- TiO_2 (011) is (2×1) reconstructed. The structure of r- TiO_2 (011)-(2×1) as suggested by X-ray diffraction and density functional theory (DFT) calculations^{23, 24} are shown in Fig. 1B. Different from r- TiO_2 (110), inequivalent types of under-coordinated Ti and O atoms exist,

namely the valley Ti_{5c} , ridge Ti_{5c} , top O_b and bridge O_b . The top O_b atoms are displayed in a zig-zag style, such that they shade the ridge Ti_{5c} sites severely. Missing of the top O_b atoms creates O_v . The saw tooth structure of α - $TiO_2(101)$ is also shown in Fig. 1C. The most prominent feature of this surface structure, in comparison with other surfaces, is the absence of surface oxygen vacancies.²⁵

In this article, we will provide a rather complete review on the recent progresses in the photocatalytic chemistry of hydrogen, water, oxygen, carbon monoxide, alcohols, aldehydes, ketones and carboxylic acids on TiO_2 single crystals, mostly on r - TiO_2 surfaces. Since the knowledge of the adsorption state is the prerequisite to understand the photocatalytic chemistry on surfaces, we will describe the detailed adsorption behavior of the adsorbates firstly, then discuss the photochemistry. Furthermore, the current challenges in experimental photocatalysis studies will be discussed. From the systematic studies of photocatalysis of methanol, water and other molecules on r - $TiO_2(110)$ under vacuum conditions, as well as similar observations in solution, a photocatalysis model based on nonadiabatic dynamics and ground state surface reactions has been proposed and will be discussed in details, which demonstrates the importance of surface dynamics in photocatalysis. Finally, we will discuss the possible directions for future studies on TiO_2 photocatalysis.

2. Hydrogen on r - $TiO_2(110)$

Photocatalytic hydrogen production is the core issue in TiO_2 heterogeneous photocatalysis. How hydrogen molecules are produced over TiO_2 surfaces is an intriguing question. Investigation of the interaction between hydrogen and TiO_2 would provide some clues for understanding the mechanism of molecular hydrogen production.

While TiO_2 surfaces do not interact strongly with molecular hydrogen,²⁶⁻³⁰ atomic hydrogen readily adsorb at the basic sites, for example, bridging oxygen (O_b) atoms on TiO_2 surfaces, generating surface hydroxyls.³¹ Li *et al.* reported a barrier higher than 1 eV for H diffusion along the O_b rows of r- $\text{TiO}_2(110)$.³² Assisted by adsorbates at Ti_{5c} , Zhang *et al.* suggested the diffusion of H atoms across the O_b rows is feasible at room temperature.³³⁻³⁵ Some researchers insisted that H adatoms remain on the surface of r- $\text{TiO}_2(110)$,³⁶⁻³⁸ but the diffusion of these adsorbates into the bulk has also been proposed for r- $\text{TiO}_2(110)$,³⁹⁻⁴¹ r- $\text{TiO}_2(011)$ ⁴² and a- $\text{TiO}_2(101)$.⁴³ In addition, existence of Ti-H species on r- $\text{TiO}_2(110)$ has also been suggested.^{28, 31, 39, 44}

Even though bridging hydroxyls (OH_b) on r- $\text{TiO}_2(110)-(1\times 1)$ are thought to be photo-inactive,^{38,45} photoinduced desorption of surface hydroxyls on r- $\text{TiO}_2(011)-(2\times 1)$ has been directly imaged by Tao and co-workers (Fig. 2).⁴² After 90-minute UV irradiation, the hydroxyl features on this surface were completely removed without the appearance of O_v . The author thus inferred that H atoms were photodesorbed as hydrogen rather than abstracting the lattice oxygen to produce water. Further photo-stimulated desorption (PSD) and time-of-flight mass spectroscopy (TOF-MS) measurements are required to identify desorption species and the final state distribution. Different from the photo-inactive surface hydroxyls, Wu and co-workers discovered the photocatalytic H_2 production from Ti-H species on r- $\text{TiO}_2(110)$.⁴⁶ They naturally proposed a hole-mediated hydrogen production mechanism based on the negatively charged Ti-H predicted by DFT calculations.

3. Water on r- $\text{TiO}_2(110)$ and a- $\text{TiO}_2(101)$

Water chemistry and photochemistry on metal oxide surfaces are of great significance in solar to chemical energy conversion.¹ The adsorption of water on

r-TiO₂(110) has been extensively investigated. Although the spontaneous dissociation at O_v sites has been well established,^{35, 47-50} the exact adsorption state at the Ti_{5c} sites remains unresolved.^{11, 12, 51-53} Coexistence of molecular and dissociative adsorption of water on r-TiO₂(011)-(2×1) has also been reported by Beck and Valentin *et al.*^{54, 55} On the a-TiO₂(101) surface, He and co-workers found that monomer water adsorbed molecularly at the Ti_{5c} sites and showed a local ordered superstructure due to the charge rearrangement at the water-anatase TiO₂ interface.⁵⁶ Chemisorption and tip induced dissociation of water at Ti³⁺ related point defects on a-TiO₂(001)-(1×4) surface at 80 K have recently been reported by Wang *et al.*⁵⁷

So far, there are only a few photochemistry studies of water on TiO₂ surfaces, which is largely due to the low photochemical activity of water on these surfaces. One example for photocatalytic decomposition of water on r-TiO₂(110) in UHV was reported by Tan *et al.* (Fig. 3).⁵⁸ Scanning tunnel microscope (STM) images showed that O-H bond was cleaved under UV irradiation, generating OH_b. While the most part of remaining terminal hydroxyls (OH_t) escaped into vacuum. However, the dissociation probability was only about 4% after the surface was irradiated for two hours. In addition, the remaining OH_t on the surface will not further dissociate to produce O atom under UV irradiation. By comparing the tip electron injection induced water dissociation where only terminal hydroxyls (OH_t) or oxygen adatoms stayed at the original adsorption sites and no OH_b's were observed, Tan and co-workers proposed a hole oxidized rather than electron reduced dissociation of water during the photocatalyzed splitting of water on r-TiO₂(110). However, technically, this is still not full cycle water splitting reaction because no O₂ evolution reaction occurs.

Even in real TiO₂ catalytic systems without additives (such as sacrificial reagents,

metals, cations, and anions), in most cases almost no O₂ has been detected on TiO₂. Thus, the O₂ evolution mechanism on TiO₂ has attracted enormous attention, and contradicting mechanisms have been proposed by different researchers.⁵⁹⁻⁶² In an earlier study, Wilson⁶² speculated that the surface state may act as a possible intermediate of the O evolution. Salvador *et al.*^{60,61} pointed out that the surface OH radicals may serve as the initiation step of the O₂ evolution by using photogenerated holes. Later, Nakamura and coworkers^{63,64} have investigated primary intermediates of oxygen photoevolution reaction at the TiO₂ (rutile)/aqueous solution interface using photoluminescence (PL) and in situ multiple internal reflection infrared (MIRIR) absorption measurements. They illustrated that O₂ evolution is initiated by a nucleophilic attack of a H₂O molecule on a photo-generated hole at a surface lattice O site to form [Ti–OOH–Ti] intermediate, but not by oxidation of surface OH group by the hole. In addition, other water oxidation mechanisms on TiO₂ were also proposed.⁶⁵⁻⁷⁰ Thus far, no consensus has been achieved on the exact mechanism of water oxidation.

4. Oxygen on r-TiO₂(110) and a-TiO₂(101)

Oxygen (O₂) is usually present in the photo-oxidation of organic pollutants and photocatalytic splitting of water over TiO₂. In addition, oxygen may act as an electron scavenger, thus facilitating the photoexcited electron-hole separation process.^{2-4, 71, 72} The crucial roles oxygen plays in photo-oxidation have stimulated extensive studies of the interaction between oxygen and TiO₂ which are of both fundamental and applicable significance.

4.1 Adsorption of oxygen on r-TiO₂(110) and a-TiO₂(101)

Chemical adsorption of O₂ on TiO₂, which is both coverage- and temperature-

dependent, required the charge transfer from the surface to the substrate. The charges are usually introduced by point defects such as surface O_v 's and subsurface Ti_{int} .^{22, 73-79} This is the reason why O_2 adsorbed only physically (desorbing below 75 K) on stoichiometric $r\text{-TiO}_2(110)$.⁸⁰ At elevated adsorption temperatures (above 150 K), spontaneous dissociation of O_2 at O_v 's has been well established. An O_2 molecule healed an O_v , leaving another oxygen adatoms (O_a) at the neighboring Ti_{5c} sites.^{49, 75, 81-84} Aside from the dissociation at O_v 's, Besenbacher *et al.* discovered another channel for O_2 dissociation, i.e., splitting of O_2 at Ti_{5c} sites, producing O_a pairs, which was proposed to be facilitated by the excess charge transfer from the subsurface Ti interstitials.^{81, 83}

Despite the spontaneous dissociation of O_2 at both O_v and Ti_{5c} sites at elevated temperatures, molecular adsorption has also been investigated with temperature below 100 K. O_2 adsorbed preferentially at O_v sites at this temperature range.⁸⁵⁻⁸⁸ Temperature programmed desorption (TPD) experiments performed by Henderson *et al.* showed that chemisorbed O_2 desorbs at around 410 K with first order kinetics.⁷³ Kimmel and Petrik reported the saturation coverage of chemisorbed O_2 is twice of the O_v concentration, which meant two O_2 per O_v ($2 O_2/O_v$).⁸⁵ Based on the TPD and electron stimulated desorption (ESD) results, they proposed a tetraoxygen species when the initial $2 O_2/O_v$ structure was annealed between 200 and 400 K. This finding was consistent with the result of an earlier calculation by Pillay *et al.*,⁸⁹ which showed that the O_4^{2-} structure was more stable by 0.6-0.9 eV than $2 O_2^-$. Site specific adsorption of O_2 on $r\text{-TiO}_2(110)$ has been investigated using high resolution STM by Diebold, Lyubinetsky and Wang's research groups.⁸⁶⁻⁸⁸ Molecularly adsorbed O_2 at both O_v and Ti_{5c} sites became dissociated (Fig. 4), driven by the STM tip.⁸⁷ Chemisorbed O_2 at O_v was invisible. Since O_v appeared as bright spots on the dark

bridging oxygen row in the empty state STM, one can easily see the difference before (Fig. 4 Aa) and after (Fig. 4 Ab) O₂ exposure, and molecularly adsorbed O₂ at Ti_{5c} displayed as even brighter spot on the bright Ti_{5c} rows. To retain the chemisorbed structure, mild tunneling condition should be chosen. For example, Fig. 4 Ab was taken at V=0.8 V and I=3 pA, while Fig. 4 Bb was acquired under V=0.3 V and I=1 pA. Under higher voltage and current (1.5 V and 3 pA in Fig. 4 Ac, 0.6 V and 3 pA in Fig. 4 Bc), chemisorbed O₂ was dissociated. The dissociation of an O₂ molecule at an O_v resulted in the appearance of an O_a on top of the Ti_{5c} site adjacent to the original O_v, while that at Ti_{5c} lead to O_a pair at the Ti_{5c} row.

The charge state of the chemisorbed O₂ species is a crucial property which affects the related chemistry. Peroxo (O₂⁻),^{27, 73, 81, 89-92} superoxo (O₂²⁻)^{77, 89, 92-94} and tetraoxygen (O₄²⁻)^{85, 89} have all been suggested for O₂ adsorption on r-TiO₂(110). For example, using quantum-chemical, ab-initio periodic Hartree-Fock calculations, Lare-Castells and co-workers found O₂⁻ was the most stable O₂ species adsorbed at the defect sites of r-TiO₂(110).⁹⁰ Based on the O_v to O₂ charge transfer and the absence of magnetic moment, Tilocca and Selloni proposed the O₂²⁻ like species using first-principles molecular dynamics approach.⁷⁹ Changing the number of chemisorbed O₂ per O_v, Pillay *et al.* calculated the structure, bonding and energetics of these oxygen species and proposed a tetraoxygen structure, i.e., O₄²⁻,⁸⁹ which was consistent with the experimental result by Kimmel and Petrik.⁸⁵ Direct spectroscopic investigation of the charge state of chemisorbed O₂ on r-TiO₂(110) has been performed by Henderson *et al.*^{73, 93} These studies found that a new loss feature at 2.8 eV appeared at the expense of the Ti 3d derived defect states in electron energy loss spectroscopy (EELS) spectra. Examination of the loss feature at 2.8 eV, however, gave rise to different conclusions in Ref. 73 and Ref. 93. The loss feature was

assigned to O_2^- in Ref. 73 and O_2^{2-} species in Ref. 93, respectively. The fact that no consensus has been reached thus far indicates the complexity of O_2 adsorption on TiO_2 .

O_2 adsorption on a- $TiO_2(101)$ surface has also been investigated.^{22, 95-103} Due to the absence of surface O_v on a- $TiO_2(101)$,²⁵ subsurface O_v 's are responsible for the charge transfer from this TiO_2 substrate to O_2 .²² DFT calculations by Aschauer *et al.* suggested the most stable species varied from O_2^- to O_2^{2-} , as the O_2 coverage increased from below one O_2 per defect to above 1.5 O_2 per defect.⁹⁶ Combined STM and DFT calculations carried out by Setvin and co-workers showed that O_2^{2-} was transformed into an O_2^- by reacting with a subsurface O_v and further placed into an anion surface lattice, generating a bridging oxygen dimer.¹⁰¹ Chemisorption and tip induced dissociation of O_2 at Ti^{3+} related point defects on a- $TiO_2(001)-(1\times 4)$ surface at 80 K have recently been reported by Wang *et al.*⁵⁷ At room temperature, O_2 was still adsorbed molecularly at these point defects, but became dissociated at higher temperature.

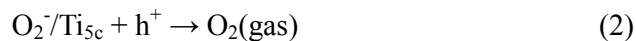
4.2 Photochemistry of oxygen on r- $TiO_2(110)$

Photochemistry of O_2 on r- $TiO_2(110)$ have been extensively studied using photostimulated desorption (PSD)^{93, 104-110} and photoinduced dissociation.¹¹¹⁻¹¹⁵ Yates' group have systematically studied the PSD of O_2 from $TiO_2(110)$ and built a hole mediated desorption model,^{13, 16, 116} which consisted of band gap excitation, diffusion of holes to the surface, trapping of holes at the surface, and finally the transfer of positively charged holes to the anion O_2 , leading to the desorption (reaction 1).



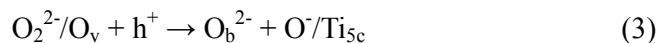
Lu *et al.*^{104, 105} discovered two chemisorption states of O_2 on a reduced

r-TiO₂(110), of which one state could assist the photooxidation of CO while the other could not. The finding of two different O₂ adsorption states was consistent with the velocity distribution measurements using time-of-flight (TOF) by Sporleder *et al.*¹¹⁰ Coverage-dependent O₂ PSD has been further quantitatively investigated by Petrik and Kimmel (Fig. 5).¹¹³ On a reduced r-TiO₂(110) with 0.08 ± 0.01 ML O_v, adsorption of ¹⁸O₂ at 28 K was followed by a subsequent TPD to 100 K (squares in Fig. 5). Thereafter, 300 s PSD was performed at 28 K (triangles in Fig. 5). No ¹⁸O₂ TPD signal was detected until the saturated chemisorption (2 O₂/O_v⁸⁵) was reached, since ramping to 100 K could only remove the physisorbed species.^{80, 117} The increase of ¹⁸O₂ PSD signal with initial ¹⁸O₂ coverage could be fitted by two straight lines with slopes of 0.14 and 0.57 below one O₂ per O_v (1 O₂/O_v) and between 1 O₂/O_v and 2 O₂/O_v, respectively. These authors argued the increase of the slope resulted from the sharing of the excess electrons of the chemisorbed O₂, which meant the charge state was more O₂²⁻ like before all the O_v sites were occupied and favored O₂⁻ which was the reagent of the hole mediated O₂ desorption thereafter. Photodesorption of O₂ at Ti_{5c} sites has recently been observed by Wang *et al.* using high resolution STM (HRSTM) (Fig. 6 A).¹¹⁴ Therefore, reaction 1 shown above could be revised as follows (reaction 2):



Besides photostimulated desorption, UV light induced dissociation of O₂ on r-TiO₂(110) has also been examined.¹¹¹⁻¹¹⁵ Fig. 7 summarized the quantitative analysis of the chemisorbed, photodesorbed and photodissociated oxygen species by Petrik and Kimmel using a combined TPD and PSD study.¹¹¹ θ_{rem} , θ_X , θ_{diss} stood for the coverage of O₂ that retained on the surface, remained undissociated, became dissociated after UV irradiation, respectively. While θ_{occ} , $\theta_{2\text{nd}}$ represented the amount

of occupied and unoccupied sites after exposure to UV light respectively, where the latter was determined by the TPD measurements after a second O₂ exposure following the UV irradiation. In this work, the authors proposed an electron mediated mechanism of photoinduced dissociation at O_v sites (reaction 3),



which was complemented by the hole mediated photodesorption. The increase of photodesorption fraction and the decrease of photodissociation fraction (Fig. 7) with the initial O₂ coverage are consistent with this proposed mechanism. The amount of O₂⁻ increased as the coverage of O₂ was bigger than that of O_v. Therefore, enhanced photodesorption and depressed photodissociation is expected. Petrik and Kimmel's further work using isotope labeling showed that although there were chemisorbed O₂ species which were photoinactive, they could exchange atoms with physisorbed O₂.¹¹² The exchange rate reached a maxima if the O₂ covered r-TiO₂(110) was preheated to 350 K. Even though the exact structure of this oxygen species remained unknown, the authors proposed two possible candidates, i.e., O₂ at O_v sites and tetraoxygen. O₂ photodissociation on TiO₂(110) was also investigated by Wang *et al.*¹¹⁴ Using HRSTM, photoinduced desorption at Ti_{5c} sites (Fig. 6A) and photoinduced dissociation at O_v sites (Fig. 6B) have been directly observed. While complementary oxidative and reductive reaction in photocatalysis are expected to proceed at substantial and balanced rates, the observed kinetics of hole mediated photodesorption and electron mediated photodissociation in this study differed significantly from each other (Fig. 8). If the diffusion rate of charge carriers is the rate-determining step of the reactions, photodissociation will be faster than photodesorption of molecular oxygen in this system since holes diffuse more slowly than electrons.^{13, 18} This is obviously not the case in the current study. There must be other factors (e.g., the dynamics of the

charge transfer processes and the barrier of reactions) governing the reaction kinetics.

5. Carbon Monoxide on r-TiO₂(110)

The interaction between CO and TiO₂ is also of great importance in a variety of applications, ranging from low temperature CO oxidation¹¹⁸ to CO hydrogenation and water-gas shift reaction.¹¹⁹ CO bound weakly on the stoichiometric r-TiO₂(110) surface due to the weak electron donation ability of the substrate and the weak back donation of the Ti ions,⁸⁰ which was in accord with an ab initio molecular orbital calculation.¹²⁰ X-ray photoelectron spectroscopy (XPS) and EELS investigation by Gopel and co-workers suggested O_v's were the adsorption sites for CO,^{27, 121} which was consistent with some theoretical work.^{29, 120} Whereas TPD examination carried out by Linsebigler *et al.* showed that Ti_{5c} sites were favored, and this conclusion was supported by many other theoretical calculations.¹²²⁻¹²⁸ STM study by Zhao *et al.* discovered that though O_v's could assist the diffusion of CO across the O_b rows, they themselves and their nearest Ti_{5c} sites were not suitable for CO adsorption at 80 K.¹²⁹ Instead, the next nearest Ti_{5c} sites were the most favored sites. For other Ti_{5c} sites, the adsorption probability decreases with the distance between Ti_{5c} and O_v. The authors suggested the delocalized distribution of the excess charge on the r-TiO₂(110) surface¹³⁰ should be responsible for the CO adsorption behavior observed. Infrared reflection adsorption spectroscopy (IRAS) study on the adsorption geometry of CO as a function of coverage by Petrik and Kimmel showed that CO adsorbed with its axis oriented perpendicularly to the r-TiO₂(110) surface on top of Ti_{5c} sites below 1 ML, afterwards it bound to the O_b atoms with the molecular axis along the [1 $\bar{1}$ 0] azimuth.

By means of PSD, Yates and co-workers observed a CO₂ signal together with the O₂ one upon UV irradiation on reduced r-TiO₂(110) covered with O₂ and CO at 105

K.^{131, 132} A threshold of the photon energy of 3.1 eV, which corresponded to the band gap of rutile, was found to initiate the surface reaction, suggesting the reaction is a substrate mediated photooxidation. The reaction could only proceed on reduced r-TiO₂(110), indicating that chemisorbed O₂ rather than dissociated O₂ was involved in the photooxidation process.

Later on, Petrik and Kimmel reexamined photooxidation of CO on r-TiO₂(110).¹³³ Besides CO₂ and O₂, CO was also detected by PSD in the presence of chemisorbed O₂. The yield of all these desorption products were similar. Both oxygen coverage dependent and isotope labeling studies supported that O₂ chemisorbed at O_v's were responsible for this photooxidation reaction, while those at Ti_{5c} sites were likely inactive. Desorption of CO₂ was peaked at 40 degree with respect to the surface normal along the [1 $\bar{1}$ 0] azimuth. Such an angular distribution of the product desorption indicated a specific transition state which was consistent with theoretical prediction.^{127, 134} The authors also proposed a model (Fig. 9) for the photooxidation of CO on O₂ covered reduced r-TiO₂(110). No intermediate was detected by IRAS in the photooxidation of CO over r-TiO₂(110).¹³⁵ Petrik and Kimmel found that the reaction kinetics obtained with millisecond time resolution is deviated from that of one step reaction mechanism, based on this, they proposed this reaction involved multiple reaction steps, and both electron-mediated and hole-mediated reactions were needed.¹³⁶

Using first principles calculations, Raina Wanbayor *et al.*¹³⁷ found that positive charge on the anatase (101) surface increases the adsorption energy of CO, allows its conversion to CO₂. This hole-assisted CO → CO₂ conversion can be spontaneous, and would be endothermic without the presence of a hole. With these results, the authors proposed that oxidation of CO on the anatase (001) surface could be an efficient

photocatalytic process.

Using IRAS, Xu and co-workers compared the cross section of photooxidation of CO on r-TiO₂(110) and a-TiO₂(101) quantitatively.¹³⁸ Seen in Fig. 10a, the vibration feature of physisorbed CO₂ at 2340 cm⁻¹ increased with the irradiation ($h\nu = 3.40$ eV) time, while that of CO chemisorbed on top of Ti_{5c} around 2180 cm⁻¹ declined apparently on a-TiO₂(101) which was held at 100 K in the presence of O₂. Based on the IR data, the calculated cross section (Fig. 10b) of this photoreaction was 2×10^{-17} cm² on a-TiO₂(101), which was one order of magnitude larger than that on r-TiO₂(110) under identical experimental conditions. Using contactless transient photoconductance method, the electron-hole lifetime is determined to be about an order of magnitude larger for anatase than for rutile. Thus, these authors proposed that the longer lifetime of electron-hole pairs in anatase facilitates the translocation of the photon-excited electrons and holes from the bulk to the surface, where the photochemical reactions take place.

6. Alcohols on r-TiO₂(110) and a-TiO₂(101)

Photocatalytic reactions of alcohols, especially methanol and ethanol, on TiO₂ have attracted great interests in recent years due to its related application in H₂ production, oxidative remediation of organic wastes, and biomass conversion to fuels and useful synthetic chemicals. Since surface science studies on single crystal surfaces under UHV conditions could provide fundamental insights into these important processes, both thermal chemistry and photochemistry on TiO₂ especially the r-TiO₂(110) surface have been investigated with a variety of experimental and theoretical approaches.^{33, 34, 45, 108, 139-184} In this section, we will provide a detailed reviews on both the thermal chemistry and photochemistry of alcohols on TiO₂

surfaces. Studies of methanol (CH_3OH) will be described first, followed by discussion on other aliphatic alcohols.

6.1 Methanol on TiO_2 surfaces

6.1.1 Adsorption of Methanol on TiO_2 surfaces

On reduced r- $\text{TiO}_2(110)$, TPD spectra of CH_3OH yielded five prominent features at 150, 165, 295, 350 and 480 K.¹⁴⁵ The 150 and 165 K peaks were assigned to multilayer desorption, the feature at 295 K was assigned to the desorption of molecularly adsorbed CH_3OH on Ti_{5c} sites, and the broad tail around 480 K was attributed to the recombinative desorption of dissociated CH_3OH at O_v 's. A small 350 K shoulder was also observed, Henderson *et al.* suggested that this shoulder was due to CH_3OH dissociated at non-defective sites of the surface, probably Ti_{5c} , on the basis of similar behavior of the 350 K and 480 K peaks following electron bombardment.¹⁸⁵ However, no obvious 350 K shoulder was detected in recent TPD studies of CH_3OH on reduced r- $\text{TiO}_2(110)$ with gentle surface treatment.¹⁷⁸ Therefore, the origin of the small 350 K shoulder of methanol TPD on reduced r- $\text{TiO}_2(110)$ is not clear.

Petek *et al.*^{150, 151} provided some indirect evidences that part of CH_3OH adsorbed at the Ti_{5c} sites dissociatively. Using two-photon photoemission spectroscopy (2PPE), an empty wet electron state at about 2.3 ± 0.2 eV above Fermi level (E_F) was detected on both reduced and stoichiometric r- $\text{TiO}_2(110)$. However, in the case of H_2O , this excited state could only be observed on reduced r- $\text{TiO}_2(110)$ surfaces with simultaneous presence of monolayer water and OH_b (resulting from spontaneous dissociation of water at O_v 's⁴⁹), and the electron distribution in this state was reported to encompass several adsorbate H sites.¹⁸⁶ While on the water covered stoichiometric r- TiO_2 surface, this state was totally absent. By analogy with the properties of the

excited state at $\text{H}_2\text{O}/\text{r-TiO}_2(110)$ interface, those authors argued that methanol on $\text{r-TiO}_2(110)$ surface is partially dissociated.

In a high resolution STM study, Zhang *et al.*³³ found that CH_3OH dissociated at the O_v sites spontaneously to form methoxy (CH_3O) and hydroxyl on the primarily neighboring O_b sites. Further investigation showed that molecular methanol can diffuse along the Ti_{5c} rows at room temperature (RT), indicating that CH_3OH is not dissociated at these sites. Theoretical work regarding CH_3OH adsorption on $\text{r-TiO}_2(110)$ were also carried out.^{142, 154, 160} Most results indicated the molecularly adsorbed state of CH_3OH was nearly iso-energetic to the dissociated state with former being slightly more stable, and the energy barrier for the transformation between these two states was quite low. These results are consistent with STM observation at both liquid nitrogen temperature¹⁶³ and RT,³³ although it is not clear this good agreement will stand at high surface coverage. Theoretical calculations showed that dissociative adsorption of CH_3OH on O_v sites is thermodynamically more favorable than molecular adsorption by 0.5 eV,¹⁵⁴ which is also consistent with TPD and STM experimental results.

6.1.2 Photocatalytic chemistry of methanol on TiO_2 surfaces

Methanol/ TiO_2 is an important model system because of remarkable enhancement of photocatalytic hydrogen production from water-methanol mixture over TiO_2 ,¹⁸⁷ the potential applications of CH_3OH in photocatalytic selective oxidation,¹⁸⁸ environmental photocatalysis,¹⁸⁹ and photocatalytic reforming reactions.¹⁸⁸ Meanwhile, as one of the simplest organic compounds, CH_3OH is often chosen as a probe for the fundamental studies of photocatalytic chemistry on oxide surfaces.

Recently, the methanol on r-TiO₂(110) system was investigated using 2PPE, STM and DFT calculations by Zhou *et al.*¹⁶³ They also observed an excited state at about 2.4 eV above E_F by irradiating a saturated layer of CH₃OH (0.77 ML)¹⁶⁹. In this work, a 1 ML covered r-TiO₂(110) surface was irradiated with 400 nm femtosecond laser pulse, very similar to the previous 2PPE measurement on this surface,¹⁵¹ where the unoccupied excited state was assigned to be an intrinsic “wet electron state” on the CH₃OH covered r-TiO₂(110) surface. However, Zhou *et al.*'s results showed the excited resonance peak was absent at the beginning of laser irradiation (Fig. 11A), suggest that this excited does not exist initially for the CH₃OH covered r-TiO₂(110) surface. The excited state signal, however, increased with the laser irradiation time and saturated after a 15-minute irradiation, accompanied by a peak shift towards lower energy. This interesting result unambiguously demonstrated that the excited resonance state, which was located at 2.4 eV above E_F, was a photoinduced surface state rather than a wet electron state that was intrinsically present on the CH₃OH /r-TiO₂(110) surface. The lifetime of the excited state was measured to be ~ 20 fs by time-resolved two-pulse correlation.¹⁷⁵ This value was in agreement with Petek's result.¹⁵¹

In order to understand this photoinduced process, Zhou *et al.*¹⁶³ also employed STM (acquired at 80 K) to reveal the nature of the photochemical changes detected by 2PPE (Fig. 12). Fig. 12A shows an STM image of the bare r-TiO₂(110) surface with about 4% O_v's (labeled as “BBO_v” in the Figure). The bright and dark lines corresponded to the Ti_{5c} and O_b rows respectively, while the bright spots on the dark lines represented the O_v's. After adsorption of 0.02 ML CH₃OH, most of the CH₃OH molecules adsorbed on the Ti_{5c} sites and appeared as clear bright round spots (Fig. 12B). These bright round spots could move along the Ti_{5c} row as a whole or desorb

driven by the STM tip, implying that CH_3OH molecules adsorbed on the Ti_{5c} sites molecularly first, which was consistent with previous STM results.³³ After 10-minute UV (< 400 nm) irradiation, the majority of the bright round spots became elongated (marked by black arrows in Fig. 12C). By manipulating one of these elongated species (labeled “m1” in Fig. 12C) with the STM tip, the species was then separated into two components. One of the components left on the O_b site was confirmed to be an OH_b group.¹⁹⁰ This clearly suggested that the CH_3OH molecule after UV irradiation was dissociated. Similar STM experiments using >400 nm light have also been carried out. No evidence for CH_3OH dissociation was found, suggesting that the dissociation of CH_3OH was a substrate mediated photocatalytic process.

Given the coverage difference in the 2PPE and STM experiments, Zhou and coworkers also performed additional 2PPE measurements at lower surface coverage. The irradiation dependence of the excited resonance state was found to be similar for the CH_3OH coverage at 0.77, 0.39 and 0.12 ML, suggesting the photochemical change is not dependent on the CH_3OH coverage, although the reaction kinetics seems to be dependent on the coverage. Therefore, the STM and 2PPE results could be directly related. The photocatalyzed dissociation of CH_3OH imaged by STM suggested the photoinduced excited state detected by 2PPE comes from photodecomposition of CH_3OH on this surface. DFT calculations of the electronic structure are also consistent with experimental results. Molecularly adsorbed CH_3OH had little effect on the density of states (DOS) of Ti 3d due to the relative weak interaction between CH_3OH and Ti_{5c} , however, the adsorbate-substrate interaction became much stronger when CH_3OH deprotonated. The strong interaction between CH_3O and the Ti_{5c} ion led to the appearance of a new band which was centered at 2.5 eV above the E_F , in agreement with the 2PPE measurement. Since both the initial

state (band gap state) and the intermediated state in the 2PPE measurement were of Ti 3d character, the transition between the two states was forbidden in octahedral field. However, due to the presence of the surface, the octahedra became distorted, thus allowing weak $d \rightarrow d$ transition.

Zhou *et al.* suggested that photodissociation of CH₃OH goes through O-H bond cleavage, as illustrated in the reaction:



Since the excited state was associated with the dissociation of CH₃OH, the irradiation time dependent excited resonance signal illustrated essentially the kinetics of photocatalyzed dissociation of CH₃OH on r-TiO₂(110). The integrated time dependent excited resonance signal (Fig. 11B) could not be described by a single exponential model, while a fractal-like kinetics model (equation 5)^{191, 192} simulated the data well.

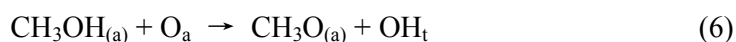
$$I = I_0(1 - \exp(-\frac{k_0}{1-h} t^{1-h})) \quad (5)$$

where k_0 is the rate at $t=1$, and h is equal to $1-d_s/2$, where d_s is the spectral dimension of the heterogeneous reaction media. Previous study suggested the fractal-like kinetics of photochemistry on TiO₂ surface can attributed to the trapping and detrapping of charge carriers.¹⁰⁹

As a model photoreaction, photocatalyzed decomposition of fully deuterated methanol (CD₃OD) on TiO₂ has been used by Zhou *et al.*¹⁶⁸ to investigate the differences in the photocatalytic activities of the oxidized and reduced r-TiO₂(110) surfaces. The excited resonance state at about 5.5 eV was observed by 2PPE on both surfaces covered with CD₃OD, whereas the rise times of the excited resonance signal on these two surfaces were significantly different (Fig. 13). It took 37 seconds for the

excited resonance signal to reach 90% of its maximum level on the reduced surface, whereas on the stoichiometric one, the rise time was 640 seconds. The varied photoactivity was attributed to the concentration difference of point defects on these two surfaces. The amount of both surface and subsurface defects on the reduced r-TiO₂(110) surface were significantly larger than those on the stoichiometric surface. They suggested that the surface and/or subsurface defects could accelerate methanol photolysis on r-TiO₂(110) surface. Unfortunately, it was difficult to characterize whether the surface defects or subsurface defects play a more important role in the acceleration of methanol photolysis on r-TiO₂^{77, 193} due to the difficulty in quantitative characterization of the density of the subsurface defects. The observed higher photoactivity on reduced TiO₂ surface was consistent with improved photocatalytic hydrogen production via self Ti³⁺ doping, probably due to the enhanced light absorption.¹⁹⁴

As discussed above, dissociation of the CH₃O–H bond occurred on CH₃OH covered reduced and stoichiometric r-TiO₂(110) surfaces under UV irradiation. However, both 2PPE and STM methods were not able to identify the photochemical species on the surface. Recently, CH₃OH photolysis on r-TiO₂(110) has been studied using the TPD method by Henderson *et al.*^{171, 172, 178} They proposed that the adsorption state of CH₃OH was crucial to its photochemistry on TiO₂. By co-adsorption of CH₃OH and O₂ on r-TiO₂(110) to control the thermal dissociation of CH₃OH, CH₃O is formed on TiO₂(110) from the reaction of molecularly adsorbed CH₃OH and an O adatom,



where OH_t is a thermal hydroxyl group on a Ti_{5c} site. Henderson *et al.*¹⁷¹ concluded

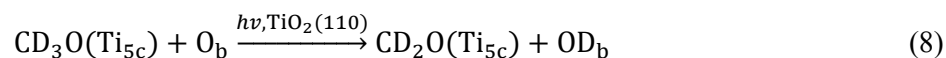
that CH_3O , rather than molecular CH_3OH , was the photoactive species in photochemical reactions of CH_3OH on TiO_2 . Their results also suggested that formaldehyde (CH_2O) was produced from photochemistry of thermally dissociated CH_3OH on the Ti_{5c} sites, which was initiated by defects, coadsorbed O adatoms or OH_t groups, but not by O_v sites (under UHV conditions), and not from photodissociation of molecular CH_3OH on the Ti_{5c} sites.

Guo *et al.* have extended the investigation of CH_3OH photolysis systematically also using the TPD method, in combination with laser surface photocatalysis. They investigated the photo-induced dissociation of partially deuterated methanol (CD_3OH) on $r\text{-TiO}_2(110)$ using 400 nm laser irradiation without coadsorbed O_2 .¹⁷⁶ Fig. 14A shows TPD spectra collected at a mass-to-charge ratio (m/z) of 33 (CD_2OH^+) after surfaces of $r\text{-TiO}_2(110)$ were dosed with 0.5 ML CD_3OH and then irradiated by the laser for various durations. The observed CD_3OH signal decreased monotonically with the laser irradiation time, suggesting that the CD_3OH molecules adsorbed on the Ti_{5c} sites of $r\text{-TiO}_2(110)$ were photocatalytically dissociated. Concomitant to the decrease of the CD_3OH TPD peak, a new peak at 270 K appeared in the TPD spectra for $m/z = 32$ (CD_2O^+) and increased with laser irradiation time (Fig. 14B), corresponding to desorption of molecularly adsorbed CH_2O from the Ti_{5c} sites. The released H/D atoms transferred to the O_b sites were confirmed by the characteristic recombinative desorption of OH_b from this surface around 460 K.^{195, 196} The photodecomposition of methanol into formaldehyde and OH_b 's on $\text{TiO}_2(110)$ has recently also been directly observed using high resolution STM technique by Wei *et al.*¹⁹⁷

DFT calculations on the ground state potential energy surface showed that the O-H dissociation energy of CH_3OH was slightly endoergic by only 0.03 eV, with a

barrier of 0.25 eV. While, the dissociation energy of the second dissociation step (the C-H dissociation) to produce CH₂O and H was highly endoergic (1.03 eV), and the barrier was also much higher (1.57 eV). The barrier for the reverse reaction was therefore 0.54 eV (Fig. 15). Similar energetics for the CH₃OH /r-TiO₂(110) model system have been reported by Lang *et al.*¹⁸⁴ A recent study on the recombination of formaldehyde and H_b atoms by Mao *et al.*¹⁹⁸ using 2PPE and STM suggested the calculated energetics were reasonable. CH₃OH at Ti_{5c} sites could only be dissociated under UV irradiation (<400 nm) (Spontaneous and tip induced (V = +1.25 V, I = 100 pA) dissociation of CH₃OH at Ti_{5c} sites were not observed). However, spontaneous and tip induced recombination of formaldehyde and H_b atoms were detected, suggesting the lower stability of the products and a high and low barrier for the forward (dissociation) and reverse (recombination) reaction, respectively. This was consistent with the calculation of the energetics for the CH₃OH/r-TiO₂(110) system.

Therefore, Guo and co-workers proposed that CD₃OH was photodissociated into CD₂O at Ti_{5c} sites in a two-step process, leaving eventually H and D atoms on the O_b sites:



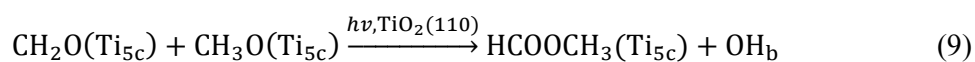
These experimental results clearly demonstrated that photocatalytic CD₃OH dissociation on r-TiO₂(110) occurred on Ti_{5c} sites rather than O_v's, and clarified the exact active photocatalytic site on this surface.

Photocatalyzed dissociation of methanol on r-TiO₂(110) clearly provided a strategy to continuously vary the surface hydroxyls without affecting the subsurface

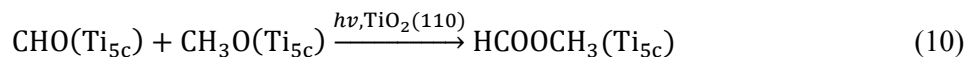
defects. Mao *et al.* thus revisited the long standing issue of the origin of band gap states in r-TiO₂(110) by exploring the correlation between the DOS of the band gap states and the concentration of surface hydroxyls prepared via CH₃OH photodissociation.¹⁹⁹ The intensity of band gap states measured by ultraviolet photoelectron spectroscopy (UPS) scaled linearly with surface hydroxyls characterized by TPD with a small intercept, suggesting surface defects made a major contribution to the band gap states, which in turn indicates the importance of surface defects in changing the electronic structure of TiO₂ which dictated the surface chemistry.

In addition to the formation of CH₂O from CH₃OH photocatalysis on r-TiO₂(110), Guo *et al.*¹⁷⁹ observed further photocatalytic oxidation to form methyl formate (HCOOCH₃) with 0.5 ML CH₃OH covered r-TiO₂(110) surface. As seen in Fig. 16, during the first 10 minutes of irradiation, the amount of CH₂O formed rose rapidly to a maximum, while little HCOOCH₃ was formed. Longer irradiation times lead to a steady decrease of the amount of CH₂O and a concomitant increase of that of HCOOCH₃. After 90 minutes of irradiation, very little CH₂O remained on the surface. Thus, the formation of HCOOCH₃ appeared to be directly correlated with the depletion of CH₂O. Similar phenomena were also observed by Phillips *et al.*¹⁸¹ and Yuan *et al.*¹⁸²

According to a series of thermal catalytic investigations on gas-phase dehydrogenation of CH₃OH to HCOOCH₃ over copper-based catalysts,²⁰⁰⁻²⁰² Guo *et al.* suggested that HCOOCH₃ was produced through cross coupling of CH₂O and CH₃O.¹⁷⁹



While, Phillips *et al.*¹⁸¹ proposed that CH₃O on Ti_{5c} sites underwent photo-oxidation to HCOOCH₃ in a two-step process where the CH₃O dissociated to CH₂O and a cross-coupling reaction involving a formyl (HCO) intermediate led to the formation of HCOOCH₃:



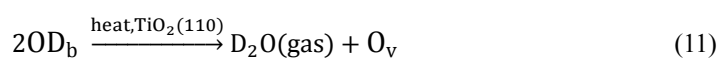
Recently, Lang and co-workers¹⁸⁴ have investigated the two pathways mentioned above for CH₃OH oxidation into HCOOCH₃ on perfect r-TiO₂(110) and defective r-TiO₂(110) based on first-principles calculations. The huge difference in the energy barriers for HCO and hemiacetal production suggested that CH₃OH oxidation on both surfaces facilely proceeded through the intermediate hemiacetal to produce HCOOCH₃.

Photooxidation of CH₃OH has recently been studied by Mao *et al.*²⁰³ to assess the relative photoactivity of r-TiO₂(110)-(1×1) and r-TiO₂(011)-(2×1), with the latter has been reported to have higher activity towards photooxidation reactions.^{204, 205} The reaction pathways were similar on these two surfaces. CH₂O, HCOOCH₃ have been detected. The most prominent difference of the photooxidation of CH₃OH on these two surfaces came from the reaction kinetics. The reaction rate on r-TiO₂(011)-(2×1) was only 42% of that on r-TiO₂(110)-(1×1), contradicting with previous reports in aqueous environments where characterization of TiO₂ structure was difficult.^{204, 205}

The effect of surface atomic structure on the activity of a crystal in heterogeneous reactions is known to be greatly related to the number of unsaturated coordinated atoms on the surface. The higher the percentage of undersaturated coordinated atoms, the more reactive the crystal is. The results obviously did not

comply with this rule since the percentage of Ti_{5c} was 100% on $r-TiO_2(011)-(2\times 1)$ and 50% on $r-TiO_2(110)-(1\times 1)$. In addition, this result was not in agreement with a previous electronic structure study which expected that the electron trapping and electron-hole separation on the $r-TiO_2(011)-(2\times 1)$ surface were more efficient than on $r-TiO_2(110)-(1\times 1)$ surface, based on the higher binding energy of the band gap states of the former.²⁰⁶ Theoretical studies^{184, 203} suggest that the rate determining step of photooxidation of CH_3OH on both surfaces were the C-H bond cleavage, however, the barrier of this elementary step was 0.2 eV higher on $r-TiO_2(011)-(2\times 1)$ due to the distinct atomic configuration. They then tentatively linked the correlation between the photoactivity and the surface structure of TiO_2 .

As we can see from the above experimental studies, the photooxidation of CH_3OH on $r-TiO_2(110)$ proceeded through multiple elementary reaction steps. After CH_3OH dissociation, the dissociated H-atoms transferred to nearby O_b sites, prompting the question of how molecular hydrogen might be formed during CH_3OH photocatalysis. Recent experimental investigation on the photocatalysis of CD_3OD on $r-TiO_2(110)$ by Xu and co-workers⁴⁵ suggested that molecular hydrogen (D_2) was not formed from photoinduced recombination of dissociated D-atoms. Whereas, during TPD process, D-atoms desorbed from the surface in form of D_2O and D_2 (Fig. 17).



Both D_2O and D_2 recombination signal increased with laser irradiation time, and the peaks gradually shift to lower temperature. Meanwhile, the desorption of D_2 starting from ~ 375 K, which is about 50 K higher than that of D_2O , indicating that D_2 desorption was more difficult than D_2O desorption. The yields of these two products

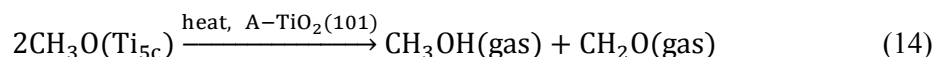
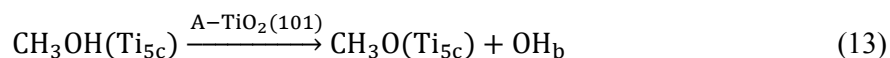
indicated that less than ~7% of total D-atoms from CD₃OD photolysis desorbed as D₂, demonstrating that D₂ formation is much less facile than D₂O formation.

It is generally believed that the thermalization of charge carriers produced from UV irradiation of the TiO₂ surface, as well as the relaxation to their respective band edges, occurs in the hundred-fs scale. As a result, photolysis on TiO₂ is driven by separated electrons or holes that are energetically located at the band edges. The reaction rate will depend on the photon flux rather than wavelength of the incident light.¹⁸ Gundlach and coworkers used 2PPE to track thermalization following electron injection from dyes adsorbed on r-TiO₂(110).²⁰⁷⁻²⁰⁹ Fast initial decay of the 2PPE signal resulting from thermalization of the injected electron occurred on the 10 fs timescale. This result suggested that excess potential energy was lost to the lattice via strong coupling with phonon modes, thus reducing the potential advantage gained by the specificity in the absorption event. Xu and coworkers have tested this idea by measuring the initial dissociation rate of CH₃OH on r-TiO₂(110) with two irradiation wavelengths, 355 nm and 266 nm.²¹⁰ Because CH₃OH and CH₂O may be desorbed by irradiation,¹⁷⁶ monitoring the yields of CH₃OH reactant and CH₂O product was not the best approach to measure the product formation rate. Another major product from CH₃OH dissociation on r-TiO₂(110) was atomic H on the O_b sites, resulting from reaction 7 and 8. Due to the high adsorption energy, these products did not desorb easily by light. Upon heating, two bridging H atoms abstracted an O_b to form a H₂O molecule, then the H₂O molecules desorbed at around 500 K, leaving an O_v on the surface (reaction 11).

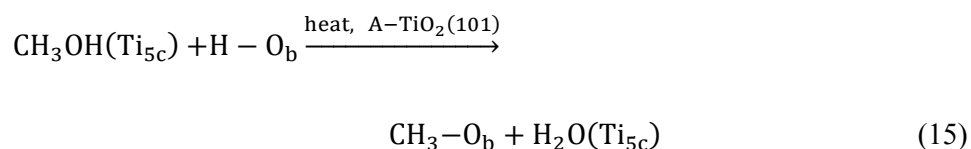
Thus, monitoring H-atom production through the desorption of H₂O was the better way to measure the product formation rate as CH₃OH underwent photocatalytic dissociation. As shown in Fig. 18, the initial rate of H₂O production was found to be

strongly dependent on photon energy, with the initial rate being about two orders of magnitude higher at 266 nm than at 355 nm. This striking result was clearly in conflict with the traditional electron-hole photocatalysis model that charge carriers in TiO₂ rapidly thermalize to their respective band edges via strong coupling with phonon modes first, which predicted that photocatalysis should not depend strongly on the photon energy. These authors speculated that reactions maybe occur on the ground electronic state, where increased converted photon energy should be more efficient in driving chemical reactions. The new phenomenon reported by Xu and coworkers challenges the traditional electron-hole photocatalysis model, and calls for the development of a more sophisticated surface photocatalysis model that incorporates the effect of photon energy, which is expected to enhance the understanding of fundamental processes in photocatalysis.

Kavan and colleagues²¹¹ found that anatase is the more photoactive polymorph for the photocatalytic production of hydrogen from H₂O oxidation and is the only polymorph that can produce hydrogen without applying an external bias. However, the availability of large size and high quality single crystal anatase is very limited. As yet, only a few experimental studies^{212, 213} on CH₃OH chemistry on a well-defined a-TiO₂(101) surface have been done. On the reduced a-TiO₂(101) surface, five desorption features observed at 142 K, 188 K, 270 K, 410 K, and 650 K are observed in TPD spectra of CH₃OH (Fig. 19).^{212, 213} By analogy with the behavior of CH₃OH on r-TiO₂(110), the 142 and 188 K peaks are assigned to multilayer desorption, the feature at 270 K is assigned to the desorption of molecularly adsorbed CH₃OH on Ti_{5c} sites, and the broad tail around 410 K is attributed to the recombinative desorption of dissociated CH₃OH on defect sites. The 650 K peak is likely due to CH₃O disproportionation at the Ti_{5c} sites, as on the r-TiO₂(110) surface.¹⁷¹



Recently, Xu and coworkers²¹³ have done some preliminary study of CH₃OH photolysis on a-TiO₂(101) using TPD method. As shown in Fig. 20, the 650 K peak in mass 30 and 31 TPD decreased rapidly after 5 second irradiation while the 300 K peak changed little implies that CH₃O has a much higher reactivity than molecular CH₃OH on this surface. Photocatalytic products, CH₂O and HCOOCH₃, have been detected with different laser irradiation times (Fig. 20B and C), implying that the photocatalytic mechanisms for the formation of these products are similar to that on the r-TiO₂(110) surface.¹⁷⁹ These authors have also detected dissociated H-atoms from photocatalysis of CH₃OH on the a-TiO₂(101) surface by collecting TPD spectra of H₂O and H₂ products (Fig. 21A and B). Whereas, a rather sharp peak at *m/z* = 18 was observed near 260 K after different laser irradiation times, which was assigned to H₂O desorption from Ti_{5c} sites. No obvious H₂O desorption signal was detected at higher temperature. Concomitant to the increase of the H₂O TPD peak, a broad methyl radical feature stretching from 400-700 K was also detected at mass 15, keeping the same increasing rate with that of H₂O. Referring to the earlier theoretical work by Tilocca and Selloni,²¹⁴ these authors suggest that the H₂O TPD peak at 260 K is due to the following thermally driven exchange reaction,



Same as D₂ formation on r-TiO₂(110), H₂ formation from CH₃OH photocatalysis on a-TiO₂(101) may occur via photocatalytic dissociation of CH₃OH followed by thermal

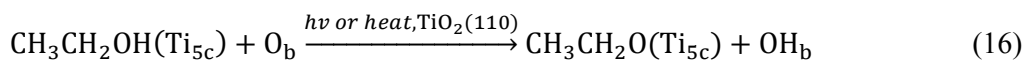
recombination of H-O_b. The formation of molecular H₂ and H₂O were comparable on the a-TiO₂(101) surface, indicating that the H₂ formation process should be more efficient on the a-TiO₂(101) surface than on r-TiO₂(110) surface.

Beside participating the photochemical reaction directly, methanol and other organic adsorbates have also been usually treated as hole scavengers. By density functional studies, Cristiana Di Valentin *et al.*²¹⁵ have shown that surface dipole originated by the molecular adsorption reduces the energy cost to form a hole at a surface oxygen. The hole can then be trapped by the organic adsorbate if proton dissociation takes place. The scavenging power follows the trend glycerol > tert-butanol > iso-propanol > methanol > formic acid.

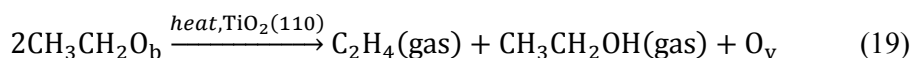
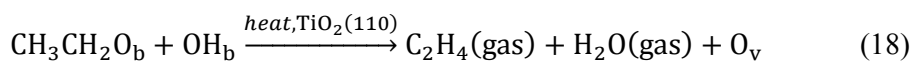
6.2 Ethanol Photolysis

Compare to methanol, less studies have been done for ethanol (C₂H₅OH) chemistry and photochemistry on r-TiO₂(110)^{139, 147, 149, 156, 158, 165, 166, 170, 174, 216-218}. Although the TPD profiles of C₂H₅OH are very similar to those of CH₃OH, the adsorption state on Ti_{5c} sites is different. As yet, no direct experimental evidence demonstrated that CH₃OH dissociatively adsorbs on the Ti_{5c} sites. However, XPS study by Idriss *et al.*¹⁵⁶ and STM study by Hansen *et al.*¹⁶⁵ showed that part of C₂H₅OH dissociated at Ti_{5c} sites spontaneously to form ethoxy (C₂H₅O) and OH_b on r-TiO₂(110). The photochemistry of C₂H₅OH on the r-TiO₂(110) surface was first investigated by Idriss *et al.*^{156, 170} using XPS and TPD methods. These authors observed thermal conversion of adsorbed C₂H₅OH to acetaldehyde and ethylene (C₂H₄) during TPD process after C₂H₅OH adsorption at 300 K. Upon UV excitation in the presence of O₂, adsorbed ethanol on r-TiO₂(110) reacts to produce acetaldehyde and then to carboxylates.

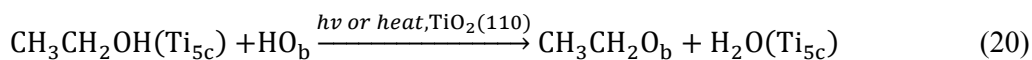
Recently, the photochemistry of C₂H₅OH on r-TiO₂(110) has been re-studied using TPD method by Ma *et al.* (Fig. 22).²¹⁷ In the absence of O₂, they illustrated the photoinduced dehydrogenation of C₂H₅OH was similar to CH₃OH photochemistry on r-TiO₂(110),



Aside from the recombinative desorption of OH_b to produce H₂O at ~500 K, another H₂O desorption feature grew at about 250 K with UV irradiation, and was assigned to H₂O species on Ti_{5c} sites. As the H₂O TPD peak at 250 K increases, a broad C₂H₄ TPD peak from 500-650 K via two possible reactions 18²¹⁹ and 19¹³⁹ appears at mass 26, in the same increasing rate with that of the H₂O TPD peak,



where C₂H₄ formation was the dominant process. Combined with early studies of C₂H₅OH on hydroxylated TiO₂ powders,²²⁰⁻²²² these authors suggest that the increased H₂O desorption feature at 250 K was likely accomplished by the replacement of C₂H₅OH molecules and OH_b to produce adsorbed H₂O on Ti_{5c} sites and bridging ethoxy,



These authors also investigated photochemistry of C₂H₅OH on a new r-TiO₂(110) sample and an old r-TiO₂(110) sample having experienced hundreds cycle of sputtering and annealing. Interestingly, on the new r-TiO₂(110) sample, reaction 20

rarely occurs. The main difference between the two samples is the density of subsurface defect, which was much higher in the old sample. Thus, these authors speculated that subsurface defects may affect surface chemistry on r-TiO₂(110) in a different way, compared to surface defects.

Photochemistry of 2-propanol on r-TiO₂(110) has been investigated by Brinkley and Engel^{141, 146} using TPD and molecular beam techniques. With a mixed beam of O₂ and 2-propanol in a 7 : 1 ratio directed at the surface, when the light was switched on, intense signals associated with acetone and H₂O products were detected by a mass spectrometer, both of which decayed very rapidly in a few seconds, then kept a constant until the light was switched off. The yields of acetone and H₂O were approximately the same, indicating that one 2-propanol molecule reacted with O₂ molecule to form one acetone and one H₂O molecule, and O₂ was necessary for this photochemical process.

7. Aldehydes on r-TiO₂(110)

Surface chemistry and photochemistry of aldehydes have been intensively studied motivated by both applied and fundamental reasons. Aldehydes may be used for the catalytic production of numerous useful synthetic chemicals. They are also atmospheric pollutants with potential carcinogenic effects, as well as additives and byproducts in the combustion of alcohols as automotive fuels.²²³ As a result, photocatalytic degradation of aldehydes, as a potential commercial technique to remove aldehydes from environment, has attracted enormous scientific interest, leading to the extensive study of the thermal chemistry and photochemistry of aldehydes on r-TiO₂(110).^{193, 223-242} The photochemistry of acetaldehyde is very similar to that of ketones.²³⁶ Thus, acetaldehyde photochemistry will be treated

together with ketones (see section 8). In this section, we will mainly focus on the photochemistry of formaldehyde (CH_2O).

7.1 Formaldehyde on r-TiO₂(110)

Yates and coworkers²²⁵ studied the thermal chemistry of CH_2O on r-TiO₂(110) surface. Using TPD method, these authors observed reductive coupling of CH_2O adsorbed at O_v sites to yield C_2H_4 , with O_v playing a key role in the reaction. They also speculated that the product C_2H_4 was due to the recombination of two dioxy-methylene ($-\text{OCH}_2\text{O}-$) groups at higher surface temperatures (~ 500 K), which was formed through the reaction of the initially adsorbed CH_2O at O_v sites with an adjacent O_b , leading to the formation of a $-\text{OCH}_2\text{O}-$ species. Later, Qiu and coworkers²³⁰ investigated the thermal chemistry of CH_2O on the r-TiO₂(110) surface with TPD and HREELS methods. In their work, paraformaldehyde yielded from polymerization of Ti_{5c} -bound CH_2O molecules was proposed as the dominant product based on the HREELS results when exposing the perfect r-TiO₂(110) surface to CH_2O at 100 K, and reductive coupling of CH_2O to produce C_2H_4 via a diolate ($-\text{OCH}_2\text{CH}_2\text{O}-$) surface intermediate by CH_2O adsorbed at the O_v 's of defective surface was demonstrated. More recently, in analogy with the adsorption of other oxygenates on r-TiO₂(110) and polymerization of CH_2O on $(\text{WO}_3)_3/\text{r-TiO}_2(110)$, Kim and coworkers concluded that CH_2O molecules adsorbed at Ti_{5c} sites in the monomer form.²³¹

A series of theoretical works^{193, 228, 229, 242} illustrated that η^2 dioxymethylene CH_2O , which bound to a Ti_{5c} site and nearby O_b , was the preferred adsorption structure, compared to an η^1 CH_2O adsorption at Ti_{5c} sites on stoichiometric r-TiO₂(110). On reduced surface, O_v was the most stable adsorption site, and η^2

dioxymethylene configuration was also formed with carbon binding to two O_b 's. However, a recent STM study²⁴² of CH_2O on reduced r-TiO₂(110) observed clearly that the O_v -bound CH_2O started to diffuse along the O_b row at ~170 K. While the Ti_{5c} -bound ones started to diffuse along the Ti_{5c} row as an intact molecule at ~215 K, the binding structure, i.e., η^2 or η^1 , could not be identified.

The most well-studied aldehydes on r-TiO₂(110) in terms of photochemistry is formaldehyde (CH_2O).²³³⁻²³⁵ Using the highly sensitive TPD method, Xu and co-workers²³³ have investigated the photo-induced (400 nm) decomposition of CH_2O on reduced r-TiO₂(110). Without irradiation, the 280 K peak in TPD spectra at $m/z = 28$ and $m/z = 29$ (Fig. 23A and B) was the result of dissociative ionization of the desorbed parent CH_2O molecule in the electron-bombardment ionizer. Upon irradiation, the intensity of the 280 K CH_2O peak in TPD spectra at $m/z = 29$ decreased monotonically as the laser irradiation time. Meanwhile, two additional new desorption peaks at 486 K and 580 K grew in the $m/z = 29$ TPD spectrum. Compared to previous investigations of HCOOH adsorbed on r-TiO₂(110),²⁴³⁻²⁴⁶ these authors assigned the 486 K TPD peak to the recombination of surface formates with surface hydroxyl groups at O_b rows, and the 580 K TPD peak to the desorption of formate. The increased CO TPD signal for $m/z = 28$ at 580 K was a result of the decomposition of the formate species. The large TPD signal for desorbed CO indicated that formate is an important photo-induced product.

In order to produce formate, the carbon atom of the CH_2O molecule must acquire a second O atom to form O- CH_2O structure first. Thus, they suggested that²³³, in the absence of O_2 , the second O atom may come either from an O_b row or from another CH_2O molecule adsorbed on a Ti_{5c} site of the surface. As shown in Fig. 23D, the increase of the C_2H_4 signal yielded by the carbon-carbon coupling reaction of two

CH₂O molecules adsorbed at O_v sites with irradiation time strongly demonstrated that methylene groups were transferred to O_b's during UV irradiation to leave the O atom of the CH₂O molecule at Ti_{5c} sites, which was most likely to occur via a dioxymethylene intermediate with the carbon atom of the CH₂O molecule binding to an O_b nearby. This conclusion was further supported by the appearance and increase of CH₃ products on O_b's after UV irradiation (Fig. 23E). While, the increasing intensity of recombinative desorption peak of HCOOH suggested that H atoms of CH₂O molecules were transferred to O_b sites during UV irradiation.

With careful experimental investigations, these authors²³³ proposed a schematic model for the photo-induced decomposition of CH₂O on r-TiO₂(110), as depicted in Fig. 24. In the absence of O₂, the Ti_{5c}-bound CH₂O adsorbed in η^2 structure or η^1 structure. Then the methylene of CH₂O might transfer to an O_b nearby via the η^2 structure through a photo-induced process, with the O atom of CH₂O left on a Ti_{5c} site. This O atom might react with a nearby CH₂O to form a CH₂O-O complex. Finally, formate is produced with an H atom of CH₂O-O complex transferring to an O_b site by UV irradiation, and this is the main reaction channel for formate production. Meanwhile, the η^2 structure Ti_{5c}-bound CH₂O may also react to form formate, which is a minor channel.

Cremer and co-workers²³⁴ further investigated the photo-oxidation of CH₂O on both reduced and oxygen-riched r-TiO₂(110) surfaces. On the reduced surface, the source of the additional O atoms for CH₂O oxidation to form formate was generated from a less efficient and more complex photodecomposition pathway of CH₂O. Therefore the efficiency for photo-oxidation of CH₂O on reduced TiO₂(110) was very low, which was similar to the results obtained by Xu and coworkers.²³³ With increasing bulk reduction of the crystal, the photochemical activity on the reduced

surface was severely diminished. Thus, they suggested that O_v 's could quench photo-oxidation. They also found that the efficiency of formate production on a highly reduced surface was about four times smaller than on one with similar bulk reduction but containing surface O adatoms, indicating that the efficiency of photo-oxidation of CH_2O to produce formate on $r-TiO_2(110)$ was strongly dependent on the degree of reduction of the surface and near-surface region.

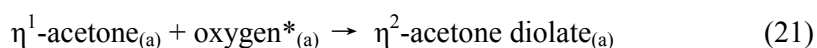
7.2 Ketones on $r-TiO_2(110)$

7.2.1 Acetone on $r-TiO_2(110)$

The adsorption of acetone, the simplest ketone, on $r-TiO_2(110)$ has been studied using TPD and EELS in combination by Henderson.^{167, 247-249} On the reduced surface with 7% ML O_v , submonolayer acetone bound molecularly in an η^1 configuration via the donation of the lone pair electrons of the carbonyl oxygen to the empty 3d states of Ti_{5c} . The desorption temperature shifted from 345 K at low coverage to 175 K at around 1 ML due to the strong intramolecular repulsion. Moreover, Henderson found no evidence for preferential binding at the O_v 's, which are usually the favorite adsorption sites for many adsorbates.¹² Exposure of $r-TiO_2(110)$ surfaces to molecular O_2 prior to acetone significantly affected the adsorption behavior of acetone. A small fraction of the adsorbed acetone underwent irreversible dissociation. Concomitantly, 0.25 ML acetone was stabilized until 375 K. This desorption state was assigned to an η^2 configuration acetone-oxygen complex according to the oxygen isotope-labeled TPD experiments and the 1425 cm^{-1} feature in the HREELS. The additional oxygens in the acetone-oxygen complex were most likely the reactive oxygen adatoms at the Ti_{5c} sites which stem from the dissociation of molecular oxygen at O_v 's^{73, 117} and/or Ti_{5c} sites.^{81, 83} The formation of η^2 acetone-oxygen complex was consistent with

STM^{250, 251} and DFT studies.²⁵²

The photochemistry of acetone on r-TiO₂(110) surface has been investigated systematically by Henderson and White *et al.*²⁵³⁻²⁵⁹ The η^1 bounded acetone was inert on r-TiO₂(110) when exposed to UV light, while the η^2 acetone-oxygen complex, i.e., the acetone diolate, was photoactive.²⁵³ Post-irradiation TPD results suggested acetone diolate was photocatalytically converted into acetate (Fig. 25A). PSD measurements in Fig. 25B clearly revealed the ejection of methyl radical. The methyl signal showed a spike when the acetone covered TiO₂(110) was initially exposed to the UV light in O₂ background. Despite the quick shrink in the first five seconds, methyl signal did not vanish during the whole UV irradiation period (300 s). The author attributed the difference in the reaction rate of acetone photooxidation to the availability of reactive oxygen species required for the production of acetone diolate. The generation of reactive oxygen species is associated with Ti³⁺. Henderson proposed the Ti³⁺ related to the fast process originated from the creation of O_v's, whereas those for the slow one were generated through trapping photoexcited electrons at surfaces. Henderson thus suggested a two-step reaction for the photooxidation of acetone on TiO₂ which could be described as follows:²⁵³



This two-step reaction involved a first thermal reaction of η^1 -acetone with reactive oxygen species to generate η^2 -acetone diolate which had a reaction barrier of about 10 kJ/mol, and a second photocatalytic decomposition of η^2 -acetone diolate into gas phase methyl radical and adsorbed acetate.

Followed by Henderson's finding of a fast and slow production of methyl radical

during the photooxidation of acetone on r-TiO₂(110), Wilson and coworkers measured the velocity distribution of ejected methyl radical directly using pulsed laser based TOF technique.²⁵⁸ As expected, they observed two components of the translation energy distribution with the average energies of 0.19 eV and 0.03 eV respectively (Fig. 26). By analogy with the dynamics of gas phase dissociative ionization of acetone, the authors suggested the hole mediated decomposition of the acetone diolate at the excited rather than ground state. Further state-resolved measurements of the CD₃ radical using (2+1) resonance enhanced multiphoton ionization (REMPI) by Kershis *et al.* revealed the production of both ground ($\nu = 0$) and excited ($\nu = 1$) vibrational state in the umbrella mode (Fig. 26).²⁵⁹ The ratio between the yield at $\nu = 0$ to that at $\nu = 1$ suggested a rather cold vibrational temperature of 151±15 K, indicating the existence of a late transition state during the photocatalytic decomposition of the acetone diolate. The mean translational energies in the fast methyl channel differ by 30 meV between $\nu = 0$ and $\nu = 1$ products, which is of the same order of magnitude but not equal to the vibrational level spacing of the umbrella mode (57 meV)²⁶⁰. Such a discrepancy indicated the substrate and/or other internal states might involve in the energy transfer process.

7.3 Other ketones on r-TiO₂(110) surface

Aside from acetone, the photochemistry of a series of other ketones, for example, butanone,²⁶¹⁻²⁶⁴ pinacolone,^{257, 265} halogen-substitute acetone,^{256, 257, 266, 267} acetyl chloride²⁵⁷ and acetophenone,^{31, 257} has also been investigated. Similar to acetone, the photodecomposition of these ketones could also be described as a two-step process illustrated in Fig. 27.²⁵⁷ The first step, a thermal conversion of the weakly bounded η^1 -ketone (R₁(CO)R₂) into strongly adsorbed η^2 -ketone diolate via the interaction with reactive oxygen species at the r-TiO₂(110) surface, was followed by the facile

photodecomposition of the η^2 -ketone diolate, ejecting a ligand radical into the vacuum and leaving a carboxylate species on the surface. In case of R_1 was not equal to R_2 , which ligand would be preferentially ejected? Experimental investigation by Henderson^{253, 257, 266, 267} together with theoretical analysis by Deskin *et al.*^{257, 266} and Wang *et al.*²⁵⁶ have provided a general rule for the bond cleavage in the photooxidation of ketones on r-TiO₂(110). Table 1 showed the experimentally observed products and the reaction energies for the photodecomposition of ketones in different pathways.²⁵⁷

Table 1. DFT calculated reaction energies for ejecting one of the ligands into vacuum as a radical when converting various carbonyl diolates into carboxylates on r-TiO₂(110).^a

Parent Carbonyl	Leaving Group	(kJ/mol)	Difference CH ₃ -R (kJ/mol)	Leaving Group	(kJ/mol)
Acetone	CH ₃	17			
Acetaldehyde	CH ₃	43	←21	H	64
2-Butanone	CH ₃	24	16→	CH ₂ CH ₃	8
Pinacolone ^a	CH ₃		? →	C(CH ₃) ₃	<<0
Acetophenone	CH ₃	-1	←39	C ₆ H ₅	38
Acetyl Chloride	CH ₃	10	53→	Cl	-43
1-Chloroacetone	CH ₃	41	51→	CH ₂ Cl	-10
1,1-Dichloroacetone	CH ₃	45	81→	CHCl ₂	-36

1,1,1-Trichloroacetone	CH ₃	-6	116→	CCl ₃	-122
1,1,1-Trifluoroacetone	CH ₃	26	50→	CF ₃	-24
Hexafluoroacetone	CF ₃	-65			

^a The middle column show the energy difference between the two different reaction pathways, with the arrow pointing towards the theoretically preferred product. Products in bold were detected experimentally. A bound state for the pinacolone diolate was not found with DFT. Modified with permission from Ref. 257. Copyright 2011 Elsevier.

For acetone, acetaldehyde, butanone, acetophenone, acetyl chloride, 1-chloroacetone and 1,1-dichloroacetone, the experimental observation agreed well with the DFT prediction. In these cases, weak C-R bond dissociated, suggesting the reaction was governed by thermodynamics. However, in the case of 1,1,1-trichloroacetone and 1,1,1-trifluoroacetone, besides the detection of CO which did not involve the diolate, both CH₃ and CX₃ (X=Cl, F) radicals were liberated through the photodecomposition of the diolate,²⁶⁶ which contradicted with the theoretical calculation that showed only CX₃ was produced. Given the discrepancy between experimental results and theoretical calculations, Henderson and coworkers proposed the dynamics of charge transfer in the heavy halogen substituted ketones might affect the reaction pathway. TOF measurements carried out by Wilson *et al.* showed the energy of the fast methyl ejection channel of photooxidation of CH₃COR (R=H, CH₃, CH₂CH₃ and C₆H₅) on r-TiO₂(110) increased with the weight of R ligand.²⁶⁸

8 Carboxylic Acids on Rutile and Anatase TiO₂ Surfaces

The adsorption and thermal chemistry of carboxylic acids on r-TiO₂(110) has been systematically reviewed by Pang *et al.*¹⁵ In general, carboxylic acids adsorbed dissociatively on TiO₂ surfaces, producing a surface hydroxyl and a η^2 -carboxylate bound to two adjacent Ti_{5c} ions. Such a strong binding structure facilitates the anchoring of organic functional groups onto TiO₂ surfaces, which could modify the structures and properties of interfaces, for example, in dye sensitized solar cells (DSSC's).²⁶⁹ For small R (R = H, CH₃, C(CH₃)₃) groups, a saturated carboxylic acid (RCOOH) coverage of ~ 0.5 ML resulted in an ordered (2 \times 1) overlayer.^{38, 270, 271}

Despite the above general rules, exceptions of carboxylic acid adsorption on TiO₂ surface have also been reported. Employing in-situ STM at 350 K, Aizawa and coworkers observed other two types of O_v involved adsorption of formate on r-TiO₂(110), i.e., monodentate formate resided in the O_v and bidentate formate with the two oxygen atoms filling the O_v and binding to an adjacent Ti_{5c} respectively.²⁴⁶ On r-TiO₂(011)-(2 \times 1) surface, Tao *et al.* reported the different adsorption dynamics of acetic acid from r-TiO₂(110) by means of TPD, UPS and STM.²⁷² At room temperature, acetic acid could not adsorb onto the surface until an O_v was encountered due to the severe steric hindrance on this surface. The pre-adsorbed acetic acid at O_v then facilitated the growth of a quasi one-dimensional structure. Based on the coverage of the adsorbed acetate molecule and the charge transfer between the adsorbate and substrate, the authors proposed a monodentate adsorption structure of acetate on the r-TiO₂(011). In a joint STM and HREELS study, Lyubinetsky and coworkers proposed a dynamical bonding of the dissociated acidic hydrogen to a pair of O_b's due to the electrostatic interaction with the trimethyl acetate (TMA) groups, leading to the invisibility of OH feature.²⁷³ Bidentate TMA binding to an O_v and a Ti_{5c} has also been reported by Lyubinetsky *et al.*²⁷⁴

In spite of the fact that formate was photo-inactive on r-TiO₂(110) even under UV irradiation, Ariga *et al.* provided the first evidence for visible light photocatalysis on pure TiO₂, using the formate/r-TiO₂(001) model system.²⁷⁵ Fig. 28 summarized their results: In the presence of O₂, surface hydroxyls were produced when the formate/TiO₂ surface was exposed to UV (a) or visible (b) light. Most interestingly, a photon energy threshold of 2.1-2.3 eV, which was significantly below the band gap of bulk rutile, was found for this photocatalytic reaction. Further EELS measurements confirmed the band gap narrowing which was attributed to the existence of low coordination atoms according to DFT calculations. Photoreaction of acetic acid on r-TiO₂(110) and (011) surfaces have also been investigated in Idriss's group.^{276, 277} Gas phase O₂ was indispensable in these reactions.

Although there were only a few studies concerning the photochemistry of formate and acetate on single crystal TiO₂ surfaces, the photodecomposition of TMA on r-TiO₂(110) has been extensively studied by Henderson and coworkers.^{38, 278-286} Upon UV irradiation of the TMA/r-TiO₂(110) interface at low temperature (<300 K), TMA species underwent a rapid hole mediated reaction to eject CO₂, leaving tert-butyl radicals on the surface. While heating to RT, tert-butyl radicals underwent thermal reaction to produce mainly isobutene along with some isobutane.²⁸⁷ EELS measurements suggested the photogenerated electrons were trapped at the surface.²⁷⁸ It was clear that carbon containing products of photodecomposition of TMA on r-TiO₂(110) were readily removed, thus this reaction provided a strategy to prepare hydroxylated TiO₂ with OH coverage up to 0.5 ML.³⁸ The difficulty of this method was the relatively low vapor pressure of TMAA (~0.5 torr at RT) which lead to a long dosing time. A combined STM, EELS and DFT study by Wang *et al.* revealed that the photodecomposition of TMA on r-TiO₂(110) occurred exclusively at Ti_{5c} sites,

providing a site-specific understanding of this model reaction.²⁸⁶ The authors proposed that the localized excess electrons around O_v 's quenched the photogenerated holes effectively, screening the TMA species at the O_v sites (Fig. 29).

Photodecomposition of TMA on a-TiO₂(001) surfaces were also investigated. Owing to the lack of high quality anatase single crystals, Ohsawa *et al.* prepared a-TiO₂(001) films using molecular beam epitaxy (MBE) technique and studied the photolysis of TMA on this film.²⁸³ They found both the reaction mechanism and reaction rate on a-TiO₂(001) were similar to those on r-TiO₂(110). Photodecomposition of TMA has been chosen to explore the effect of TiO₂ crystallography and orientation on the photoreactivity by Ohsawa and coworkers.²⁸⁴²⁸⁵ The N doped TiO₂ (Ti_{2-x}N_x, x≤0.2) films were prepared by MBE growth. By measuring the reaction kinetics, the authors proposed the N sites were effective hole trapping sites in r-TiO₂(110), while this function of doped N in a-TiO₂(001) became negligible.²⁸⁴ In Ref. 285, Ohsawa *et al.* suggested the hole trapping ability of doped N in r-TiO₂(100) was more transient compared to those in r-TiO₂(110) and r-TiO₂(001).

9 Challenges

As an ideal model of semiconductor photocatalyst, TiO₂ has been widely investigated because of its relatively efficient photoactivity, high chemical stability, low cost, as well as its low toxicity for both humans and the environment. Unfortunately, the ζ parameter (defined as the rate of the formation of reaction products divided by the incident photon flow)⁶¹ of TiO₂ catalysts is usually rather small. In fact, time-resolved spectroscopic studies demonstrate that most of the photogenerated electron-hole pairs (~90%) recombine rapidly after excitation. This is

proposed to be one main reason for the relatively low ζ (<10%) for TiO₂-based photocatalytic reactions.⁶¹

A variety of approaches have been proposed to promote the efficiency of charge separation in TiO₂, including heterojunctions, cocatalysts (such as metal, metal oxide, hydroxide, sulfide) and bulk dopants (i.e., metal, carbon, nitrogen). The metal doping in TiO₂ can redshift the threshold of the TiO₂ absorption into the visible light region (decrease the band gap energy of TiO₂) and enhance the efficiency of charge separation.²⁸⁸ For example, Grätzel *et al.*²⁸⁹ found that the quantum yield of H₂ generation in the overall water splitting reaction can be achieved to ~30% at 310 nm by using a bifunctional colloidal TiO₂ loaded with Pt and RuO₂. In this system, Pt is the H₂ evolution site, while RuO₂ is the O₂ evolution site. In a recent review, Li and coworkers⁸ have presented the perspectives of TiO₂-based photocatalysts for production of hydrogen by biomass conversion and water splitting as well as generation of carbon-based chemical fuels by photo-reduction of CO₂, and the plausible mechanisms of H₂O splitting and CO₂ reduction have also been summarized.

In addition to the metal doping methods, the synergistic effect of the localized surface plasmon resonance (SPR) absorption by metal nanoparticles loading has been considered to be another promising approach for the enhancement of photocatalytic activity of TiO₂ photocatalysts. Whereas, despite lots of exciting results,²⁹⁰⁻²⁹⁷ the exact mechanisms responsible for SPR-enhanced photocatalysis remains unclear. For instance, Han and coworkers²⁹¹ has reported that the rate of hydrogen generation under visible light irradiation using the Janus Au-TiO₂ photocatalysts with 70 nm Au nanoparticles is higher than that with 30 nm Au nanoparticles. Based on a series of results, these authors proposed that the efficient visible-light hydrogen generation

with Janus Au-TiO₂ photocatalysts is due to the enhanced optical absorption of TiO₂ itself caused by the strong SPR-enhanced electromagnetic (EM) fields close to the Au-TiO₂ interface, leading to enhanced electron-hole pairs generation. Meanwhile, Silva and coworkers²⁹⁰ have shown that Au-TiO₂ with 1.87 nm Au nanoparticles has the best activity for hydrogen generation, and these authors claimed that the injection of photo-induced hot electrons from Au nanoparticles to the conduction band of TiO₂ plays a key role in the enhanced photocatalytic activity. Obviously, such a controversial understanding of the role of plasmonic metals impedes the development of new photocatalytic materials for efficient visible-light-driven H₂O reduction to produce H₂.

For these real catalytic systems, many elementary reactions are involved, and it is a big challenge to identify all elementary reaction steps and related active sites. Furthermore, electron and energy transfers occur in reactions simultaneously, whereas, the concept that reactions are promoted by separated holes and electrons transfer is usually over-emphasized, while the dynamics of electron transfer and the energy transfer process in photocatalysis is rarely investigated in literatures. Thus, in addition to investigation of the elementary reaction steps of these real catalytic systems experimentally, development of theoretical understanding of photocatalytic processes at the most fundamental level from the dynamics point of view is also quite important. In the previous published works,^{176, 210, 298-300} one surprising fact is that certain well controlled experimental results obtained are not fully consistent with the well accepted photocatalysis model based on the concept that electrons and holes are the driving force.⁴ For example, methanol can be photocatalyzed on *r*-TiO₂(110) at 400 nm while water cannot at the exactly same wavelength,¹⁷⁶ as well as the strong photon energy dependence of methanol and water photocatalysis on *r*-TiO₂(110).²¹⁰ It is

therefore fair to question whether this traditional photocatalysis model is only the good model to explain all heterogeneous photocatalytic processes. From the dynamics point of view, the traditional photocatalysis model is essentially a model that is based on excited state reactions where electron and holes are separated (Fig. 30). We have proposed a new model (Fig. 30) based on nonadiabatic dynamics and ground state surface reactions, which can qualitatively explain some recent experimental results for the photocatalysis of water and methanol on r-TiO₂(110). This new model described the importance of the surface dynamics in photocatalysis. However, our model is proposed based on studies of photocatalysis of methanol and water on TiO₂ under vacuum conditions. However, whether this model is applicable in other photocatalysis systems needs to be further tested with well controlled photocatalysis experiments in the future. In addition, theoretical studies of surface nonadiabatic processes and surface reaction dynamics are also urgently needed in order to gain clear and fundamental insights into the photocatalysis processes.

10 Concluding Remarks

In this review, we have summarized recent progress made in the study of elementary processes in photocatalysis of several organic and inorganic molecules on TiO₂ surfaces. The photochemical products, reaction pathways and chemical kinetics obtained through site-specific STM imaging and/or ensemble-averaging desorption/photonic/electronic spectroscopy contributed significantly to our knowledge of TiO₂ heterogeneous photocatalysis. The reaction sites, pathways and kinetics clearly provided clues for analyzing the charge transfer process. Despite the achievements made in photocatalytic chemistry on TiO₂ surfaces, more investigations are still required in order to understand the dynamics of photocatalytic reactions on surfaces at the most fundamental level.

Measuring the reaction and interfacial charge transfer dynamics is always challenging. Thus far, the photochemistry on TiO₂ surfaces was monitored in minute, second and even millisecond time scales. These macroscopic kinetics measurements definitely helped us to understand the macroscopic pictures of photochemical reaction processes. However, it would be hard to derive the microscopic dynamical picture of photocatalytic processes just from these macroscopic measurements. Studies of ultrafast dynamics on these surfaces would certainly help us to understand better the microscopic photocatalytic dynamics on these surfaces.

Direct detection of the transition state is considered as a Holy Grail in chemistry research, even though detecting transition states on surface reactions is extremely challenging. Development of new techniques, such as free electron lasers (FEL), provides great opportunities in this area. Recently breakthroughs have been made in the detection of chemical bonds cleavage and construction on metal surfaces. By using femtosecond time-resolved X-ray absorption and emission spectroscopy (XAS and XES), Nilsson *et al* observed the first bond cleavage and construction on surfaces in the studies of CO desorption from Ru(0001)³⁰¹ and CO interaction with O on the same surface,³⁰² respectively. However, the direct detection of transition states in photocatalytic chemistry hasn't been reported thus far, investigation of the femtosecond time evolution of the valence structure of adsorbates in photocatalytic systems by using time-resolved photoelectron spectroscopy (e.g., ultraviolet photoelectron spectroscopy realized by FEL or high order harmonic generation in the extremely ultraviolet/soft X-ray regime) might bring breakthroughs in this direction. Femtosecond time-resolved UV pump and IR/sum frequency generation (SFG) probe is also a promising method to study the ultrafast dynamics which could provide important insights into the reaction mechanism.

Although ultrafast electron transfer from the excited dye molecules and quantum dots to the TiO₂ acceptor have been directly monitored,^{303,304} studies on photoexcited charge transfer from TiO₂ single crystals to adsorbates are still rare. Future work making use of 2PPE could help us understanding the mechanism of charge transfer from the substrate to adsorbates. The electronic structure of TiO₂ substrate, the adsorbate and the matching between them are crucial to the charge transfer. Hot photoexcited charge carriers were regarded to thermalize at an ultrafast time scale to the respective band edges, making the construction of specific TiO₂-adsorbate structures which facilitate even faster interfacial charge transfer a promising subject. The use of ultrafast techniques would certainly help us to understand better these hot electron processes. Another strategy for making good use of the photon energy is the multi-exciton generation (MEG) which has been realized in quantum dots and nanocrystals.³⁰⁵⁻³⁰⁷

The existence of surface faces and surface state make the surface different from the bulk, introducing distinct chemical and photochemical properties. For example, Tao *et al.*³⁰⁸ prepared a new two-dimensional phase which introduced a surface state of Ti4sp character in the band gap by annealing the r-TiO₂(011)-(2×1) surface in oxygen background. Such a surface state successfully closed the band gap to 2.1 eV, a step towards visible light photocatalysis. Another example for surface mediated visible light photocatalysis on pure TiO₂ was provided by Ariga and co-workers.²⁷⁵ The nanostructured r-TiO₂(001) surface layer had a surface band gap which was significantly smaller than the bulk, this smaller surface band gap facilitates the photooxidation of formate under visible light irradiation. Latest works in our laboratory showed that the previously reported excited state which was located at 2.4 eV above E_F at r-TiO₂(110) interface was actually an intrinsic state of Ti³⁺ rather than

adsorbate induced. Similarly to the well-studied gap state at ~ 1.0 eV below E_F , this excited state was found to come from the Jahn-Teller induced splitting of the $3d-t_{2g}$ orbitals of Ti^{3+} ions in reduced TiO_2 . This state could be accessed via $3d \rightarrow 3d$ transitions from the gap state and contributed significantly to the photoabsorption of TiO_2 (Figure 31).³⁰⁹ Though the lifetime of this excited was less than 20 fs, the possibility of interfacial charge transfer via this state still could not be ruled out. This localized excitation will extend the photoabsorption to the visible range, consistent with the observed enhancement of the photocatalytic activity of TiO_2 under visible light irradiation through Ti^{3+} self-doping.^{194, 310-313}

Surface orientation also has a significant effect on the photoactivity of TiO_2 .³¹⁴ Synthesizing TiO_2 with specific facets and constructing TiO_2 heterojunctions that exhibit distinct properties at different facets has become a promising field.^{203, 315-317} Besides the surface atomic configuration, electronic structure and energetics, the anisotropic charge carrier transportation, trapping, detrapping and transfer should also be taken into account to understand the orientation dependence of the photoactivity of TiO_2 .^{318, 319} In addition, the exact role (e.g., reaction sites and charge separation) of co-catalyst such as Pt in the photoactivity of TiO_2 should also be investigated closely. Furthermore, photocatalysis studied under high pressure and in solution using photon-in and photon-out techniques such as surface sensitive second harmonic generation (SHG), SFG and X-ray absorption spectroscopy (XAS) are also desirable.

Acknowledgement

We acknowledge the financial support from the National Natural Science Foundation of China (Grant No. 21203189, 21321091, 21173212, 21403224 and

21322310), National Basic Research Program of China (Grant No. 2013CB834605), the Key Research Program of the Chinese Academy of Science (KGZD-EW-T05) and the State Key Laboratory of Molecular Reaction Dynamics (ZZ-2014-02).

Biographical Information

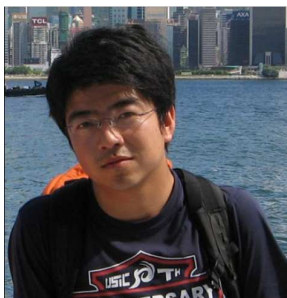


Qing Guo received his B. S. degree in chemical physics from University of Science and Technology of China (USTC) in 2007, and Ph. D. from State Key Laboratory of Molecular Reaction Dynamics, Dalian Institute of Chemical Physics, CAS in 2013 under the supervision of Prof. Xueming Yang. He is now an assistant research fellow at the State Key Laboratory of Molecular Reaction Dynamics. His current research is focused on the dynamic/mechanistic aspects of photocatalytic reactions on model semiconductor photocatalysts.



Chuanyao Zhou received his B. S. degree in chemical physics from University of Science and Technology of China (USTC) in 2005, and Ph. D. from State Key Laboratory of Molecular Reaction Dynamics, Dalian Institute of Chemical Physics, CAS in 2011 under the supervision of Prof. Xueming Yang. He is now an associated professor at the State Key Laboratory of Molecular Reaction Dynamics. His present

research interests are in the area of surface chemistry and photochemistry, especially the ultrafast electron spectroscopic study of photocatalysis.



Zhibo Ma graduated from University of Science and Technology of China in 2006. He then studied with Prof. Xueming Yang at Dalian Institute of Chemical Physics, Chinese Academy of Sciences, working on two-photon photoemission spectroscopy and Scanning Tunneling Microscope. He obtained his Ph. D. in 2012 and worked as an assistant research fellow. His research focuses on the dynamical information of photo-reaction on metal oxide in real-space, photoelectric conversion of dye molecules on TiO_2 and the growth and chemical property of two-dimensional (2D) materials.



Zefeng Ren was born in 1981 in Jiangsu, China, and received his B.S. degree in University of Science and Technology of China in 2004 and his Ph. D. in physical chemistry under the supervision of Prof. Xueming Yang in Dalian Institute of Chemical Physics, CAS in 2009. After postdoctoral works with Prof. Martin Wolf in Fritz Haber Institute of Max Planck Society in Berlin, he became an associate

professor in Peking University in 2011. His present research interest is in the area of surface chemistry and ultrafast surface dynamics using surface nonlinear spectroscopy.



Hongjun Fan received his BS degree in Chemistry from Zhejiang University in 1994, MS degree in Physical Chemistry from Fujian Institute of Research on the Structure of Matter in 1997, and Ph. D. in Chemistry from the University of Siegen (Germany) in 2004. He did postdoctoral research at Indiana University Bloomington from 2005 to 2009, and joined the Dalian Institute of Chemical Physics in 2009 as a member of the Chinese Academy of Science “100 Talent Program”. From 2009 he worked in State Key Laboratory of Molecular Reaction Dynamics, in the field of photochemistry, heterogeneous and homogeneous catalysis.



Xueming Yang obtained his Ph. D. in chemistry at University of California at Santa Barbara in 1991. After spending four years at Princeton and Berkeley as a postdoc, he became an associate research fellow at the Institute of Atomic and Molecular Sciences,

Academia in 1995, and was promoted to the rank of full research fellow with tenure in 2000. He moved to the Dalian Institute of Chemical Physics, Chinese Academy of Sciences in 2004. He is now a research fellow of the State Key Laboratory of Molecular Reaction Dynamics. His research interests focus mainly on gas-phase and surface reaction dynamics.

Figures and Captions

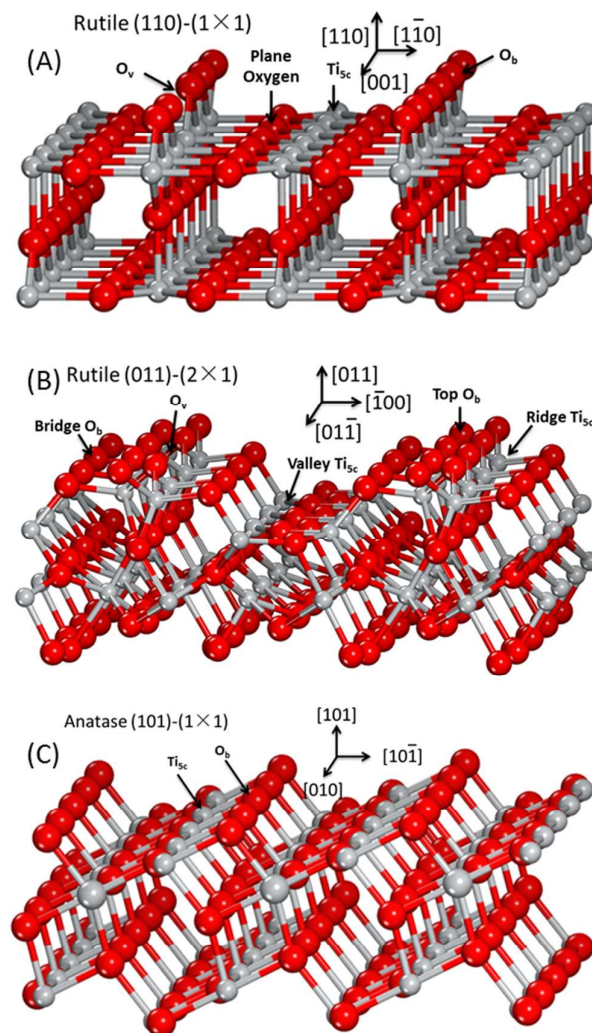


Fig. 1 Structure model of (A) rutile (110)-(1×1) (r-TiO₂(110)-(1×1)), (B) rutile (011)-(2×1) (r-TiO₂(011)-(2×1)) and (C) anatase (101)-(1×1) (a-TiO₂(101)-(1×1)). Red and grey balls stand for oxygen and titanium ions, respectively.

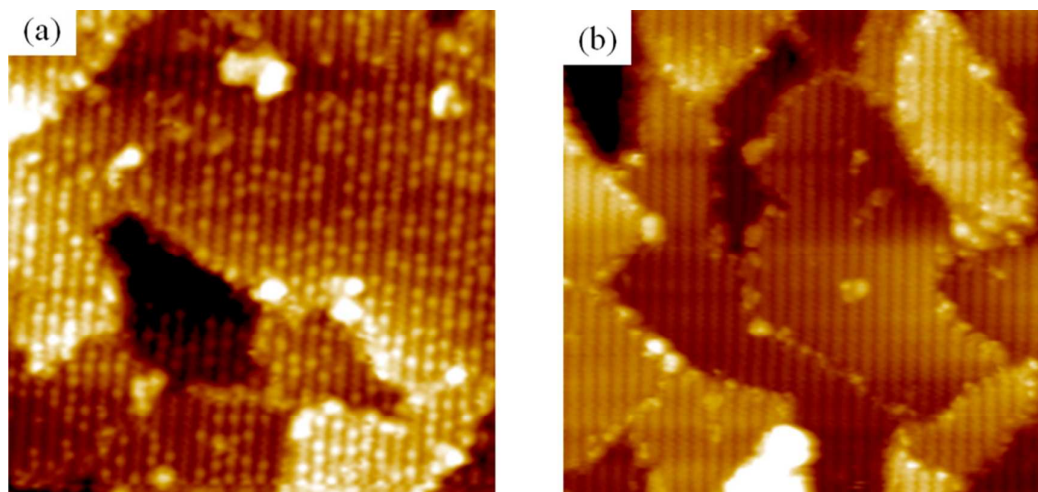


Fig. 2 STM images ($20 \times 20 \text{ nm}^2$) of a hydroxylated $r\text{-TiO}_2(011)\text{-}(2 \times 1)$ before (a) and after (b) 90-minute UV illumination in UHV at room temperature taken at $V=1.2 \text{ V}$ and $I=0.3 \text{ nA}$. Reproduced with permission from Ref. 42. Copyright 2012 American Chemical Society.

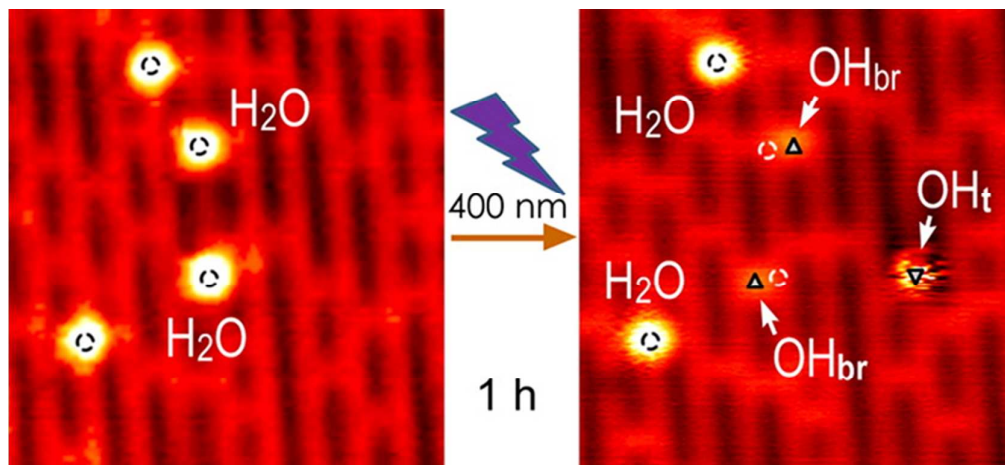


Fig. 3 STM images ($6.3 \times 6.6 \text{ nm}^2$, imaged at 1.0 V, 10 pA and 80 K) showing the photocatalyzed splitting of water on $r\text{-TiO}_2(110)$. (Black circles, adsorbed water at Ti_{5c} sites; white circle, sites for dissociated water; triangles, OH_b ; inverted triangles, OH_t) Modified with permission from Ref. 58. Copyright 2012 American Chemical Society.

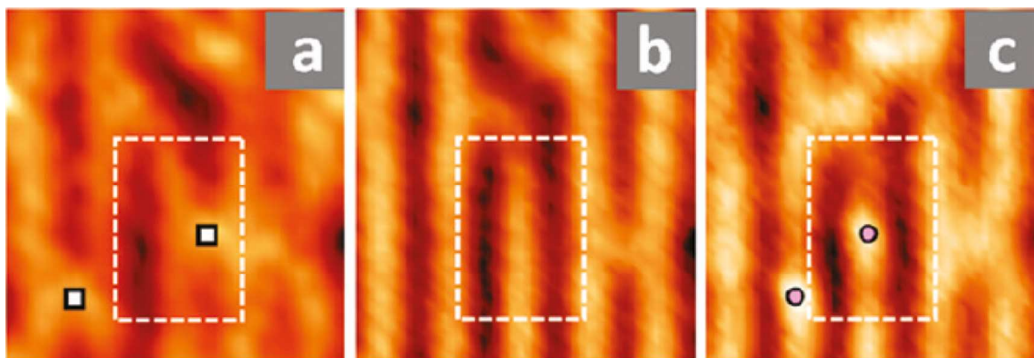
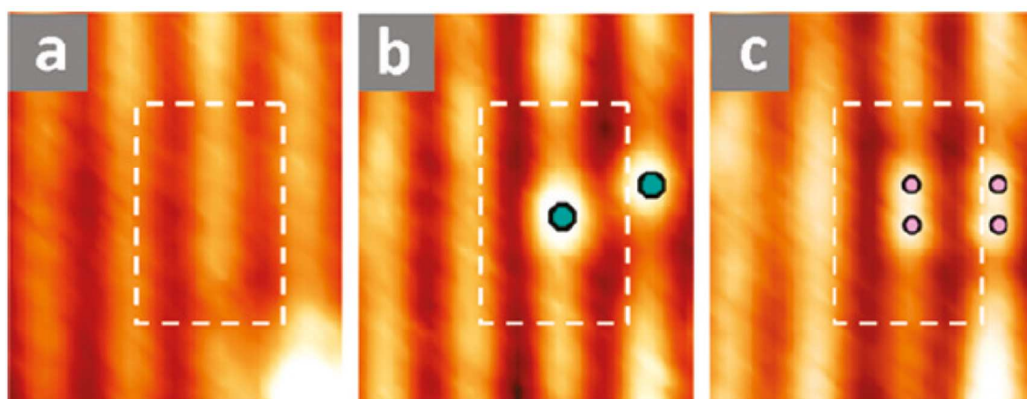
A. Tip induced dissociation of oxygen molecules at O_v B. Tip induced dissociation of oxygen molecules at Ti_{5c} 

Fig. 4 STM images showing the tip induced dissociation of oxygen molecules at O_v (A) and Ti_{5c} (B) sites respectively. a, b and c represent the $TiO_2(110)$ surface before, after O_2 exposure and after UV illumination. Modified with permission from Ref. 87. Copyright 2010 American Chemical Society.

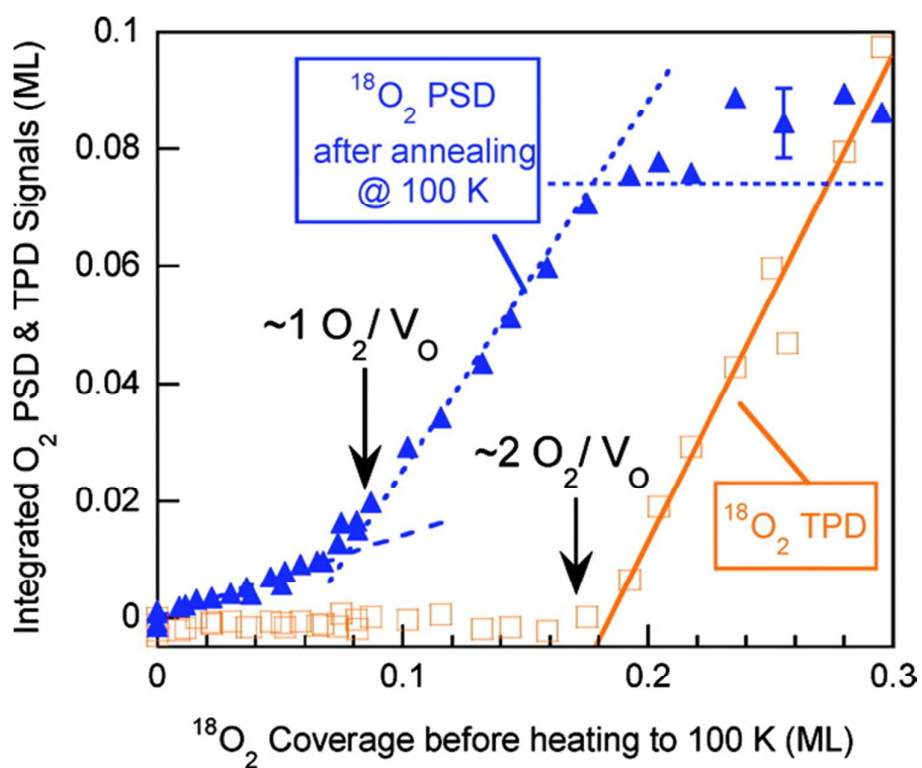


Fig. 5 ¹⁸O₂ PSD (blue) and TPD (orange) signal as a function of initial coverage. Reproduced with permission from Ref. 113. Copyright 2011 American Chemical Society.

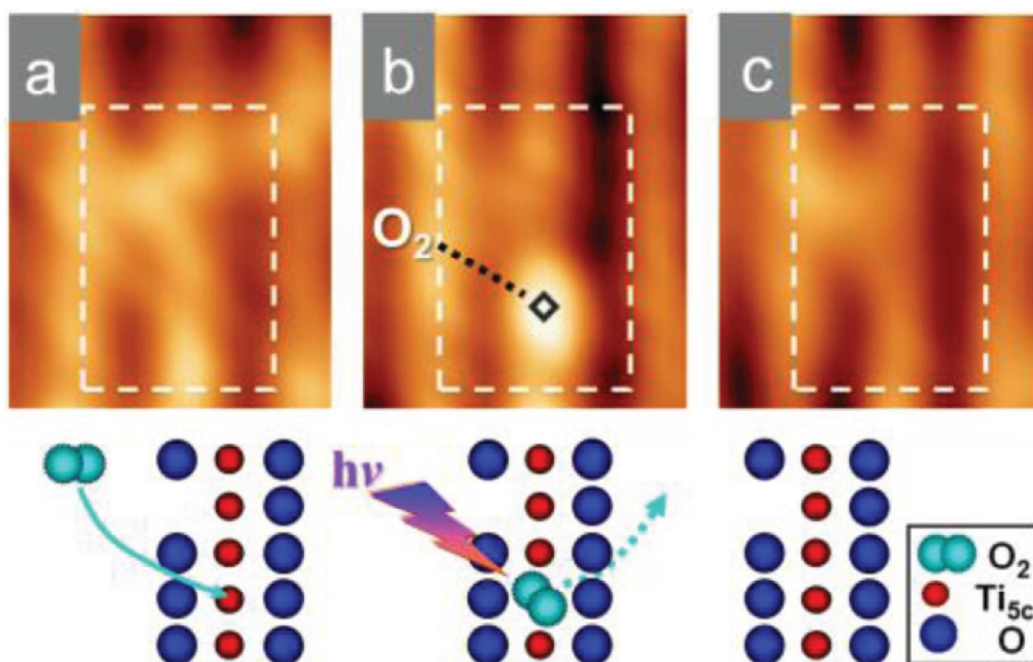
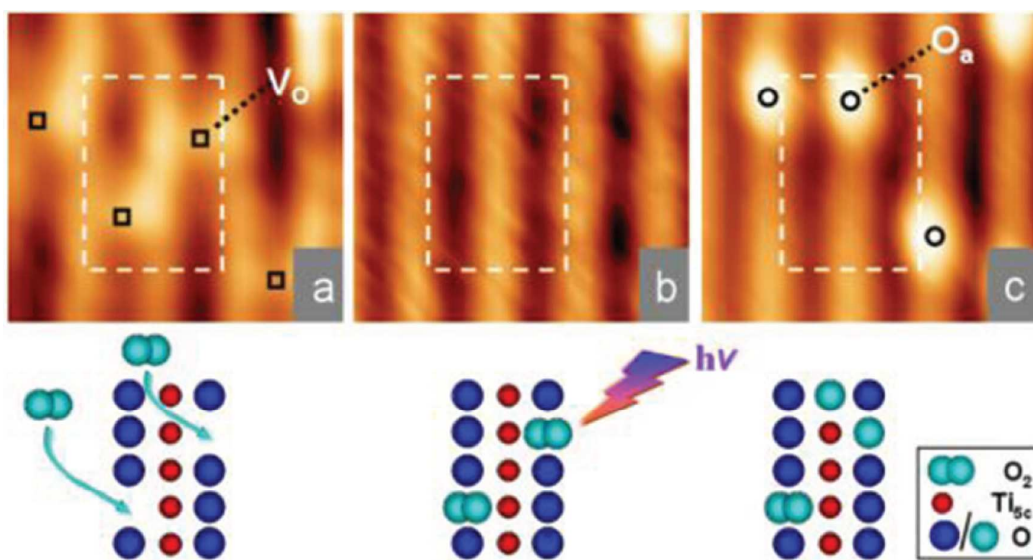
A. Photodesorption of oxygen at Ti_{5c} B. Photodissociation of oxygen at O_v 's

Fig. 6 STM images and cartoons showing the photodesorption of O_2 at Ti_{5c} sites (A) and photodissociation of O_2 at O_v 's (B). Modified with permission from Ref. 114. Copyright 2012 American Chemical Society.

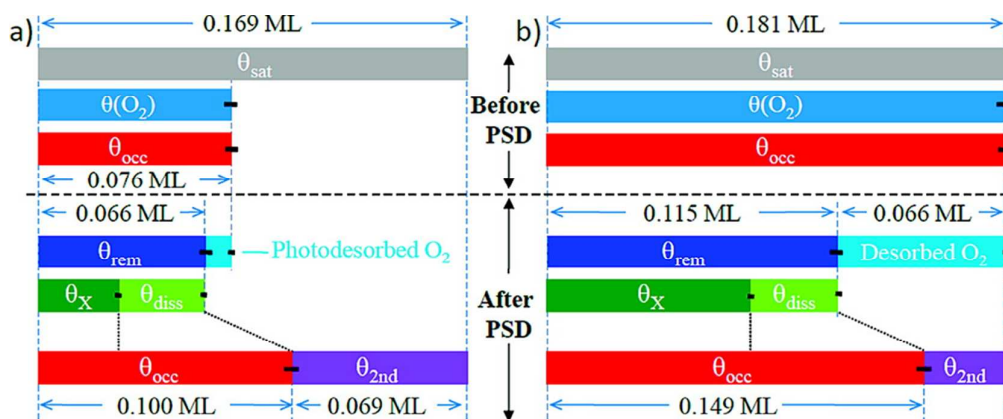


Fig. 7 The amount of adsorbed, photodesorbed, photodissociated and nondissociated O₂ before and after UV irradiation for (a) $\theta(O_2) = \theta(O_v)$ and (b) $\theta(O_2) = 2\theta(O_v)$. Reproduced with permission from Ref. 111. Copyright 2010 American Chemical Society.

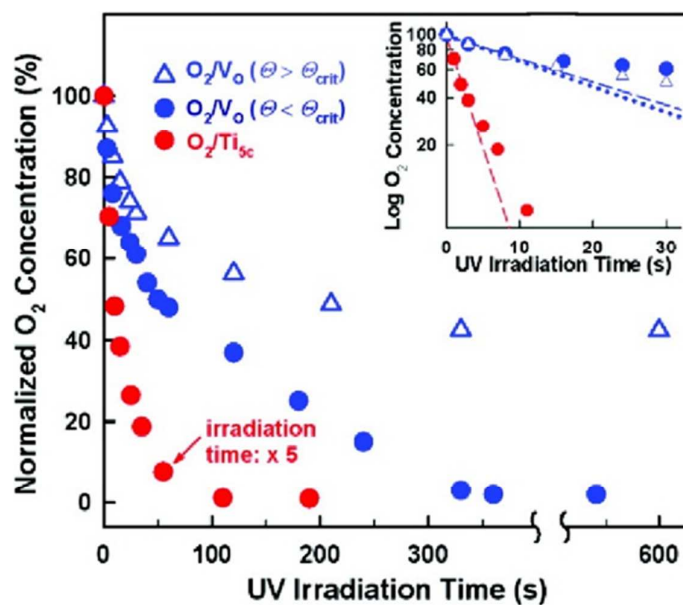


Fig. 8 Normalized UV irradiation time dependent amount of O₂ at O_v and Ti_{5c} sites. Inset graph shows the initial regions of the plot in a semilog scale. Reproduced with permission from Ref. 114. Copyright 2012 American Chemical Society.

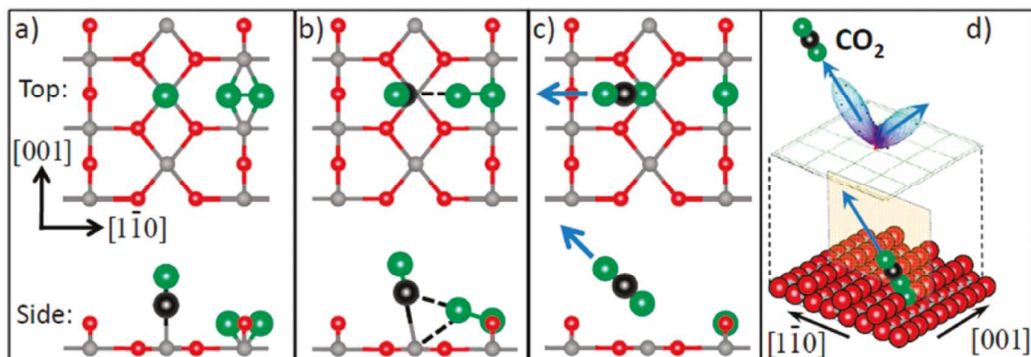


Fig. 9 Schematic showing the mechanism of photooxidation of CO on O_2 precovered $r\text{-TiO}_2(110)$. Reproduced with permission from Ref. 133. Copyright 2010 American Chemical Society.

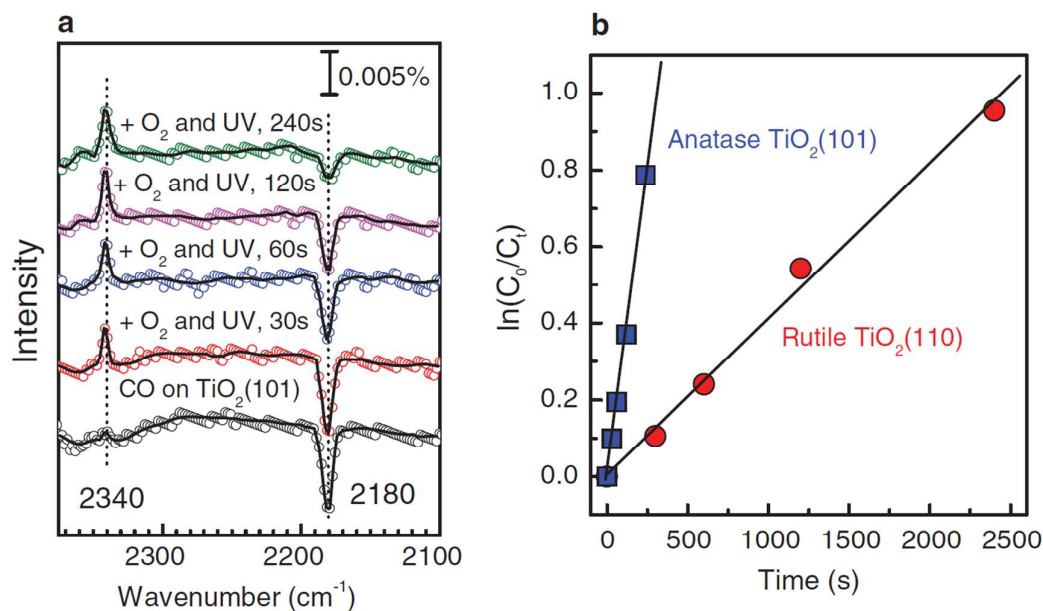


Fig. 10 (a) UV (3.4 eV) irradiation time dependent IRAS spectra for CO and CO_2 during the photooxidation of CO on $\text{a-TiO}_2(101)$ surface in the presence of O_2 . (b) Comparison of the cross section of photooxidation of CO on $\text{a-TiO}_2(101)$ and $\text{r-TiO}_2(110)$. Reproduced with permission from Ref. 138. Copyright 2011 American Physical Society.

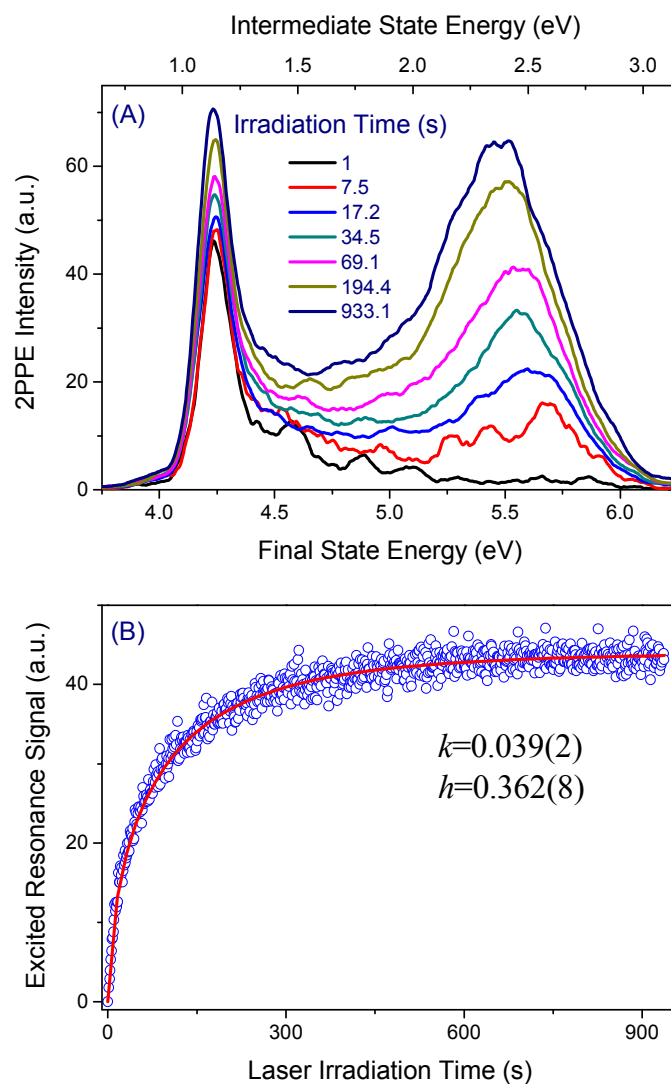


Fig. 11 (A) 2PPE spectra for CH₃OH adsorbed stoichiometric r-TiO₂(110) after the interface was exposed to the probe light for different periods. (B) Time-dependent excited resonance signal integrated from (A) and the fractal-like kinetics model fitting. Modified with permission from Ref. 163, 175. Copyright 2010, 2012 the Royal Society of Chemistry.

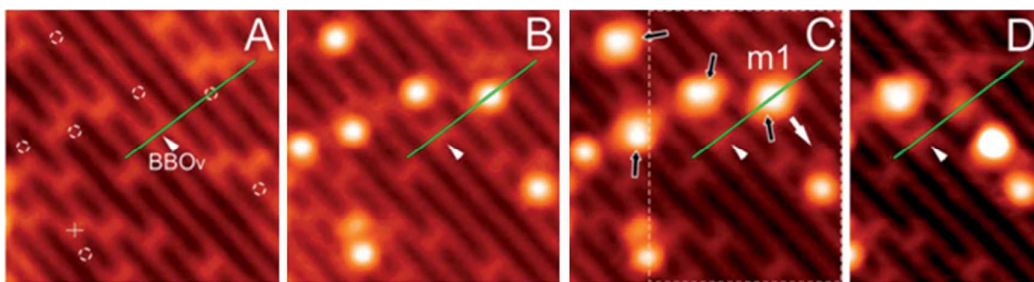


Fig. 12 STM images (acquired at bias of 1.0 V and set point current of 10 pA, size of $7.3 \times 7.3 \text{ nm}^2$) showing the photocatalyzed dissociation of methanol. (A) bare $\text{r-TiO}_2(110)\text{-}1 \times 1$ surface. (B) surface with adsorbed CH_3OH (0.02 ML). (C) after 10-minute irradiation by 400 nm light. Dashed circles in (A), sites for CH_3OH adsorption on Ti_{5c} row; Cross, sites for CH_3OH on O_v (labeled as BBO_v in the Figure). Black arrows in (C) indicate the four dissociated molecules after UV irradiation. (D) STM image after manipulation (0.4 V, 700 pA) of the dissociated molecule m1 in the marked area of (C). Modified with permission from Ref. 163. Copyright 2010 the Royal Society of Chemistry.

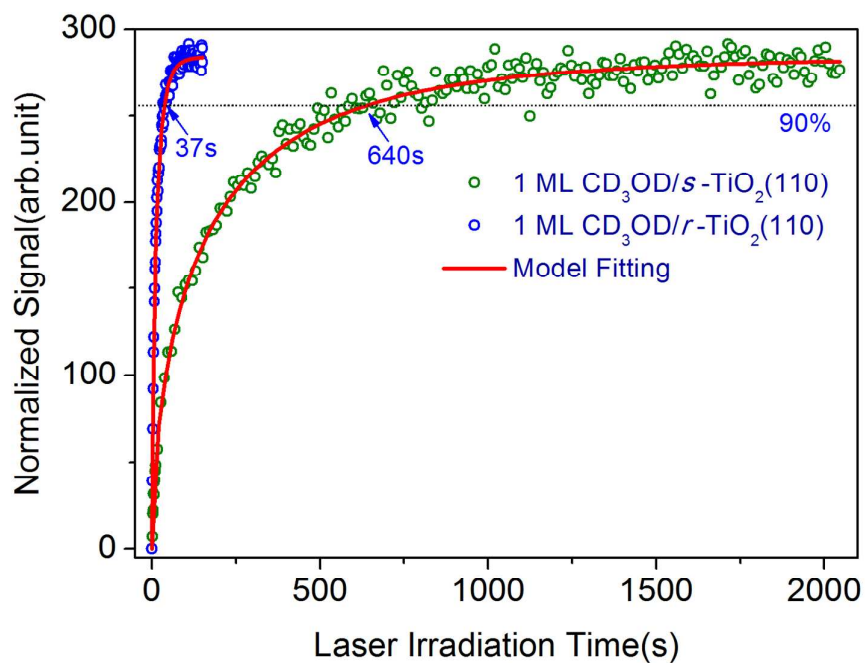


Fig. 13 Normalized time-dependent signal of the excited resonance of 0.77 ML CD₃OD covered stoichiometric (olive circle) and reduced (blue circle) r-TiO₂(110) surface and the fractal-like kinetics model fitting (red line). Reproduced with permission from Ref. 168. Copyright 2010 the Royal Society of Chemistry.

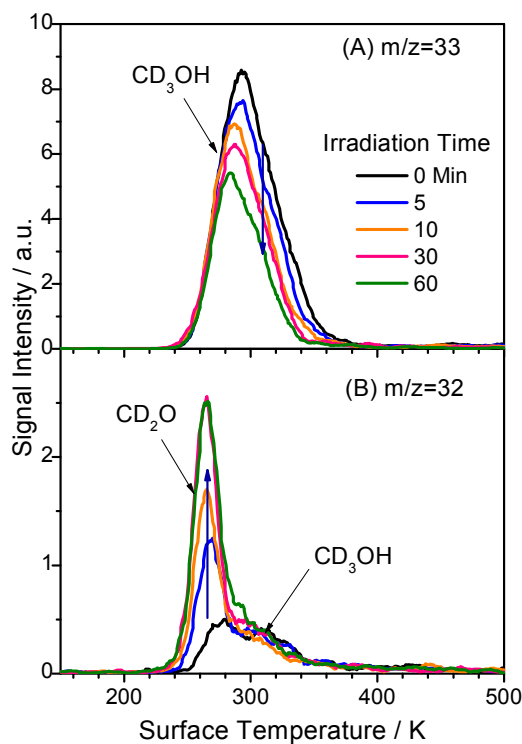


Fig. 14 (A) Typical TPD spectra collected at $m/z = 33$ (CD_2OH^+) after 0.5 ML CD_3OH was adsorbed on r- $TiO_2(110)$ at 110 K and irradiated at 400 nm for various times.. CD_2OH^+ is formed by dissociative ionization of the desorbed parent CD_3OH molecule in the electron-bombardment ionizer. (B) Typical TPD spectra collected at $m/z = 32$ (CD_2O^+) following different laser irradiation times. The $m/z = 32$ (CD_2O^+) signal has three components: the parent ion signal of formaldehyde (CD_2O), as well as the ion-fragment signals of the parent CD_3OH molecule and the photocatalyzed CD_3OD product. Reproduced with permission from Ref. 176. Copyright 2012 American Chemical Society.

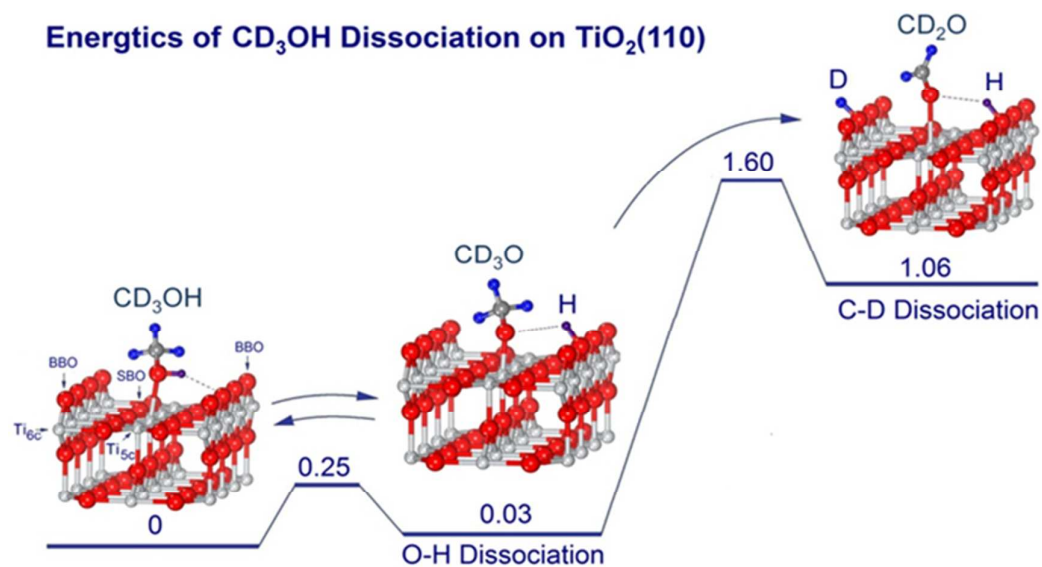


Fig. 15 Calculated energetics of the two-step dissociation of CD₃OH on the r-TiO₂(110) surface. The structures shown are simplified schematics. Modified with permission from Ref. 176. Copyright 2012 American Chemical Society.

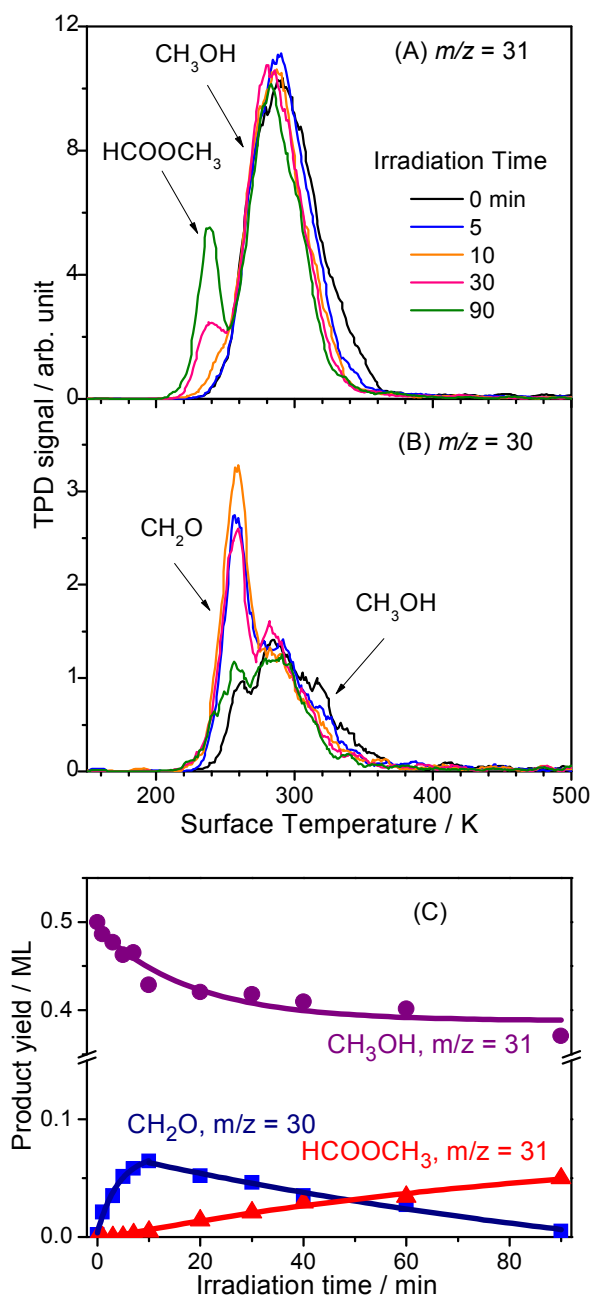


Fig. 16 (A) TPD spectra acquired at $m/z = 31$ (CH_3O^+) after 0.5 ML CH_3OH was adsorbed on $\text{r-TiO}_2(110)$ at 120 K and irradiated at 400 nm for various times. (B) TPD spectra acquired at 30 (CH_2O^+) after 0.5 ML CH_3OH was adsorbed on $\text{TiO}_2(110)$ at 120 K and irradiated at 400 nm for various times. (C) Yields of CH_3OH , CH_2O , and HCOOCH_3 as a function of irradiation time, derived from data in Fig. 16 (A) and (B). Modified with permission from Ref. 179. Copyright 2013 American Chemical Society.

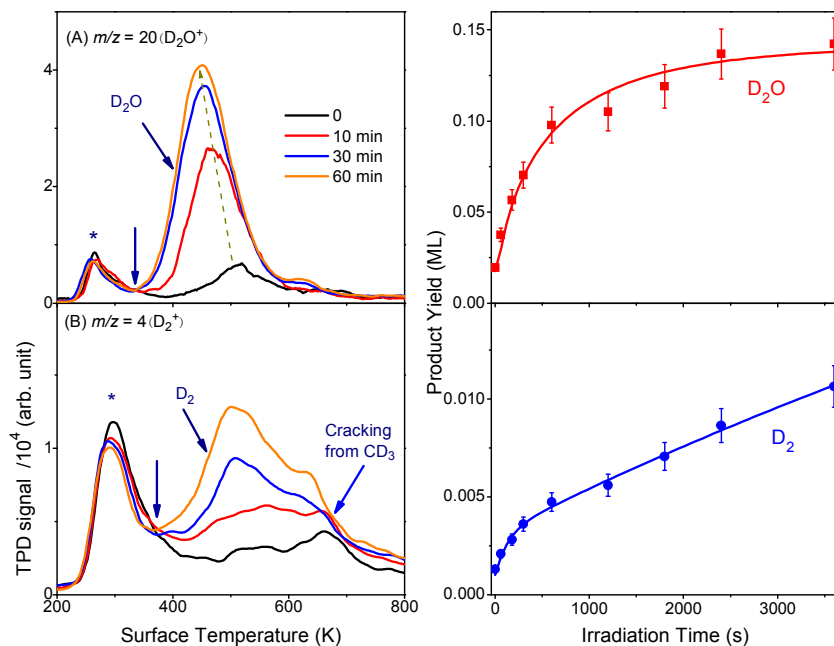


Fig. 17 (A) Typical TPD spectra collected at $m/z = 20$ (D_2O^+) after 0.5 ML CD_3OH was adsorbed on $r-TiO_2(110)$ at 100 K and irradiated at 400 nm for various times., the peak (marked with *) slightly below 300 K is attributed to the dissociative ionization signal of molecular adsorbed CD_3OD in the electron-impact ionizer and impurity of D_2O in CD_3OD . (B) Typical TPD spectra collected at $m/z = 4$ (D_2^+) following different laser irradiation times at 400 nm, the peak (marked with *) slightly below 300 K is attributed to the dissociative ionization signal of molecular adsorbed CD_3OD in the electron-impact ionizer. The right shows TPD product yield for D_2O and D_2 as a function of irradiation time, derived from data in Fig. 17 (A) and (B). Reproduced with permission from Ref. 45. Copyright 2013 American Chemical Society.

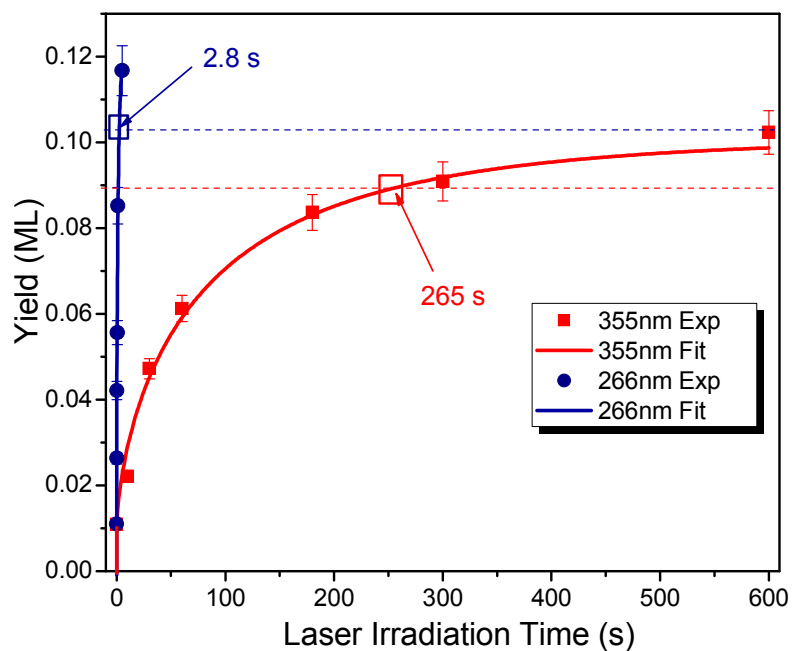


Fig. 18 The laser irradiation time dependence of the water yield at both 355 nm (red solid square) and 266 nm (blue solid circle) photolysis from a 0.5 ML methanol covered r-TiO₂(110) surface. The solid squares and circles are the experimental data (calibrated), while the solid lines are the fits using the fractal models described in the text. The unfilled squares indicate the rise times at 90% of the asymptotic values of the fits for both 355 nm and 266 nm photocatalysis. Reprinted with permission from Ref. 210. Copyright 2013 American Chemical Society.

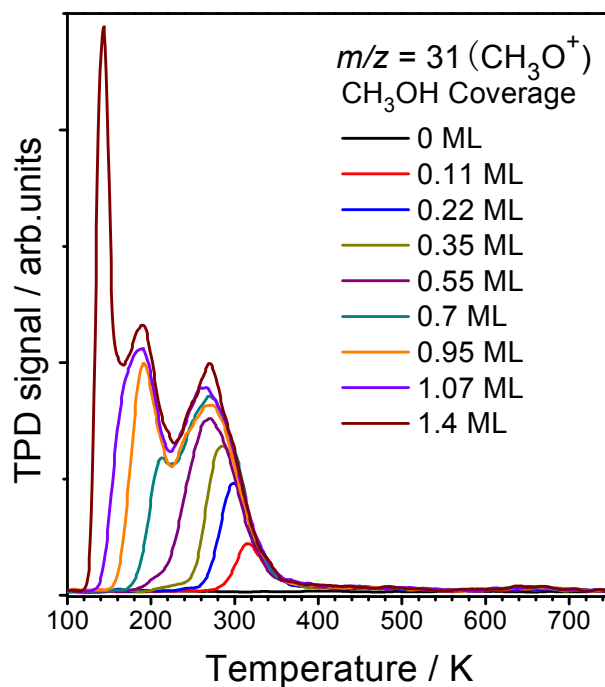


Fig. 19 CH_3OH TPD spectra ($m/z = 31$) spectra from various exposures of CH_3OH on the $\alpha\text{-TiO}_2(101)$ surface at 100 K. Reprinted with permission from Ref. 213. Copyright 2014 American Chemical Society.

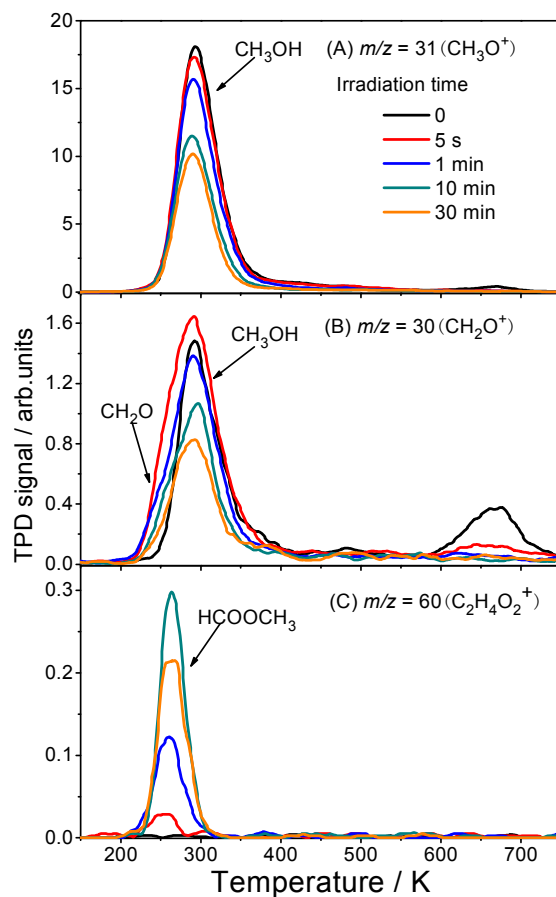


Fig. 20 0.38 ML of CH_3OH were dosed to the $\alpha\text{-TiO}_2(101)$ surfaces at 100 K. (A) Typical TPD spectra collected at $m/z = 31$ (CH_2OH^+) as a function of irradiation time with a photon flux of 1.9×10^{17} photons $\text{cm}^{-2} \text{s}^{-1}$. CH_2OH^+ is formed by dissociative ionization of the desorbed parent CH_3OH molecule in the electron-bombardment ionizer. (B) Typical TPD spectra collected at $m/z = 30$ (CH_2O^+) as a function of irradiation time. The $m/z = 30$ (CH_2O^+) signal has two components: the parent ion signal of formaldehyde (CH_2O), as well as the ion-fragment signals of the parent CH_3OH molecule. (C) Typical TPD spectra collected at $m/z = 60$ ($\text{C}_2\text{H}_4\text{O}_2^+$) as a function of irradiation time. The $m/z = 60$ ($\text{C}_2\text{H}_4\text{O}_2^+$) signal is from the parent ion signal of HCOOCH_3 molecule. Reprinted with permission from Ref. 213. Copyright 2014 American Chemical Society.

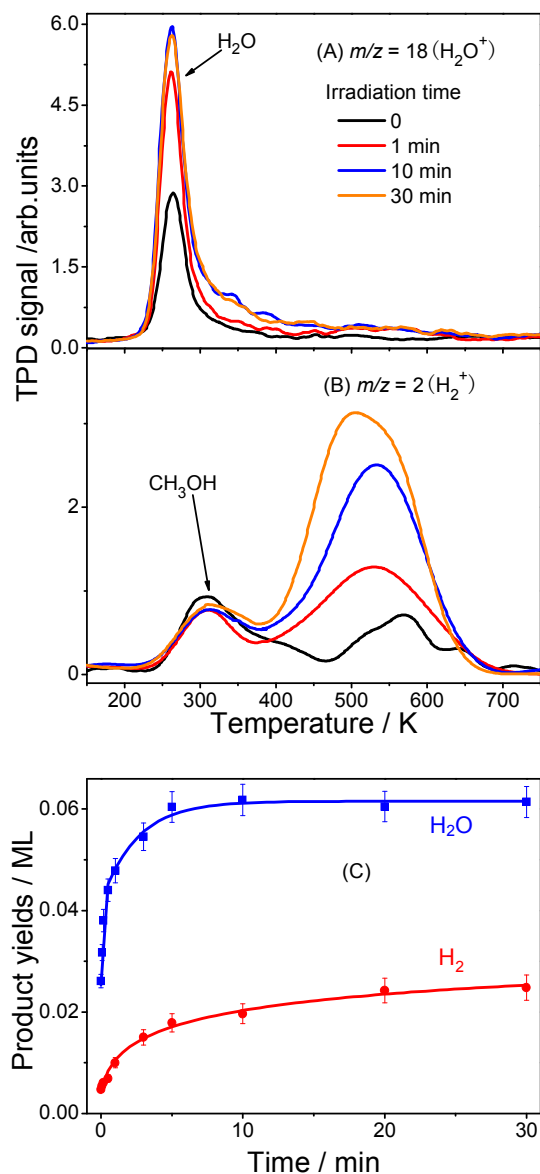


Fig. 21 TPD spectra collected at $m/z = 2$, and 18, from photocatalysis of 0.38 ML of CH_3OH covered $\alpha\text{-TiO}_2(101)$ at 100 K with a photon flux of 1.9×10^{17} photons $\text{cm}^{-2} \text{s}^{-1}$. Fig. 21(C) Yields of the molecular hydrogen (H_2), water (H_2O) TPD product as a function of laser irradiation time, derived from data in Fig. 21 (A) and (B). Reprinted with permission from Ref. 213. Copyright 2014 American Chemical Society.

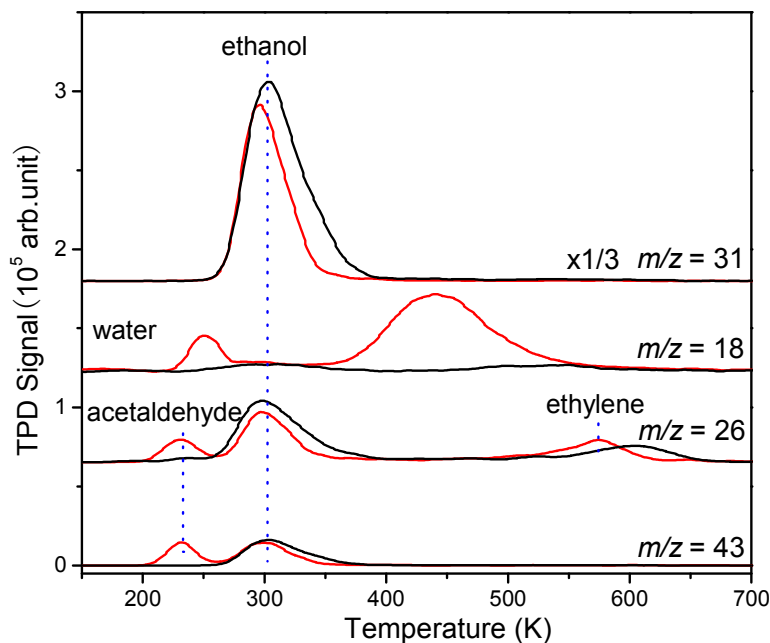


Fig. 22 Typical TPD spectrum after 0.35 ML ethanol covered r-TiO_2 (110) has been illuminated by laser light (400 nm, 460 mW) for 0 (black line) and 20 (red line) minutes. All the detectable products with a typical tracing mass to charge ratio are shown here. The profiles are offset vertically for clarity. Reprinted with permission from Ref. 217. Copyright 2013 American Chemical Society.

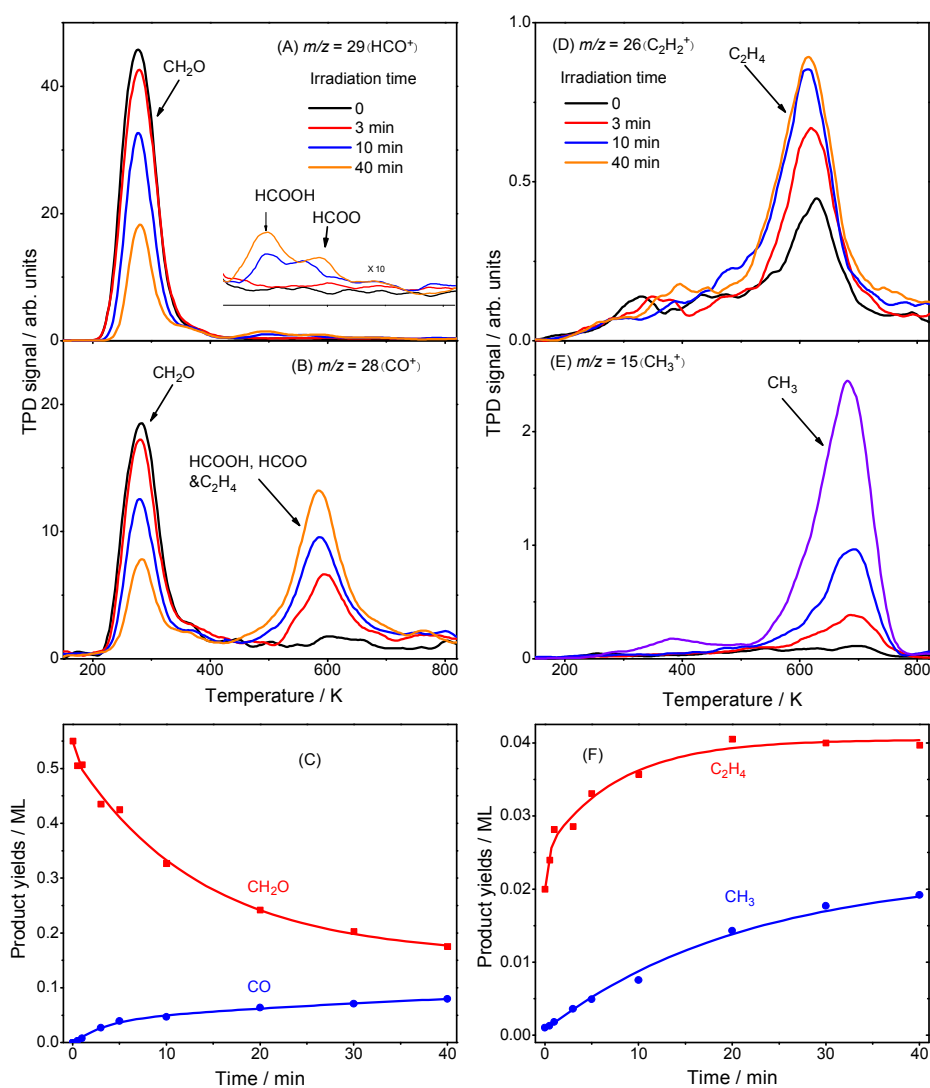


Fig. 23 Reduced r-TiO₂(110) was dosed with 0.55 ML of CH₂O at 110 K. (A) Typical TPD spectra collected at $m/z = 29$ (HCO^+) following different laser irradiation times. (B) Typical TPD spectra collected at $m/z = 28$ (C_2H_4^+ , CO^+) following different laser irradiation times. (C) Yields of CH₂O and CO (from formate) as a function of irradiation time, derived from data in Fig. 23 (A) and (B). The contribution of C₂H₄ has been subtracted. (D) Typical TPD spectra collected at $m/z = 26$ (C_2H_2^+) following different laser irradiation times. (E) Typical TPD spectra collected at $m/z = 15$ (CH_3^+) following different laser irradiation times. (F) Yields of C₂H₄ and CH₃ as a function of irradiation time, derived from data in Fig. 23 (D) and (E). Reproduced with permission from Ref. 233. Copyright 2013 American Chemical Society.

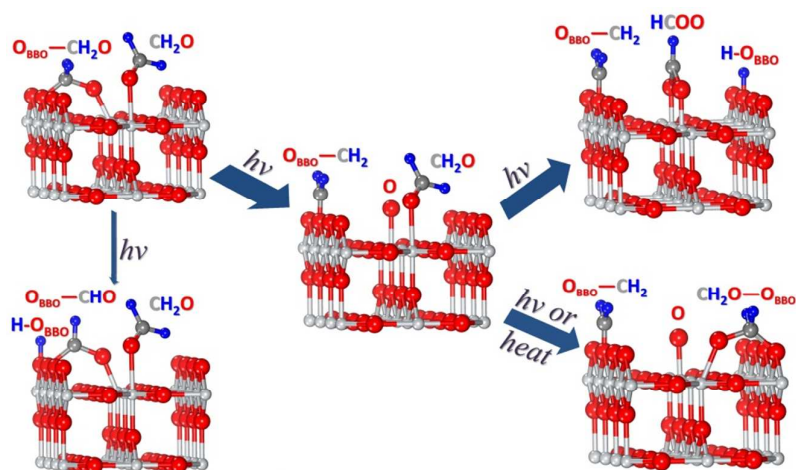


Fig. 24 Schematic model for bridging-oxygen-assisted, photo-induced decomposition of CH_2O on reduced $\text{r-TiO}_2(110)$. Reprinted with permission from Ref. 233. Copyright 2013 American Physical Society.

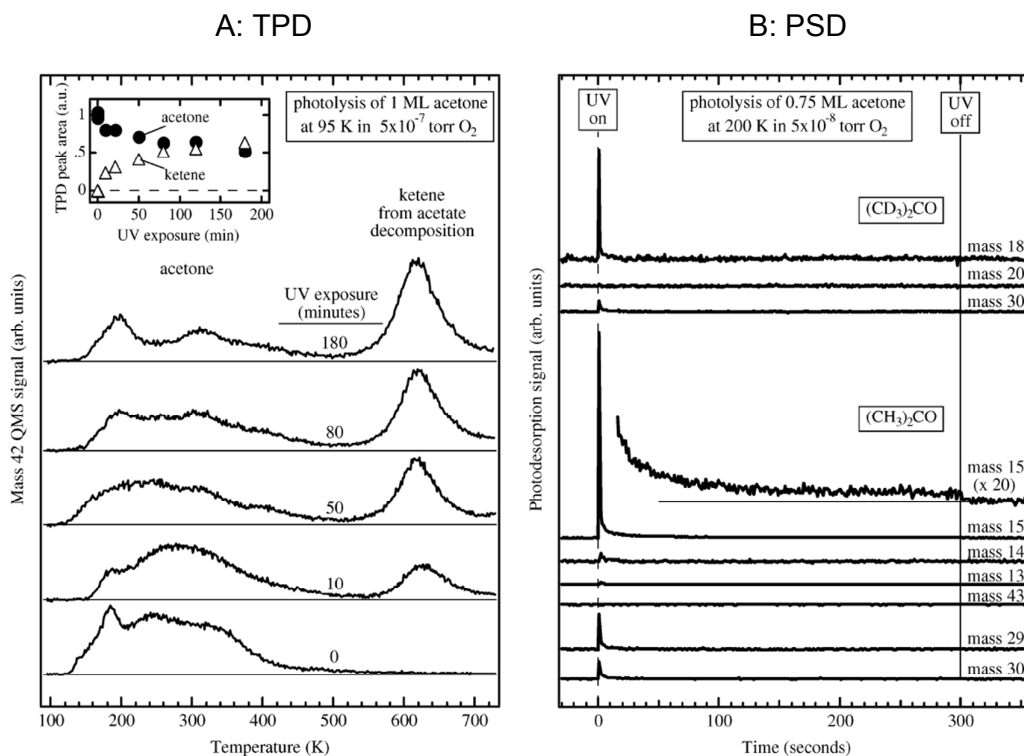


Fig. 25 (A) Postirradiation TPD spectra ($m/z = 42$) of 1 ML acetone on r-TiO₂(110) as a function of UV exposure in an oxygen background of 5×10^{-7} torr. (B) PSD spectra of various masses during the exposure of 0.75 ML acetone adsorbed r-TiO₂(110) which was held at 200 K to UV illumination in an oxygen background of 5×10^{-8} torr. Isotope labeled experiments clearly suggests the ejection of methyl radical. Modified with permission from Ref. 253. Copyright 2005 American Chemical Society.

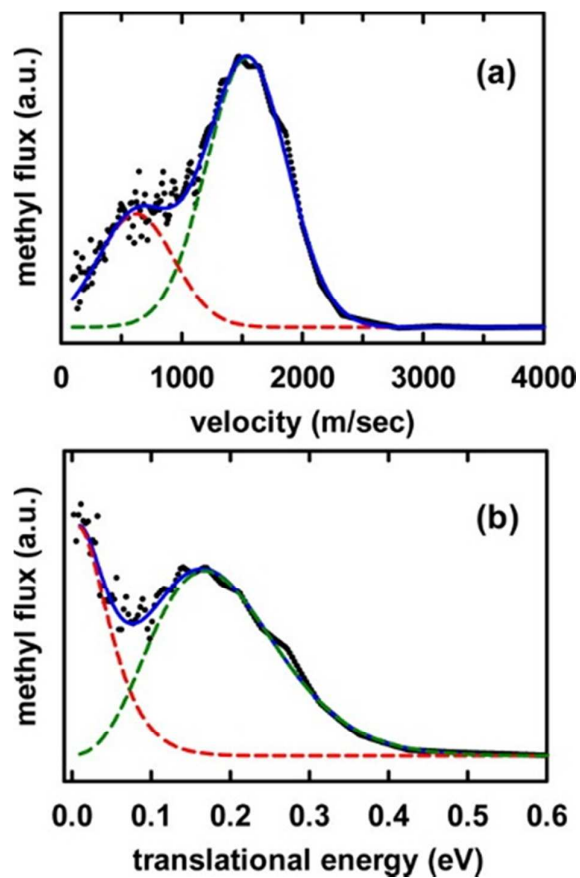


Fig. 26 Velocity (a) and translational energy (b) distribution of methyl radical ejected from the photooxidation of acetone on r-TiO₂(110) surface which was exposed to 80 L oxygen and ~1.1 ML acetone at 100 K. The photocatalytic chemistry was initiated by a 335 nm pulse with a typical photon fluence of 10^{13} - 10^{14} photons/(cm⁻² s). Reproduced with permission from Ref. 258. Copyright 2012 American Chemical Society.

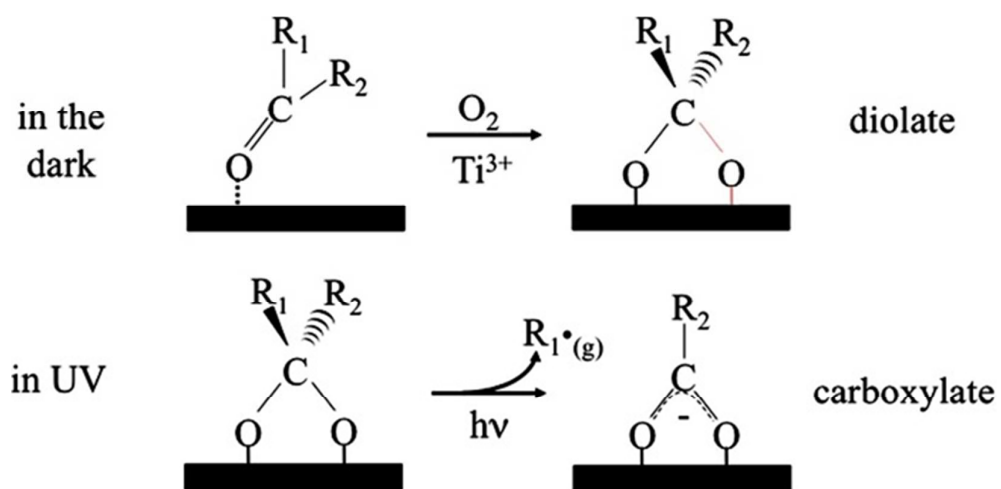


Fig. 27 Schematic of the two-step photooxidation of ketones on $r\text{-TiO}_2(110)$.

Reproduced with permission from Ref. 257. Copyright 2011 Elsevier.

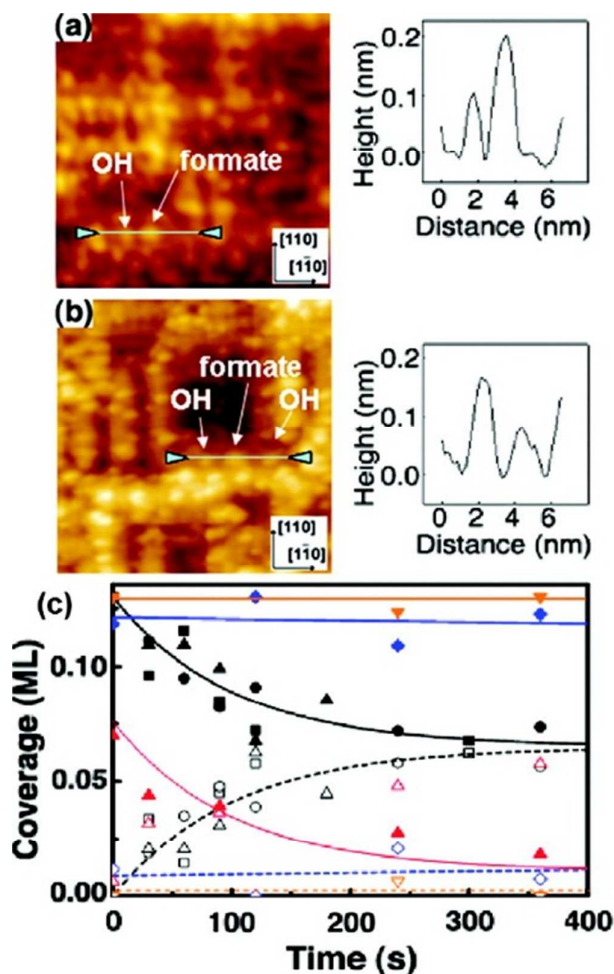


Fig. 28 STM images ($20 \times 20 \text{ nm}^2$, imaged at 2.00 V, 0.05 nA and RT) of the TiO₂(001) surface after exposure to formic acid, followed by (a) UV light ($5 \times 10^{17} \text{ photon cm}^{-2} \text{ s}^{-1}$) and (b) visible light ($2 \times 10^{18} \text{ photon cm}^{-2} \text{ s}^{-1}$) irradiation in the presence of O₂. Line profiles between white arrowheads in the images are shown in the right panels. (c) Time dependence of formate (solid) and hydroxyl (open) coverages under 3.4 eV (square), 2.1–2.8 eV (circle), 2.3 eV (triangle), and 2.1 eV (diamond) light irradiation in the presence of O₂ (black, blue, and red). The same plots under UV light irradiation but without O₂ are also shown with orange markers. Reproduced with permission from Ref. 275. Copyright 2009 American Chemical Society.

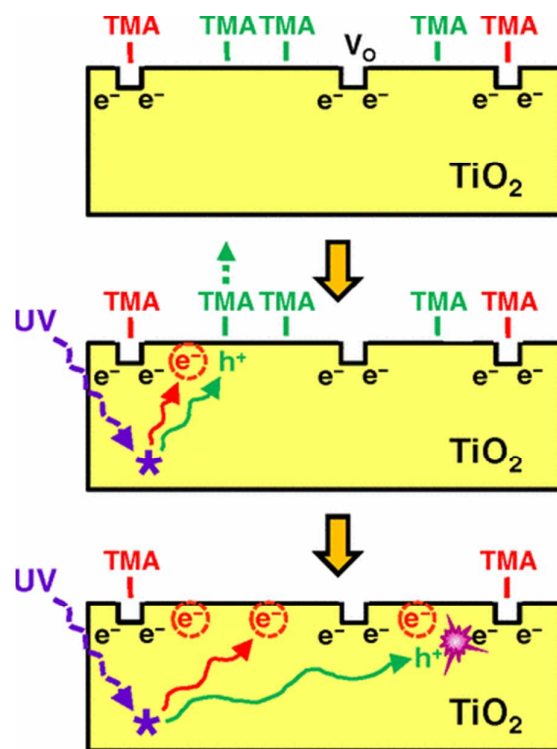


Fig. 29 Schematic showing the site-specific photodecomposition of TMA on r-TiO₂(110). Reproduced with permission from Ref. 286. Copyright 2012 American Physical Society.

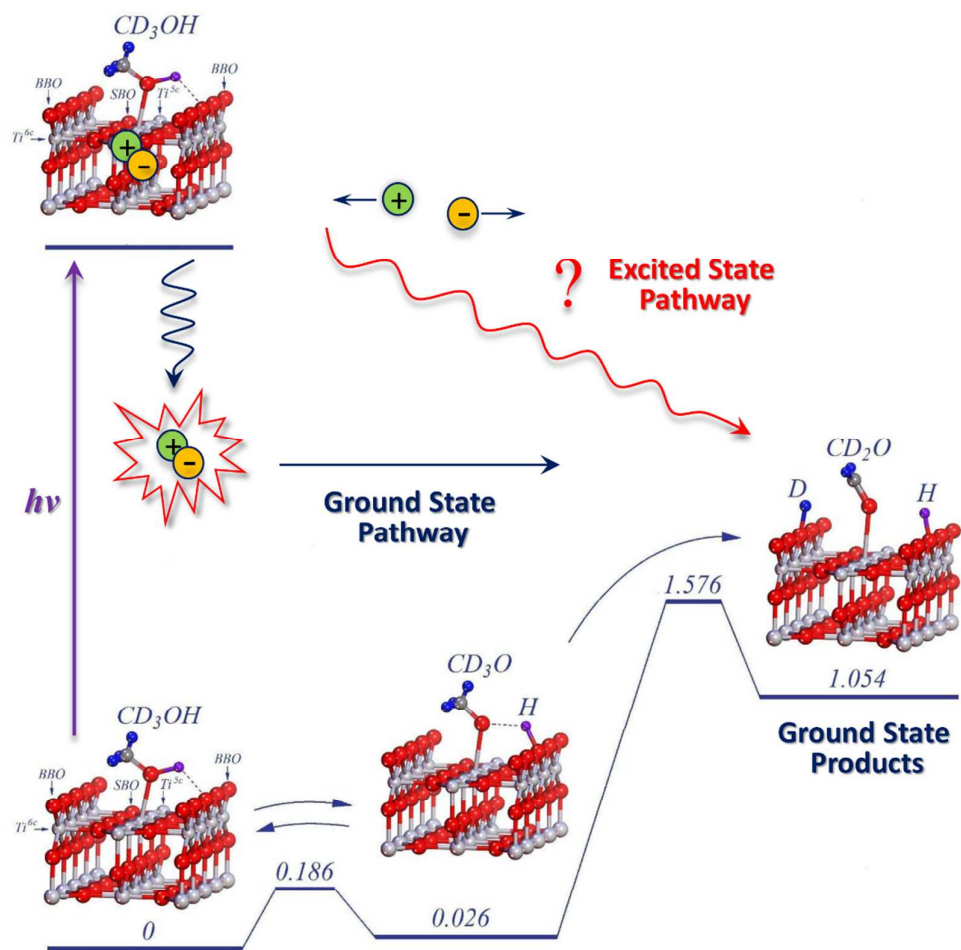


Fig. 30 A possible photocatalysis model based on nonadiabatic dynamical processes and ground state reactions. In this model, photoexcited electron-hole pairs are nonadiabatically recombined to convert the excited electronic state energy to the ground state energy, which drives the chemical reactions on the ground state surface.

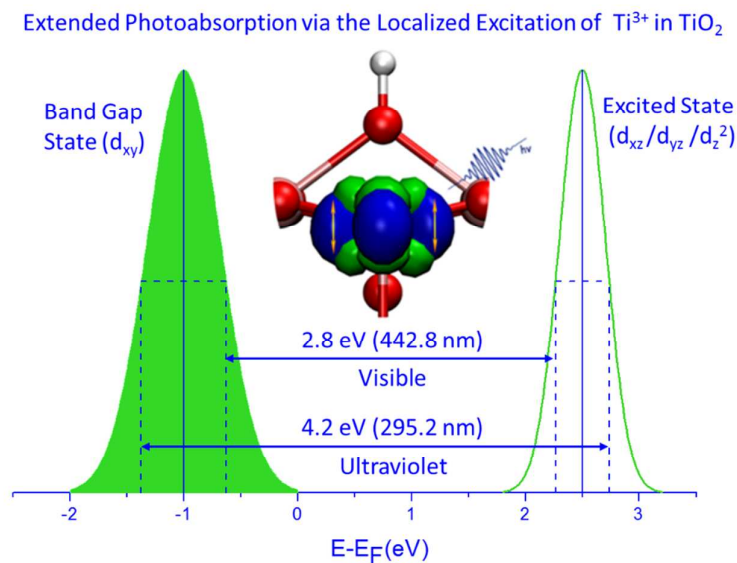


Fig. 31 Schematic of the enhanced and extended photoabsorption via $3d \rightarrow 3d$ transitions from the band gap state to the excited resonant state at 2.5 ± 0.2 eV in reduced TiO_2 . Blue and green charge density isosurfaces in the middle panel represent the band gap and excited states, respectively. Reproduced with permission from Ref. 309. Copyright 2015 American Chemical Society.

References:

1. A. Fujishima and K. Honda, *Nature*, 1972, **238**, 37-38.
2. A. Mills, R. H. Davies and D. Worsley, *Chem Soc Rev*, 1993, **22**, 417-425.
3. M. R. Hoffmann, S. T. Martin, W. Choi and D. W. Bahnemann, *Chem Rev*, 1995, **95**, 69-96.
4. A. L. Linsebigler, G. Q. Lu and J. T. Yates, *Chem Rev*, 1995, **95**, 735-758.
5. A. Fujishima, T. N. Rao and D. A. Tryk, *Journal of Photochemistry and Photobiology C: Photochemistry Reviews*, 2000, **1**, 1-21.
6. X. Chen and S. S. Mao, *Chem Rev*, 2007, **107**, 2891-2959.
7. X. Chen, S. Shen, L. Guo and S. S. Mao, *Chem Rev*, 2010, **110**, 6503-6570.
8. Y. Ma, X. Wang, Y. Jia, X. Chen, H. Han and C. Li, *Chem Rev*, 2014, **114**, 9987-10043.
9. D. Y. C. Leung, X. L. Fu, C. F. Wang, M. Ni, M. K. H. Leung, X. X. Wang and X. Z. Fu, *Chemsuschem*, 2010, **3**, 681-694.
10. A. Fujishima, X. Zhang and D. A. Tryk, *Surf. Sci. Rep.*, 2008, **63**, 515-582.
11. M. A. Henderson, *Surf. Sci. Rep.*, 2002, **46**, 1-308.
12. U. Diebold, *Surf. Sci. Rep.*, 2003, **48**, 53-229.
13. T. L. Thompson and J. T. Yates, *Chem Rev*, 2006, **106**, 4428-4453.
14. J. Zhao, B. Li, K. Onda, M. Feng and H. Petek, *Chem Rev*, 2006, **106**, 4402-4427.
15. C. L. Pang, R. Lindsay and G. Thornton, *Chem Soc Rev*, 2008, **37**, 2328-2353.
16. J. T. Yates, *Surface Science*, 2009, **603**, 1605-1612.
17. Z. Dohnalek, I. Lyubinetsky and R. Rousseau, *Prog Surf Sci*, 2010, **85**, 161-205.
18. M. A. Henderson, *Surf. Sci. Rep.*, 2011, **66**, 185-297.
19. M. A. Henderson and I. Lyubinetsky, *Chem Rev*, 2013, **113**, 4428-4455.
20. C. L. Pang, R. Lindsay and G. Thornton, *Chem Rev*, 2013, **113**, 3887-3948.
21. C. M. Friend, *Chem. Rec.*, 2014, **14**, 944-951.
22. Y. F. Li, U. Aschauer, J. Chen and A. Selloni, *Acc Chem Res*, 2014, **47**, 3361-3368.
23. X. Torrelles, G. Cabailh, R. Lindsay, O. Bikondoa, J. Roy, J. Zegenhagen, G. Teobaldi, W. A. Hofer and G. Thornton, *Phys Rev Lett*, 2008, **101**, 185501.
24. X. Q. Gong, N. Khorshidi, A. Stierle, V. Vonk, C. Ellinger, H. Dosch, H. Z. Cheng, A. Selloni, Y. B. He, O. Dulub and U. Diebold, *Surface Science*, 2009, **603**, 138-144.
25. Y. B. He, O. Dulub, H. Z. Cheng, A. Selloni and U. Diebold, *Phys Rev Lett*, 2009, **102**.
26. V. E. Henrich and R. L. Kurtz, *Phys Rev B*, 1981, **23**, 6280-6287.
27. W. Gopel, G. Rocker and R. Feierabend, *Phys Rev B*, 1983, **28**, 3427-3438.
28. J. M. Pan, B. L. Maschhoff, U. Diebold and T. E. Madey, *J. Vac. Sci. Technol. A-Vac. Surf. Films*, 1992, **10**, 2470-2476.
29. M. Menetrey, A. Markovits and C. Minot, *Surface Science*, 2003, **524**, 49-62.
30. Y. Yang, M. Sushchikh, G. Mills, H. Metiu and E. McFarland, *Appl Surf Sci*, 2004, **229**, 346-351.
31. S. Suzuki, K.-i. Fukui, H. Onishi and Y. Iwasawa, *Phys Rev Lett*, 2000, **84**, 2156-2159.
32. S. C. Li, Z. Zhang, D. Sheppard, B. D. Kay, J. M. White, Y. Du, I. Lyubinetsky, G. Henkelman and Z. Dohnalek, *J Am Chem Soc*, 2008, **130**, 9080-9088.
33. Z. R. Zhang, O. Bondarchuk, J. M. White, B. D. Kay and Z. Dohnalek, *J Am Chem Soc*, 2006, **128**, 4198-4199.
34. Z. R. Zhang, E. Bondarchuk, B. D. Kay, J. M. White and Z. Dohnalek, *J Phys Chem C*, 2007, **111**, 3021-3027.

35. Z. Zhang, O. Bondarchuk, B. D. Kay, J. M. White and Z. Dohnalek, *J Phys Chem B*, 2006, **110**, 21840-21845.
36. G. H. Enevoldsen, H. P. Pinto, A. S. Foster, M. C. R. Jensen, W. A. Hofer, B. Hammer, J. V. Lauritsen and F. Besenbacher, *Phys Rev Lett*, 2009, **102**, 136103.
37. G. H. Enevoldsen, H. P. Pinto, A. S. Foster, M. C. R. Jensen, W. A. Hofer, B. Hammer, J. V. Lauritsen and F. Besenbacher, *Phys Rev Lett*, 2010, **104**, 119604.
38. Y. Du, N. G. Petrik, N. A. Deskins, Z. Wang, M. A. Henderson, G. A. Kimmel and I. Lyubinetsky, *Physical Chemistry Chemical Physics*, 2012, **14**, 3066-3074.
39. X. L. Yin, M. Calatayud, H. Qiu, Y. Wang, A. Birkner, C. Minot and C. Woll, *Chemphyschem*, 2008, **9**, 253-256.
40. P. M. Kowalski, B. Meyer and D. Marx, *Phys Rev B*, 2009, **79**, 115410.
41. M. Calatayud, X. L. Yin, H. Qiu, Y. Wang, A. Birkner, C. Minot and C. Wöll, *Phys Rev Lett*, 2010, **104**, 119603.
42. J. Tao, Q. Cuan, X.-Q. Gong and M. Batzill, *The Journal of Physical Chemistry C*, 2012, **116**, 20438-20446.
43. M. M. Islam, M. Calatayud and G. Pacchioni, *The Journal of Physical Chemistry C*, 2011, **115**, 6809-6814.
44. J. Leconte, A. Markovits, M. K. Skalli, C. Minot and A. Belmajdoub, *Surface Science*, 2002, **497**, 194-204.
45. C. Xu, W. Yang, Q. Guo, D. Dai, M. Chen and X. Yang, *J Am Chem Soc*, 2013, 10206-10209.
46. Z. F. Wu, W. H. Zhang, F. Xiong, Q. Yuan, Y. K. Jin, J. L. Yang and W. X. Huang, *Physical Chemistry Chemical Physics*, 2014, **16**, 7051-7057.
47. I. M. Brookes, C. A. Muryn and G. Thornton, *Phys Rev Lett*, 2001, **87**, 266103-266106.
48. R. Schaub, P. Thostrup, N. Lopez, E. Laegsgaard, I. Stensgaard, J. K. Nørskov and F. Besenbacher, *Phys Rev Lett*, 2001, **87**, 266104-266107.
49. O. Bikondoa, C. L. Pang, R. Ithnin, C. A. Muryn, H. Onishi and G. Thornton, *Nat Mater*, 2006, **5**, 189-192.
50. S. Wendt, R. Schaub, J. Matthiesen, E. K. Vestergaard, E. Wahlstrom, M. D. Rasmussen, P. Thostrup, L. M. Molina, E. Laegsgaard, I. Stensgaard, B. Hammer and F. Besenbacher, *Surface Science*, 2005, **598**, 226-245.
51. P. J. D. Lindan, N. Harrison and M. Gillan, *Phys Rev Lett*, 1998, **80**, 762-765.
52. L. E. Walle, A. Borg, P. Uvdal and A. Sandell, *Phys Rev B*, 2009, **80**, 235436-235440.
53. D. A. Duncan, F. Allegretti and D. P. Woodruff, *Phys Rev B*, 2012, **86**.
54. T. J. Beck, A. Klust, M. Batzill, U. Diebold, C. Di Valentin, A. Tilocca and A. Selloni, *Surface Science*, 2005, **591**, L267-L272.
55. C. Di Valentin, A. Tilocca, A. Selloni, T. J. Beck, A. Klust, M. Batzill, Y. Losovyj and U. Diebold, *J Am Chem Soc*, 2005, **127**, 9895-9903.
56. Y. B. He, A. Tilocca, O. Dulub, A. Selloni and U. Diebold, *Nat Mater*, 2009, **8**, 585-589.
57. Y. Wang, H. Sun, S. Tan, H. Feng, Z. Cheng, J. Zhao, A. Zhao, B. Wang, Y. Luo, J. Yang and J. G. Hou, *Nat Commun*, 2013, **4**, 2214.
58. S. Tan, H. Feng, Y. Ji, Y. Wang, J. Zhao, A. Zhao, B. Wang, Y. Luo, J. Yang and J. G. Hou, *J Am Chem Soc*, 2012, **134**, 9978-9985.
59. Y. Nakato, A. Tsumura and H. Tsubomura, *The Journal of Physical Chemistry*, 1983, **87**, 2402-2405.

60. P. Salvador, *J Electrochem Soc*, 1981, **128**, 1895-1900.
61. P. Salvador and C. Gutierrez, *J Phys Chem-Us*, 1984, **88**, 3696-3698.
62. R. H. Wilson, *J Electrochem Soc*, 1980, **127**, 228-234.
63. R. Nakamura and Y. Nakato, *J Am Chem Soc*, 2004, **126**, 1290-1298.
64. R. Nakamura, T. Okamura, N. Ohashi, A. Imanishi and Y. Nakato, *J Am Chem Soc*, 2005, **127**, 12975-12983.
65. J.-i. Ueda, K. Takeshita, S. Matsumoto, K. Yazaki, M. Kawaguchi and T. Ozawa, *Photochemistry and Photobiology*, 2003, **77**, 165-170.
66. D. C. Hurum, A. G. Agrios, S. E. Crist, K. A. Gray, T. Rajh and M. C. Thurnauer, *J Electron Spectrosc*, 2006, **150**, 155-163.
67. C. P. Kumar, N. O. Gopal, T. C. Wang, M.-S. Wong and S. C. Ke, *The Journal of Physical Chemistry B*, 2006, **110**, 5223-5229.
68. P. Billik, G. Plesch, V. Brezová, L. Kuchta, M. Valko and M. Mazúr, *J Phys Chem Solids*, 2007, **68**, 1112-1116.
69. A. Lipovsky, L. levitski, Z. Tzitrinovich, A. Gedanken and R. Lubart, *Photochemistry and Photobiology*, 2012, **88**, 14-20.
70. I. R. Macdonald, S. Rhydderch, E. Holt, N. Grant, J. M. D. Storey and R. F. Howe, *Catal Today*, 2012, **182**, 39-45.
71. M. A. Fox and M. T. Dulay, *Chem Rev*, 1993, **93**, 341-357.
72. M. Ni, M. K. H. Leung, D. Y. C. Leung and K. Sumathy, *Renew. Sust. Energ. Rev.*, 2007, **11**, 401-425.
73. M. A. Henderson, W. S. Epling, C. L. Perkins, C. H. F. Peden and U. Diebold, *J Phys Chem B*, 1999, **103**, 5328-5337.
74. M. D. Rasmussen, L. M. Molina and B. Hammer, *J Chem Phys*, 2004, **120**, 988-997.
75. Y. G. Du, N. A. Deskins, Z. R. Zhang, Z. Dohnalek, M. Dupuis and I. Lyubinetsky, *Physical Chemistry Chemical Physics*, 2010, **12**, 6337-6344.
76. N. A. Deskins and M. Dupuis, *Phys Rev B*, 2007, **75**.
77. N. A. Deskins, R. Rousseau and M. Dupuis, *J Phys Chem C*, 2010, **114**, 5891-5897.
78. M. V. Ganduglia-Pirovano, A. Hofmann and J. Sauer, *Surf. Sci. Rep.*, 2007, **62**, 219-270.
79. A. Tilocca and A. Selloni, *Chemphyschem*, 2005, **6**, 1911-1916.
80. Z. Dohnálek, J. Kim, O. Bondarchuk, J. M. White and B. D. Kay, *The Journal of Physical Chemistry B*, 2006, **110**, 6229-6235.
81. S. Wendt, P. T. Sprunger, E. Lira, G. K. H. Madsen, Z. S. Li, J. O. Hansen, J. Matthiesen, A. Blekinge-Rasmussen, E. Laegsgaard, B. Hammer and F. Besenbacher, *Science*, 2008, **320**, 1755-1759.
82. N. G. Petrik, Z. R. Zhang, Y. G. Du, Z. Dohnalek, I. Lyubinetsky and G. A. Kimmel, *J Phys Chem C*, 2009, **113**, 12407-12411.
83. E. Lira, J. O. Hansen, P. Huo, R. Bechstein, P. Galliker, E. Laegsgaard, B. Hammer, S. Wendt and F. Besenbacher, *Surface Science*, 2010, **604**, 1945-1960.
84. A. C. Papageorgiou, N. S. Beglitis, C. L. Pang, G. Teobaldi, G. Cabailh, Q. Chen, A. J. Fisher, W. A. Hofer and G. Thornton, *P Natl Acad Sci USA*, 2010, **107**, 2391-2396.
85. G. A. Kimmel and N. G. Petrik, *Phys Rev Lett*, 2008, **100**, 196102-196105.
86. P. Scheiber, A. Riss, M. Schmid, P. Varga and U. Diebold, *Phys Rev Lett*, 2010, **105**, 216101.
87. Z. T. Wang, Y. G. Du, Z. Dohnalek and I. Lyubinetsky, *J Phys Chem Lett*, 2010, **1**, 3524-3529.

88. S. Tan, Y. Ji, Y. Zhao, A. Zhao, B. Wang, J. Yang and J. G. Hou, *J Am Chem Soc*, 2011, **133**, 2002-2009.
89. D. Pillay, Y. Wang and G. S. Hwang, *J Am Chem Soc*, 2006, **128**, 14000-14001.
90. M. P. de Lara-Castells and J. L. Krause, *Chem Phys Lett*, 2002, **354**, 483-490.
91. V. E. Henrich, G. Dresselhaus and H. J. Zeiger, *Journal of Vacuum Science & Technology*, 1978, **15**, 534-537.
92. Y. Wang, D. Pillay and G. S. Hwang, *Phys Rev B*, 2004, **70**.
93. M. A. Henderson, M. Shen, Z.-T. Wang and I. Lyubinetsky, *The Journal of Physical Chemistry C*, 2013, **117**, 5774-5784.
94. X. Y. Wu, A. Selloni, M. Lazzeri and S. K. Nayak, *Phys Rev B*, 2003, **68**, 241402.
95. F. Filippone, G. Mattioli and A. A. Bonapasta, *Catal Today*, 2007, **129**, 169-176.
96. U. Aschauer, J. Chen and A. Selloni, *Physical Chemistry Chemical Physics*, 2010, **12**, 12956-12960.
97. W. Zeng, T. M. Liu, Z. C. Wang, S. Tsukimoto, M. Saito and Y. Ikuhara, *Mater Trans*, 2010, **51**, 171-175.
98. Y. F. Li and A. Selloni, *J Am Chem Soc*, 2013, **135**, 9195-9199.
99. M. Setvín, U. Aschauer, P. Scheiber, Y.-F. Li, W. Hou, M. Schmid, A. Selloni and U. Diebold, *Science*, 2013, **341**, 988-991.
100. L. L. Liu, Q. Liu, Y. P. Zheng, Z. Wang, C. X. Pan and W. Xiao, *J Phys Chem C*, 2014, **118**, 3471-3482.
101. M. Setvin, B. Daniel, U. Aschauer, W. Hou, Y. F. Li, M. Schmid, A. Selloni and U. Diebold, *Physical Chemistry Chemical Physics*, 2014, **16**, 21524-21530.
102. D. C. Sorescu, S. Civiš and K. D. Jordan, *The Journal of Physical Chemistry C*, 2014, **118**, 1628-1639.
103. W. Zeng, T. M. Liu, T. M. Li and B. J. Xie, *Physica E*, 2015, **67**, 59-64.
104. G. Lu, A. Linsebigler and J. T. Yates, *The Journal of Chemical Physics*, 1995, **102**, 3005-3008.
105. G. Q. Lu, A. Linsebigler and J. T. Yates, *J. Chem. Phys.*, 1995, **102**, 4657-4662.
106. C. N. Rusu and J. T. Yates, *Langmuir*, 1997, **13**, 4311-4316.
107. C. L. Perkins and M. A. Henderson, *J Phys Chem B*, 2001, **105**, 3856-3863.
108. T. L. Thompson and J. T. Yates, *J Phys Chem B*, 2005, **109**, 18230-18236.
109. T. L. Thompson and J. T. Yates, *J Phys Chem B*, 2006, **110**, 7431-7435.
110. D. Sporleder, D. P. Wilson and M. G. White, *J Phys Chem C*, 2009, **113**, 13180-13191.
111. N. G. Petrik and G. A. Kimmel, *J Phys Chem Lett*, 2010, **1**, 1758-1762.
112. N. G. Petrik and G. A. Kimmel, *The Journal of Physical Chemistry Letters*, 2011, **2**, 2790-2796.
113. N. G. Petrik and G. A. Kimmel, *J Phys Chem C*, 2011, **115**, 152-164.
114. Z.-T. Wang, N. Aaron Deskins and I. Lyubinetsky, *The Journal of Physical Chemistry Letters*, 2012, **3**, 102-106.
115. N. G. Petrik and G. A. Kimmel, *Physical Chemistry Chemical Physics*, 2014, **16**, 2338-2346.
116. T. L. Thompson and J. T. Yates, *Top Catal*, 2005, **35**, 197-210.
117. W. S. Epling, C. H. F. Peden, M. A. Henderson and U. Diebold, *Surface Science*, 1998, **413**, 333-343.
118. M. Haruta, T. Kobayashi, H. Sano and N. Yamada, *Chem Lett*, 1987, 405-408.
119. Y. Sato, M. Koizumi, T. Miyao and S. Naito, *Catal Today*, 2006, **111**, 164-170.
120. H. Kobayashi and M. Yamaguchi, *Surface Science*, 1989, **214**, 466-476.

121. G. Rocker and W. Göpel, *Surface Science Letters*, 1986, **175**, L675-L680.
122. P. Reinhardt, M. Causa, C. M. Marian and B. A. Hess, *Phys Rev B*, 1996, **54**, 14812-14821.
123. G. Pacchioni, A. M. Ferrari and P. S. Bagus, *Surface Science*, 1996, **350**, 159-175.
124. D. C. Sorescu and J. T. Yates, *J Phys Chem B*, 1998, **102**, 4556-4565.
125. M. Casarin, C. Maccato and A. Vittadini, *J Phys Chem B*, 1998, **102**, 10745-10752.
126. D. C. Sorescu and J. T. Yates, *J Phys Chem B*, 2002, **106**, 6184-6199.
127. D. Pillay and G. S. Hwang, *The Journal of Chemical Physics*, 2006, **125**, 144706.
128. Z. X. Yang, R. Q. Wu, Q. M. Zhang and D. W. Goodman, *Phys Rev B*, 2001, **63**.
129. Y. Zhao, Z. Wang, X. F. Cui, T. Huang, B. Wang, Y. Luo, J. L. Yang and J. G. Hou, *J Am Chem Soc*, 2009, **131**, 7958-7959.
130. T. Minato, Y. Sainoo, Y. Kim, H. S. Kato, K. Aika, M. Kawai, J. Zhao, H. Petek, T. Huang, W. He, B. Wang, Z. Wang, Y. Zhao, J. L. Yang and J. G. Hou, *J. Chem. Phys.*, 2009, **130**, 124502-124512.
131. A. Linsebigler, G. Q. Lu and J. T. Yates, *J Phys Chem-Us*, 1996, **100**, 6631-6636.
132. A. Linsebigler, C. Rusu and J. T. Yates, *J Am Chem Soc*, 1996, **118**, 5284-5289.
133. N. G. Petrik and G. A. Kimmel, *J Phys Chem Lett*, 2010, **1**, 2508-2513.
134. X. Wu, A. Selloni and S. K. Nayak, *The Journal of Chemical Physics*, 2004, **120**, 4512-4516.
135. C. Rohmann, Y. M. Wang, M. Muhler, J. Metson, H. Idriss and C. Woll, *Chem Phys Lett*, 2008, **460**, 10-12.
136. N. G. Petrik and G. A. Kimmel, *The Journal of Physical Chemistry Letters*, 2013, 344-349.
137. R. Wanbayor, P. Deák, T. Frauenheim and V. Ruangpornvisuti, *The Journal of Chemical Physics*, 2011, **134**, 104701.
138. M. Xu, Y. Gao, E. M. Moreno, M. Kunst, M. Muhler, Y. Wang, H. Idriss and C. Wöll, *Phys Rev Lett*, 2011, **106**, 138302-138305.
139. L. Gamble, L. S. Jung and C. T. Campbell, *Surface Science*, 1996, **348**, 1-16.
140. D. Brinkley and T. Engel, *Surface Science*, 1998, **415**, L1001-L1006.
141. D. Brinkley and T. Engel, *J Phys Chem B*, 1998, **102**, 7596-7605.
142. S. P. Bates, M. J. Gillan and G. Kresse, *The Journal of Physical Chemistry B*, 1998, **102**, 2017-2026.
143. S. P. Bates, G. Kresse and M. J. Gillan, *Surface Science*, 1998, **409**, 336-349.
144. K. F. Ferris and L. Q. Wang, *J Vac Sci Technol A*, 1998, **16**, 956-960.
145. M. A. Henderson, S. Otero-Tapia and M. E. Castro, *Faraday Discuss.*, 1999, **114**, 313-329.
146. D. Brinkley and T. Engel, *J Phys Chem B*, 2000, **104**, 9836-9841.
147. E. Farfan-Arribas and R. J. Madix, *J Phys Chem B*, 2002, **106**, 10680-10692.
148. E. Farfan-Arribas and R. J. Madix, *Surface Science*, 2003, **544**, 241-260.
149. L. Kieu, P. Boyd and H. Idriss, *J. Mol. Catal. A-Chem.*, 2002, **188**, 153-161.
150. K. Onda, B. Li, J. Zhao and H. Petek, *Surface Science*, 2005, **593**, 32-37.
151. B. Li, J. Zhao, K. Onda, K. D. Jordan, J. L. Yang and H. Petek, *Science*, 2006, **311**, 1436-1440.
152. Y. Kim, B. Kay, J. White and Z. Dohnálek, *J Phys Chem C*, 2007, **111**, 18236-18242.
153. Y. K. Kim, B. D. Kay, J. M. White and Z. Dohnalek, *Catal Lett*, 2007, **119**, 1-4.
154. R. S. de Armas, J. Oviedo, M. A. San Miguel and J. F. Sanz, *J Phys Chem C*, 2007, **111**, 10023-10028.
155. O. Bondarchuk, Y. K. Kim, J. M. White, J. Kim, B. D. Kay and Z. Dohnalek, *J Phys Chem C*, 2007, **111**, 11059-11067.
156. P. M. Jayaweera, E. L. Quah and H. Idriss, *J Phys Chem C*, 2007, **111**, 1764-1769.

157. Z. Zhang, R. Rousseau, J. Gong, S. C. Li, B. D. Kay, Q. Ge and Z. Dohnalek, *Phys Rev Lett*, 2008, **101**, 156103.
158. S. Koppen and W. Langel, *Physical Chemistry Chemical Physics*, 2008, **10**, 1907-1915.
159. J. Oviedo, R. Sanchez-De-Armas, M. A. S. Miguel and J. F. Sanz, *J Phys Chem C*, 2008, **112**, 17737-17740.
160. J. Zhao, J. L. Yang and H. Petek, *Phys Rev B*, 2009, **80**, 235416-235426.
161. Z. R. Zhang, R. Rousseau, J. L. Gong, B. D. Kay and Z. Dohnalek, *J Am Chem Soc*, 2009, **131**, 17926-17932.
162. V. M. Sanchez, J. A. Cojulun and D. A. Scherlis, *J Phys Chem C*, 2010, **114**, 11522-11526.
163. C. Y. Zhou, Z. F. Ren, S. J. Tan, Z. B. Ma, X. C. Mao, D. X. Dai, H. J. Fan, X. M. Yang, J. LaRue, R. Cooper, A. M. Wodtke, Z. Wang, Z. Y. Li, B. Wang, J. L. Yang and J. G. Hou, *Chemical Science*, 2010, **1**, 575-580.
164. U. Martinez, L. B. Vilhelmsen, H. H. Kristoffersen, J. Stausholm-Møller and B. Hammer, *Phys Rev B*, 2011, **84**, 205434-.
165. J. Ø. Hansen, P. Huo, U. Martinez, E. Lira, Y. Y. Wei, R. Streber, E. Lægsgaard, B. Hammer, S. Wendt and F. Besenbacher, *Phys Rev Lett*, 2011, **107**, 136102.
166. Y. K. Kim and C. C. Hwang, *Surface Science*, 2011, **605**, 2082-2086.
167. M. Shen and M. A. Henderson, *Langmuir*, 2011, **27**, 9430-9438.
168. C. Zhou, Z. Ma, Z. Ren, X. Mao, D. Dai and X. Yang, *Chemical Science*, 2011, **2**, 1980-1983.
169. Z. Li, R. S. Smith, B. D. Kay and Z. Dohnálek, *The Journal of Physical Chemistry C*, 2011, **115**, 22534-22539.
170. A. M. Nadeem, J. M. R. Muir, K. A. Connelly, B. T. Adamson, B. J. Metson and H. Idriss, *Physical Chemistry Chemical Physics*, 2011, **13**, 7637-7643.
171. M. Shen and M. A. Henderson, *The Journal of Physical Chemistry Letters*, 2011, **2**, 2707-2710.
172. M. M. Shen and M. A. Henderson, *J Phys Chem C*, 2011, **115**, 5886-5893.
173. A. Y. Ahmed, T. A. Kandiel, T. Oekermann and D. Bahnemann, *The Journal of Physical Chemistry Letters*, 2011, **2**, 2461-2465.
174. P. Huo, J. O. Hansen, U. Martinez, E. Lira, R. Streber, Y. Y. Wei, E. Lægsgaard, B. Hammer, S. Wendt and F. Besenbacher, *J Phys Chem Lett*, 2012, **3**, 283-288.
175. C. Zhou, Z. Ma, Z. Ren, A. M. Wodtke and X. Yang, *Energy Environ. Sci.*, 2012, **5**, 6833-6844.
176. Q. Guo, C. Xu, Z. Ren, W. Yang, Z. Ma, D. Dai, H. Fan, T. K. Minton and X. Yang, *J Am Chem Soc*, 2012, **134**, 13366-13373.
177. M. Shen, D. P. Acharya, Z. Dohnalek and M. A. Henderson, *J Phys Chem C*, 2012, **116**, 25465-25469.
178. M. M. Shen and M. A. Henderson, *J Phys Chem C*, 2012, **116**, 18788-18795.
179. Q. Guo, C. Xu, W. Yang, Z. Ren, Z. Ma, D. Dai, T. K. Minton and X. Yang, *The Journal of Physical Chemistry C*, 2013, **117**, 5293-5300.
180. A. Migani, D. J. Mowbray, A. Iacomino, J. Zhao, H. Petek and A. Rubio, *J Am Chem Soc*, 2013, **135**, 11429-11432.
181. K. R. Phillips, S. C. Jensen, M. Baron, S. C. Li and C. M. Friend, *J Am Chem Soc*, 2013, **135**, 574-577.
182. Q. Yuan, Z. Wu, Y. Jin, L. Xu, F. Xiong, Y. Ma and W. Huang, *J Am Chem Soc*, 2013, **135**, 5212-5219.
183. C. Xu, W. Yang, Q. Guo, D. Dai, M. Chen and X. Yang, *Chinese J Catal*, 2014, **35**, 416-422.

184. X. Lang, B. Wen, C. Zhou, Z. Ren and L.-M. Liu, *The Journal of Physical Chemistry C*, 2014, **118**, 19859-19868.
185. M. A. Henderson, S. Otero-Tapia and M. E. Castro, *Surface Science*, 1998, **413**, 252-272.
186. K. Onda, B. Li, J. Zhao, K. D. Jordan, J. L. Yang and H. Petek, *Science*, 2005, **308**, 1154-1158.
187. T. Kawai and T. Sakata, *J Chem Soc Chem Comm*, 1980, 694-695.
188. G. Palmisano, V. Augugliaro, M. Pagliaro and L. Palmisano, *Chem Commun*, 2007, 3425-3437.
189. D. S. Muggli, M. J. Odland and L. R. Schmidt, *J. Catal.*, 2001, **203**, 51-63.
190. X. F. Cui, Z. Wang, S. J. Tan, B. Wang, J. L. Yang and J. G. Hou, *J Phys Chem C*, 2009, **113**, 13204-13208.
191. P. W. Klymko and R. Kopelman, *J Phys Chem-Us*, 1983, **87**, 4565-4567.
192. R. Kopelman, *Science*, 1988, **241**, 1620-1626.
193. J. Haubrich, E. Kaxiras and C. M. Friend, *Chemistry – A European Journal*, 2011, **17**, 4496-4506.
194. F. Zuo, L. Wang, T. Wu, Z. Y. Zhang, D. Borchardt and P. Y. Feng, *J Am Chem Soc*, 2010, **132**, 11856-11857.
195. C. D. Lane, N. G. Petrik, T. M. Orlando and G. A. Kimmel, *J Phys Chem C*, 2007, **111**, 16319-16329.
196. N. G. Petrik and G. A. Kimmel, *J Phys Chem C*, 2009, **113**, 4451-4460.
197. D. Wei, X. Jin, C. Huang, D. Dai, Z. Ma, W.-X. Li and X. Yang, *The Journal of Physical Chemistry C*, 2015, DOI:10.1021/acs.jpcc.5b05074.
198. X. Mao, D. Wei, Z. Wang, X. Jin, Q. Hao, Z. Ren, D. Dai, Z. Ma, C. Zhou and X. Yang, *The Journal of Physical Chemistry C*, 2015, **119**, 1170-1174.
199. X. C. Mao, X. F. Lang, Z. Q. Wang, Q. Q. Hao, B. Wen, Z. F. Ren, D. X. Dai, C. Y. Zhou, L. M. Liu and X. M. Yang, *J Phys Chem Lett*, 2013, **4**, 3839-3844.
200. L. Domokos, T. Katona and A. Molnar, *Catal Lett*, 1996, **40**, 215-221.
201. J. L. Liu, E. S. Zhan, W. J. Cai, J. Li and W. J. Shen, *Catal Lett*, 2008, **120**, 274-280.
202. T. P. Minyukova, I. I. Simentsova, A. V. Khasin, N. V. Shtertser, N. A. Baronskaya, A. A. Khassin and T. M. Yurieva, *Appl Catal a-Gen*, 2002, **237**, 171-180.
203. X. Mao, Z. Wang, X. Lang, Q. Hao, B. Wen, D. Dai, C. Zhou, L.-M. Liu and X. Yang, *The Journal of Physical Chemistry C*, 2015, **119**, 6121-6127.
204. T. Ohno, K. Sarukawa and M. Matsumura, *New J Chem*, 2002, **26**, 1167-1170.
205. H. Takahashi, R. Watanabe, Y. Miyauchi and G. Mizutani, *J. Chem. Phys.*, 2011, **134**, 154704.
206. J. G. Tao and M. Batzill, *J Phys Chem Lett*, 2010, **1**, 3200-3206.
207. L. Gundlach, S. Felber, W. Storck, E. Galoppini, Q. Wei and F. Willig, *Res Chem Intermediat*, 2005, **31**, 39-46.
208. L. Gundlach, R. Ernstorfer and F. Willig, *Prog Surf Sci*, 2007, **82**, 355-377.
209. L. Gundlach, R. Ernstorfer and F. Willig, *Phys Rev B*, 2006, **74**.
210. C. Xu, W. Yang, Z. Ren, D. Dai, Q. Guo, T. K. Minton and X. Yang, *J Am Chem Soc*, 2013, **135**, 19039-19045.
211. L. Kavan, M. Gratzel, S. E. Gilbert, C. Klemenz and H. J. Scheel, *J Am Chem Soc*, 1996, **118**, 6716-6723.
212. G. S. Herman, Z. Dohnalek, N. Ruzycki and U. Diebold, *J Phys Chem B*, 2003, **107**, 2788-2795.
213. C. Xu, W. Yang, Q. Guo, D. Dai, M. Chen and X. Yang, *J Am Chem Soc*, 2014, **136**, 602-605.

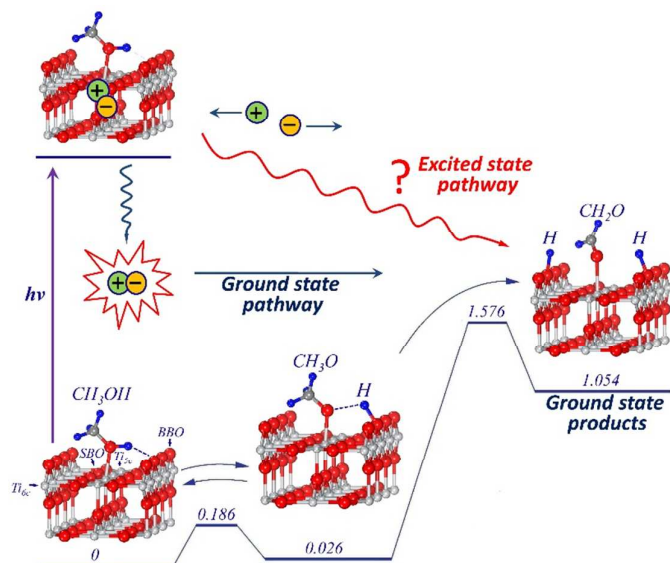
214. A. Tilocca and A. Selloni, *J Phys Chem B*, 2004, **108**, 19314-19319.
215. C. Di Valentin and D. Fittipaldi, *The Journal of Physical Chemistry Letters*, 2013, **4**, 1901-1906.
216. S. Kundu, A. B. Vidal, M. A. Nadeem, S. D. Senanayake, H. Idriss, P. Liu, J. A. Rodriguez and D. Stacchiola, *J Phys Chem C*, 2013, **117**, 11149-11158.
217. Z. Ma, Q. Guo, X. Mao, Z. Ren, X. Wang, C. Xu, W. Yang, D. Dai, C. Zhou, H. Fan and X. Yang, *The Journal of Physical Chemistry C*, 2013, **117**, 10336-10344.
218. Z. B. Ma, C. Y. Zhou, X. C. Mao, Z. F. Ren, D. X. Dai and X. M. Yang, *Chinese J Chem Phys*, 2013, **26**, 1-7.
219. H. Idriss, *Platinum Metals Review*, 2004, **48**, 105-115.
220. Y. Suda, T. Morimoto and M. Nagao, *Langmuir*, 1987, **3**, 99-104.
221. E. A. Taylor and G. L. Griffin, *J Phys Chem-Us*, 1988, **92**, 477-481.
222. I. Carrizosa, G. Munuera and S. Castanar, *J. Catal.*, 1977, **49**, 265-277.
223. J. J. Plata, V. Collico, A. M. Marquez and J. F. Sanz, *J Phys Chem C*, 2011, **115**, 2819-2825.
224. G. Busca, J. Lamotte, J. C. Lavalley and V. Lorenzelli, *J Am Chem Soc*, 1987, **109**, 5197-5202.
225. G. Q. Lu, A. Linsebigler and J. T. Yates, *J Phys Chem-Us*, 1994, **98**, 11733-11738.
226. L. Kieu, P. Boyd and H. Idriss, *J. Mol. Catal. A-Chem.*, 2001, **176**, 117-125.
227. J. Li, L. Wu and Y. Zhang, *Chem Phys Lett*, 2001, **342**, 249-258.
228. H. Z. Liu, X. Wang, C. X. Pan and K. M. Liew, *J Phys Chem C*, 2012, **116**, 8044-8053.
229. J. M. R. Muir and H. Idriss, *Chem Phys Lett*, 2013, **572**, 125-129.
230. H. Qiu, H. Idriss, Y. M. Wang and C. Woell, *J Phys Chem C*, 2008, **112**, 9828-9834.
231. J. Kim, B. D. Kay and Z. Dohnalek, *J Phys Chem C*, 2010, **114**, 17017-17022.
232. C. Di Valentin, M. Rosa and G. Pacchioni, *J Am Chem Soc*, 2012.
233. C. Xu, W. Yang, Q. Guo, D. Dai, T. K. Minton and X. Yang, *The Journal of Physical Chemistry Letters*, 2013, **4**, 2668-2673.
234. T. Cremer, S. C. Jensen and C. M. Friend, *The Journal of Physical Chemistry C*, 2014, **118**, 29242-29251.
235. Q. Yuan, Z. F. Wu, Y. K. Jin, F. Xiong and W. X. Huang, *J Phys Chem C*, 2014, **118**, 20420-20428.
236. R. T. Zehr and M. A. Henderson, *Surface Science*, 2008, **602**, 2238-2249.
237. L. Benz, J. Haubrich, R. G. Quiller, S. C. Jensen and C. M. Friend, *J Am Chem Soc*, 2009, **131**, 15026-15031.
238. L. Benz, J. Haubrich, S. C. Jensen and C. M. Friend, *Acs Nano*, 2011, **5**, 834-843.
239. S. C. Jensen, J. Haubrich, A. Shank and C. M. Friend, *Chem-Eur J*, 2011, **17**, 8309-8312.
240. L. Benz, J. Haubrich, R. G. Quiller and C. M. Friend, *Surface Science*, 2009, **603**, 1010-1017.
241. P. M. Clavin, C. M. Friend and K. Al-Shamery, *Chem-Eur J*, 2014, **20**, 7665-7669.
242. Z. R. Zhang, M. R. Tang, Z. T. Wang, Z. Ke, Y. B. Xia, K. T. Park, I. Lyubinetsky, Z. Dohnalek and Q. F. Ge, *Top Catal*, 2015, **58**, 103-113.
243. M. A. Henderson, *J Phys Chem B*, 1997, **101**, 221-229.
244. M. Bowker, P. Stone, R. Bennett and N. Perkins, *Surface Science*, 2002, **511**, 435-448.
245. D. I. Sayago, M. Polcik, R. Lindsay, R. L. Toomes, J. T. Hoeft, M. Kittel and D. P. Woodruff, *J Phys Chem B*, 2004, **108**, 14316-14323.
246. M. Aizawa, Y. Morikawa, Y. Namai, H. Morikawa and Y. Iwasawa, *J Phys Chem B*, 2005, **109**, 18831-18838.
247. M. A. Henderson, *J Phys Chem B*, 2004, **108**, 18932-18941.
248. M. A. Henderson, *Langmuir*, 2005, **21**, 3443-3450.

249. M. A. Henderson, *Langmuir*, 2005, **21**, 3451-3458.
250. M. Yasuo, A. Sasahara and H. Onishi, *J Phys Chem C*, 2010, **114**, 14579-14582.
251. Y. B. Xia, J. Y. Ye, P. Murray, A. Ali, Q. F. Ge and Z. R. Zhang, *Physical Chemistry Chemical Physics*, 2013, **15**, 13897-13901.
252. A. M. Marquez, J. J. Plata and J. F. Sanz, *J Phys Chem C*, 2009, **113**, 19973-19980.
253. M. A. Henderson, *J Phys Chem B*, 2005, **109**, 12062-12070.
254. M. A. Henderson, *J Phys Chem C*, 2008, **112**, 11433-11440.
255. M. A. Henderson, *J. Catal.*, 2008, **256**, 287-292.
256. T. H. Wang, D. A. Dixon and M. A. Henderson, *J Phys Chem C*, 2010, **114**, 14083-14092.
257. M. A. Henderson, N. A. Deskins, R. T. Zehr and M. Dupuis, *J. Catal.*, 2011, **279**, 205-212.
258. D. P. Wilson, D. Sporleder and M. G. White, *J Phys Chem C*, 2012, **116**, 16541-16552.
259. M. D. Kershish, D. P. Wilson and M. G. White, *J Chem Phys*, 2013, **138**, 204703.
260. A. Snelson, *The Journal of Physical Chemistry*, 1970, **74**, 537-544.
261. M. A. Henderson, *Surface Science*, 2008, **602**, 3188-3193.
262. R. S. Kavathekar, P. Dev, N. J. English and J. M. D. MacElroy, *Molecular Physics*, 2011, **109**, 1649-1656.
263. M. D. Kershish, D. P. Wilson, M. G. White, J. J. John, A. Nomerotski, M. Brouard, J. W. Lee, C. Vallance and R. Turchetta, *J Chem Phys*, 2013, **139**, 084202.
264. D. P. Wilson, D. P. Sporleder and M. G. White, *J Phys Chem C*, 2013, **117**, 9290-9300.
265. C. Di Valentin, G. Pacchioni and A. Selloni, *Phys Rev Lett*, 2006, **97**, 166803.
266. R. T. Zehr, N. A. Deskins and M. A. Henderson, *J Phys Chem C*, 2010, **114**, 16900-16908.
267. R. T. Zehr and M. A. Henderson, *Physical Chemistry Chemical Physics*, 2010, **12**, 8084-8091.
268. M. Miao, Y. C. Liu, Q. Wang, T. Wu, L. P. Huang, K. E. Gubbins and M. B. Nardelli, *J. Chem. Phys.*, 2012, **136**.
269. M. Gratzel, *Nature*, 2001, **414**, 338-344.
270. H. Onishi, T. Aruga and Y. Iwasawa, *J. Catal.*, 1994, **146**, 557-567.
271. H. Onishi, Y. Yamaguchi, K. Fukui and Y. Iwasawa, *J Phys Chem-US*, 1996, **100**, 9582-9584.
272. J. G. Tao, T. Luttrell, J. Bylsma and M. Batzill, *J Phys Chem C*, 2011, **115**, 3434-3442.
273. I. Lyubinetzky, Z. Q. Yu and M. A. Henderson, *J Phys Chem C*, 2007, **111**, 4342-4346.
274. I. Lyubinetzky, N. A. Deskins, Y. G. Du, E. K. Vestergaard, D. J. Kim and M. Dupuis, *Physical Chemistry Chemical Physics*, 2010, **12**, 5986-5992.
275. H. Ariga, T. Taniike, H. Morikawa, M. Tada, B. K. Min, K. Watanabe, Y. Matsumoto, S. Ikeda, K. Saiki and Y. Iwasawa, *J Am Chem Soc*, 2009, **131**, 14670-14672.
276. H. Idriss, P. Legare and G. Maire, *Surface Science*, 2002, **515**, 413-420.
277. E. L. Quah, J. N. Wilson and H. Idriss, *Langmuir*, 2010, **26**, 6411-6417.
278. M. A. Henderson, J. M. White, H. Uetsuka and H. Onishi, *J Am Chem Soc*, 2003, **125**, 14974-14975.
279. H. Uetsuka, H. Onishi, M. A. Henderson and J. M. White, *J Phys Chem B*, 2004, **108**, 10621-10624.
280. H. Uetsuka, C. Pang, A. Sasahara and H. Onishi, *Langmuir*, 2005, **21**, 11802-11805.
281. J. M. White and M. A. Henderson, *J Phys Chem B*, 2005, **109**, 14990-15000.
282. M. A. Henderson, J. M. White, H. Uetsuka and H. Onishi, *J. Catal.*, 2006, **238**, 153-164.
283. T. Ohsawa, I. V. Lyubinetzky, M. A. Henderson and S. A. Chambers, *J Phys Chem C*, 2008, **112**, 20050-20056.

284. T. Ohsawa, I. Lyubinetsky, Y. Du, M. A. Henderson, V. Shutthanandan and S. A. Chambers, *Phys Rev B*, 2009, **79**, 085401.
285. T. Ohsawa, M. A. Henderson and S. A. Chambers, *J Phys Chem C*, 2010, **114**, 6595-6601.
286. Z. T. Wang, N. A. Deskins, M. A. Henderson and I. Lyubinetsky, *Phys Rev Lett*, 2012, **109**, 266103.
287. J. M. White and M. A. Henderson, *J Phys Chem B*, 2005, **109**, 12417-12430.
288. J. Schneider, M. Matsuoka, M. Takeuchi, J. Zhang, Y. Horiuchi, M. Anpo and D. W. Bahnemann, *Chem Rev*, 2014, **114**, 9919-9986.
289. D. Duonghong, E. Borgarello and M. Graetzel, *J Am Chem Soc*, 1981, **103**, 4685-4690.
290. C. G. Silva, R. Juarez, T. Marino, R. Molinari and H. Garcia, *J Am Chem Soc*, 2011, **133**, 595-602.
291. Z. W. Seh, S. Liu, M. Low, S.-Y. Zhang, Z. Liu, A. Mlayah and M.-Y. Han, *Adv Mater*, 2012, **24**, 2310-2314.
292. F. Sastre, M. Oteri, A. Corma and H. Garcia, *Energy Environ. Sci.*, 2013, **6**, 2211-2215.
293. F. Wang, C. Li, H. Chen, R. Jiang, L.-D. Sun, Q. Li, J. Wang, J. C. Yu and C.-H. Yan, *J Am Chem Soc*, 2013, **135**, 5588-5601.
294. J. Yan, G. Wu, N. Guan and L. Li, *Chem Commun*, 2013, **49**, 11767-11769.
295. Z. Bian, T. Tachikawa, P. Zhang, M. Fujitsuka and T. Majima, *J Am Chem Soc*, 2014, **136**, 458-465.
296. K. Qian, B. C. Sweeny, A. C. Johnston-Peck, W. X. Niu, J. O. Graham, J. S. DuChene, J. J. Qiu, Y. C. Wang, M. H. Engelhard, D. Su, E. A. Stach and W. D. Wei, *J Am Chem Soc*, 2014, **136**, 9842-9845.
297. A. Tanaka, K. Hashimoto and H. Kominami, *J Am Chem Soc*, 2014, **136**, 586-589.
298. M. A. Grela, M. A. Brusa and A. J. Colussi, *J Phys Chem B*, 1997, **101**, 10986-10989.
299. M. A. Grela, M. A. Brusa and A. J. Colussi, *J Phys Chem B*, 1999, **103**, 6400-6402.
300. M. A. Grela and A. J. Colussi, *J Phys Chem B*, 1999, **103**, 2614-2619.
301. M. Dell'Angela, T. Anniyev, M. Beye, R. Coffee, A. Föhlich, J. Gladh, T. Katayama, S. Kaya, O. Krupin, J. LaRue, A. Møgelhøj, D. Nordlund, J. K. Nørskov, H. Öberg, H. Ogasawara, H. Öström, L. G. M. Pettersson, W. F. Schlotter, J. A. Sellberg, F. Sorgenfrei, J. J. Turner, M. Wolf, W. Wurth and A. Nilsson, *Science*, 2013, **339**, 1302-1305.
302. H. Öström, H. Öberg, H. Xin, J. LaRue, M. Beye, M. Dell'Angela, J. Gladh, M. L. Ng, J. A. Sellberg, S. Kaya, G. Mercurio, D. Nordlund, M. Hantschmann, F. Hieke, D. Kühn, W. F. Schlotter, G. L. Dakovski, J. J. Turner, M. P. Minitti, A. Mitra, S. P. Moeller, A. Föhlich, M. Wolf, W. Wurth, M. Persson, J. K. Nørskov, F. Abild-Pedersen, H. Ogasawara, L. G. M. Pettersson and A. Nilsson, *Science*, 2015, **347**, 978-982.
303. J. Schnadt, P. A. Bruhwiler, L. Patthey, J. N. O'Shea, S. Sodergren, M. Odelius, R. Ahuja, O. Karis, M. Bassler, P. Persson, H. Siegbahn, S. Lunell and N. Martensson, *Nature*, 2002, **418**, 620-623.
304. W. A. Tisdale, K. J. Williams, B. A. Timp, D. J. Norris, E. S. Aydil and X. Y. Zhu, *Science*, 2010, **328**, 1543-1547.
305. A. J. Nozik, *Physica E*, 2002, **14**, 115-120.
306. J. E. Murphy, M. C. Beard, A. G. Norman, S. P. Ahrenkiel, J. C. Johnson, P. Yu, O. I. Mičić, R. J. Ellingson and A. J. Nozik, *J Am Chem Soc*, 2006, **128**, 3241-3247.
307. R. D. Schaller and V. I. Klimov, *Phys Rev Lett*, 2006, **96**, 097402.
308. J. G. Tao, T. Luttrell and M. Batzill, *Nat. Chem.*, 2011, **3**, 296-300.

309. Z. Wang, B. Wen, Q. Hao, L. M. Liu, C. Zhou, X. Mao, X. Lang, W. J. Yin, D. Dai, A. Selloni and X. Yang, *J Am Chem Soc*, 2015, **137**, 9146-9152.
310. I. Justicia, P. Ordejon, G. Canto, J. L. Mozos, J. Fraxedas, G. A. Battiston, R. Gerbasi and A. Figueras, *Adv Mater*, 2002, **14**, 1399-1402.
311. F. Zuo, K. Bozhilov, R. J. Dillon, L. Wang, P. Smith, X. Zhao, C. Bardeen and P. Feng, *Angew Chem Int Ed Engl*, 2012, **51**, 6223-6226.
312. C. Y. Mao, F. Zuo, Y. Hou, X. H. Bu and P. Y. Feng, *Angew Chem Int Edit*, 2014, **53**, 10485-10489.
313. F. Zuo, L. Wang and P. Y. Feng, *Int J Hydrogen Energ*, 2014, **39**, 711-717.
314. G. Liu, H. G. Yang, J. Pan, Y. Q. Yang, G. Q. Lu and H. M. Cheng, *Chem Rev*, 2014, **114**, 9559-9612.
315. H. G. Yang, C. H. Sun, S. Z. Qiao, J. Zou, G. Liu, S. C. Smith, H. M. Cheng and G. Q. Lu, *Nature*, 2008, **453**, 638-641.
316. J. Pan, G. Liu, G. M. Lu and H. M. Cheng, *Angew Chem Int Edit*, 2011, **50**, 2133-2137.
317. M. Y. Xing, B. X. Yang, H. Yu, B. Z. Tian, S. Bagwasi, J. L. Zhang and X. Q. Gongs, *J Phys Chem Lett*, 2013, **4**, 3910-3917.
318. T. Luttrell, S. Halpegamage, J. Tao, A. Kramer, E. Sutter and M. Batzill, *Scientific reports*, 2014, **4**, 4043.
319. E. Hendry, F. Wang, J. Shan, T. F. Heinz and M. Bonn, *Phys Rev B*, 2004, **69**, 081101.

Table of contents



In this article, we review the recent advances on photoreactions of small molecules with model TiO_2 surfaces, and propose a photocatalytic model based on nonadiabatic dynamics and ground state surface reactions.